

**Effect of D-aspartate and storage temperature on
cryopreserved sperm quality and fertility in mice**

Inaugural Dissertation

zur

Erlangung des Doktorgrades
philosophiae doctor (PhD) in Health Sciences
der Medizinischen Fakultät
der Universität zu Köln

vorgelegt von

Manon Peltier

aus Chartres, France

Druckerei Hundt, Köln

2024

Betreuerin / Betreuer: Prof. Dr. Esther Mahabir-Brenner

Gutachterin / Gutachter: Prof. Dr. Maria Cristina Polidori
Prof. Dr. Marius Lemberg

Datum der Mündlichen Prüfung: 05.06.2024

Acknowledgements

I remember my arrival in Cologne, my first visit to Germany, in January 2020. A few weeks before, full of enthusiasm, I prepared my resume, learned how to count from 1 to 100 and a few other (more or less) indispensable words in German. We left Salt Lake City, the mountains and the snow. I was thrilled to come back to Europe. Starting a new life, discovering a new country and looking for a PhD position was very exciting, even though the COVID-19 pandemic had made things a little bit more difficult. I would like to thank all of the people who, in one way or another, contributed to my success, believed in me and encouraged me during my thesis.

First of all, I would like to thank Prof. Dr. Mahabir-Brenner for giving me the opportunity to complete my PhD in her research group. Obtaining a PhD is a major achievement in my life and I am grateful for her contribution in this journey. I also expressed my gratitude to my IPHS tutors, Prof. Dr. Polidori and Prof. Dr. Lemberg. I thank you very much for your time, your availability and your guidance. I am also thankful to Prof. Scavizzi and Renata for our fruitful collaboration.

To my colleagues, past and present: Daniela, Fleurand, Hannah, Lucienne, Mohamed, Ole, Pascal, Sara, Sarah, Silke and Yasmin, I am very thankful for your friendship, for your efforts to speak English when I am around and for making me feel that my skills and knowledge can be useful to someone else. Thank you for your support, for attending my presentations, for your feedback, for being present in stressful situations and for being most of my social life. Thank you all for your good vibes! A special thank you to Sarah for helping to translate the abstract into German, and to Mohamed who was a colleague, coach, interpreter, storyteller and TV-show reviewer all in one. I thank you for your infectious laugh and for always finding the positive in every situation. Your help has been precious in navigating in this sometimes-unintelligible world.

On a more personal perspective, I want to express my profound friendship to Natasha. Although you are on another continent, you always feel so close to me. You have already contributed a lot to my success when I was a master student, as well as with Franz. You welcomed me with such a warm smile, facilitated my integration into this new environment, fed me with cherry cakes and other amazing dishes that you have the secret. I will never forget everything you have done for me, thank you for your support, for your humanity, for your affection and for being you. I can't wait to get back to Utah and see you in person again. Hot-air ballooning over The Wasatch Front sounds like an amazingly very good plan! Thank you and Nestor, for being such good friends.

I am deeply grateful to my two families, Peltier and Storelli. Vous mes parents, qui m'avez toujours soutenue, qui avez su me laisser partir et me faire confiance, je vous remercie de tout ce que vous avez fait pour moi. Merci de m'avoir guidée dans la vie, de m'avoir appris à travailler dur, à m'accrocher mais aussi à profiter des choses simples de la vie. Je te remercie mon frère, avec qui j'ai partagé tant de choses, pour ton soutien, même si on est loin, même si on ne se voit pas souvent, je sais qu'on sera toujours là l'un pour l'autre. Toi aussi tu as accompli tant de choses dans ta vie et je suis incroyablement fière de toi. Un grand merci à ma famille de cœur, celle qui m'a adoptée comme une fille et une sœur. Merci de m'avoir accueillie si chaleureusement, merci pour vos encouragements dans tous les aspects de ma vie et de suivre nos péripéties depuis plus de 10 ans déjà !

I also would like to thank my emotional support animal, Gibbs, for his unconditional love and happiness. I am very pleased to be your human. Thank you for always trusting me and for making me feel like I am the most important person in the world.

Finally, I am extremely grateful to my husband, Gilles. Who would have thought that tree-climbing activity would change my life forever? Thanks to you, I have achieved things I never thought I could or even imagined. Completing my PhD would not have been possible without you. I thank you for your unwavering support, your guidance, your feedback and for the time you took to correct my dissertation in an already overloaded schedule. I also thank you for your patience, your trust and your honesty. Lastly, I thank you for sharing my life, for our daily uncontrollable laughter, for being an amazing father to Gibbs and for making me the person I am today.

Abstract

Mice have long been used in biomedical research because of their similarity to humans and ease of maintenance. Recent advances in genetic engineering have resulted in the generation of thousands of transgenic mouse lines that need to be made available to the scientific community. Assisted reproductive technologies have become essential for managing and archiving all these lines in repositories. Sperm cryopreservation appears to be the most economical and straightforward way to archive mouse lines compared to oocyte and embryo cryopreservation. Cryopreserved sperm is thawed and used for *in vitro* fertilisation (IVF), followed by embryo transfer, to recover mouse lines as needed. However, there are still major challenges in using cryopreserved sperm for IVF. In particular, cryodamage can compromise sperm integrity and fertility. Although cryopreservation protocols have been greatly improved in recent years, sperm recovery after cryopreservation remains highly variable among mouse lines. Another challenge is related to the use of liquid nitrogen (LN₂, -196°C) for sperm cryopreservation and storage due to the inherent risk of injury, cost and potential difficulty in accessing this resource. Improving sperm cryopreservation techniques to enhance success rate of IVF and developing protocols that do not rely on LN₂ would benefit the entire community of researchers working with mice.

The amino acid D-aspartate (D-Asp) improves IVF success rates with cryopreserved sperm in several mammalian species. However, how this compound exerts these effects remains poorly understood. I have investigated this phenomenon to advance our understanding of the mechanisms that preserve sperm fertility after cryopreservation. In parallel, the use of -80°C freezers is an attractive alternative to LN₂ for sperm cryopreservation. It has already shown promising results with B6N sperm, but how this temperature affects the sperm integrity in other mouse strains has not been investigated. I have therefore evaluated the effect of cryopreservation and storage at -80°C on a panel of widely used mouse strains. Finally, I tested whether D-Asp would also have a beneficial effect when mouse spermatozoa are cryopreserved at -80°C.

The results show that D-Asp administered orally to C57BL/6N (B6N) males improves sperm motility, morphology and maturation after cryopreservation in LN₂. Some of these effects were recapitulated in sperm treated *in vitro* with D-Asp, showing that this compound can act directly on spermatozoa to improve their quality after cryopreservation. D-Asp treatment was associated with a signature of oxidative stress in spermatozoa, suggesting that this amino acid acts through reactive oxygen species (ROS) to exert its cryoprotective effects. Consistent with this hypothesis, quenching ROS with antioxidant treatment suppressed the beneficial effect of D-Asp on sperm maturation after cryopreservation. Taken together, it suggests that D-Asp improves sperm function after cryopreservation by inducing the production of ROS.

In parallel, the response of a panel of widely used mouse strains to sperm cryopreservation at -80°C was assessed. IVF success rates were similar when spermatozoa from B6N, CD-1, FVB and 129 were cryopreserved and stored in LN_2 or in -80°C freezers. However, sperm from B6J and BALB/c mice showed a dramatic decrease in fertility when cryopreserved at -80°C , which was associated with a decline in viability, sperm quality and integrity. This shows that there are variations in the sensitivity to cryopreservation at -80°C among mouse strains. These strain-specific variations could limit the generalisation of sperm cryopreservation at this temperature. Given the beneficial role of D-Asp on sperm stored in LN_2 , I have tested whether this compound could improve the quality of B6J and BALB/c sperm cryopreserved at -80°C . D-Asp improved the motility, morphology and maturation of B6J and BALB/c sperm under this condition, showing that D-Asp alleviates, at least in part, the physiological limitations of cryopreservation at -80°C in these strains. D-Asp treatment could therefore be used in combination with long-term storage at -80°C to facilitate sperm cryopreservation even in the most sensitive strains, and greatly improve the workflow of research laboratories and mouse repositories.

Taken together, this study supports a model in which D-Asp acts in a cell-autonomous manner to increase cellular ROS levels, which in turn improves sperm quality after cryopreservation. D-Asp shows similar effects in sperm archived at -80°C , opening up promising perspectives for the generalisation of this cryopreservation temperature. Further investigations are required to determine how D-Asp increases ROS levels and if defined ROS are responsible for improving sperm quality after cryopreservation. It also remains to be determined whether improved sperm fertility after D-Asp treatment translates into normal embryo development and offspring health after IVF. From a broader perspective, these studies may have important implications for human assisted reproduction. The use of cryopreservation has become common practice for sperm donation or sperm preservation in the event of illness or future treatment that may affect fertility. In all cases, it is extremely important to improve sperm cryopreservation methods, especially in an ageing population where the use of assisted reproductive techniques is of increasing interest.

Zusammenfassung

Mäuse werden seit langem in der biomedizinischen Forschung eingesetzt, da sie pflegeleicht sind und dem Menschen ähneln. Jüngste Fortschritte in der Gentechnik haben zur Erzeugung tausender transgener Mauslinien geführt, die der wissenschaftlichen Gemeinschaft zur Verfügung gestellt werden müssen. Assistierte Reproduktionstechnologien sind für die Verwaltung und Archivierung all dieser Linien in Repositorien unerlässlich. Die Kryokonservierung von Spermien scheint sich gegenüber der Kryokonservierung von Eizellen und Embryonen als die wirtschaftlichste und einfachste Methode zur Archivierung von Mauslinien durchzusetzen. Das kryokonservierte Sperma wird aufgetaut und für die *In-vitro*-Fertilisation (IVF) und den anschließenden Embryotransfer verwendet, um Mauslinien zu reproduzieren. Bei der Verwendung von kryokonserviertem Sperma für die IVF gibt es jedoch noch große Probleme. Insbesondere Kälteschäden können die Integrität und Fruchtbarkeit der Spermien beeinträchtigen. Obwohl die Kryokonservierungsprotokolle in den letzten Jahren verbessert wurden, ist die Qualität der Spermien nach der Kryokonservierung innerhalb der verschiedenen Mausstämme sehr unterschiedlich. Eine weitere Herausforderung ist die Verwendung von flüssigem Stickstoff (LN₂, -196°C) für die Kryokonservierung und Lagerung von Spermien, da ein Verletzungsrisiko besteht, die Kosten hoch sind und der Zugang zu LN₂ möglicherweise schwierig ist. Die Entwicklung von Protokollen, die nicht auf LN₂ angewiesen sind und die Verbesserung der Kryokonservierungsmethoden von Spermien, um die Erfolgsrate der IVF zu erhöhen, würden allen Forschern, die mit Mäusen arbeiten, helfen.

Die Aminosäure D-aspartat (D-Asp) verbessert die IVF-Raten bei kryokonservierten Spermien in mehreren Säugetierarten. Wie D-Asp diese Wirkungen entfaltet ist jedoch noch wenig bekannt. Ich habe dieses Phänomen untersucht, um unser Verständnis für Mechanismen, welche die Fruchtbarkeit von kryokonservierten Spermien erhalten, zu verbessern. Zudem wäre die Verwendung von -80°C Gefriergeräten eine attraktive Alternative zu LN₂ für die Kryokonservierung von Spermien. Dies hat bereits vielversprechende Ergebnisse bei B6N-Spermien gezeigt, aber wie diese Temperatur die Integrität der Spermien anderer Mauslinien beeinflusst, wurde noch nicht erforscht. Daher habe ich die Auswirkungen der Kryokonservierung und Lagerung bei -80 °C bei einer Reihe weit verbreiteter Mausstämme untersucht. Zusätzlich habe ich getestet, ob D-Asp auch bei der Kryokonservierung von Mauspermien bei -80°C eine positive Wirkung hat.

Die Ergebnisse zeigen, dass die orale Verabreichung von D-Asp an C57BL/6N (B6N)-Männchen die Beweglichkeit, Morphologie und Reifung der Spermien nach der Kryokonservierung in LN₂ verbessert. Einige dieser Effekte konnten bei Spermien, die *in vitro* mit D-Asp behandelt wurden, wiederholt werden. Dies zeigt, dass diese Verbindung direkt auf die Qualität der Spermien einwirken kann, um ihre Funktion nach der Kryokonservierung zu verbessern. Die Behandlung mit D-Asp wurde mit einer Signatur von oxidativem Stress in Spermien in Verbindung gebracht, was darauf hindeutet, dass diese Aminosäure ihre kryoprotektive Wirkung über reaktive Sauerstoffspezies (ROS) ausübt. In Übereinstimmung mit dieser Hypothese führte die

Reduzierung von ROS durch eine antioxidative Behandlung die positive Wirkung von D-Asp auf die Spermienreifung nach der Kryokonservierung. Insgesamt deutet es darauf hin, dass D-Asp die Spermienfunktion nach der Kryokonservierung verbessert, indem es die Produktion von ROS anregt.

Parallel dazu wurde die Reaktion einiger weit verbreiteter Mausstämmen auf die Kryokonservierung von Spermien bei -80°C untersucht. Bei Spermien der Stämme B6N, CD-1, FVB und 129, die in -80°C Gefrierschränken kryokonserviert und gelagert waren, war die IVF-Erfolgsraten ähnlich, wie bei denen, die in LN_2 kryokonserviert und gelagert wurden. Die Spermien von B6J- und BALB/c-Mäusen zeigten jedoch einen dramatischen Rückgang der Fruchtbarkeit, wenn sie bei -80°C kryokonserviert wurden, was mit einer Verschlechterung der Lebensfähigkeit, Spermienqualität und -integrität einherging. Dies zeigt, dass die Empfindlichkeit gegenüber der Kryokonservierung bei -80°C bei verschiedenen Mausstämmen unterschiedlich ist. Diese stammspezifischen Unterschiede könnten die Generalisierung der Kryokonservierung von Spermien bei -80°C einschränken. Angesichts der positiven Wirkung von D-Asp auf Spermien, die in LN_2 gelagert werden, habe ich getestet, ob diese Verbindung die Qualität von B6J- und BALB/c-Spermien, die bei -80°C kryokonserviert wurden, verbessern könnte. D-Asp verbesserte die Beweglichkeit, die Morphologie und die Reifung von B6J- und BALB/c-Spermien unter diesen Bedingungen, was zeigt, dass D-Asp die physiologischen Einschränkungen der Kryokonservierung bei -80°C bei diesen Stämmen zumindest teilweise aufhebt. Die D-Asp-Behandlung könnte daher in Kombination mit einer Langzeitlagerung bei -80°C eingesetzt werden, um die Kryokonservierung von Spermien selbst bei den empfindlichsten Stämmen zu erleichtern und die Arbeitsabläufe in Forschungslaboren und Mauslagern zu verbessern.

Zusammenfassend stützt diese Studie ein Modell, bei dem D-Asp auf zellautonome Weise den zellulären ROS-Spiegel erhöht, was die Spermienqualität nach der Kryokonservierung verbessert. D-Asp zeigt ähnliche Effekte in Spermien, die bei -80°C archiviert wurden, was vielversprechende Perspektiven für die Generalisierung dieser Kryokonservierungstemperatur eröffnet. Um festzustellen, wie D-Asp den ROS-Spiegel erhöht und ob bestimmte ROS für die Verbesserung der Spermienqualität nach der Kryokonservierung verantwortlich sind, sind weitere Untersuchungen nötig. Es bleibt auch zu klären, ob die verbesserte Spermienfruchtbarkeit nach einer D-Asp-Behandlung zu einer normalen Embryonalentwicklung und Gesundheit der Nachkommen nach einer IVF führt. Aus einer umfassenderen Perspektive betrachtet, könnten diese Studien wichtige Auswirkungen auf die assistierte Reproduktion beim Menschen haben. Die Kryokonservierung ist inzwischen gängige Praxis für Samenspende oder die Aufbewahrung von Spermien im Falle von Krankheiten oder zukünftigen Behandlungen, die die Fruchtbarkeit beeinträchtigen können. In jedem Fall ist es äußerst wichtig, die Methoden der Kryokonservierung von Spermien zu verbessern, insbesondere in einer alternden Bevölkerung, in der der Einsatz von assistierten Reproduktionstechniken von zunehmendem Interesse ist.

Table of contents

Acknowledgements	3
Abstract	5
Zusammenfassung	7
Table of contents	9
List of figures and tables	12
Abbreviations	14
1. Introduction	17
1.1 Reproductive techniques for mouse colony management	17
1.1.1 The mouse as an animal model for biomedical research	17
1.1.2 Mouse repositories	18
1.1.3 Assisted reproductive technologies in mice	19
1.2 Overview of the male reproductive system in mice	23
1.2.1 Testis morphology and function	23
1.2.2 Spermatogenesis	23
1.2.3 Endocrinology of the male reproductive system	24
1.2.4 Spermatozoa morphology	25
1.2.5 Epididymal maturation of spermatozoa	26
1.2.6 Post-ejaculation sperm maturation	27
1.2.7 Fertilisation	28
1.2.8 Function of reactive oxygen species in male reproduction	28
1.3 Cryopreservation of spermatozoa	29
1.3.1 History and principles of sperm cryopreservation	29
1.3.2 Sperm cryopreservation protocol	31
1.3.3 Sperm thawing protocol	31
1.3.4 Sperm cryodamage	32
1.3.5 LN ₂ -free alternative protocol for mouse sperm cryopreservation	33
1.3.6 Effect of D-aspartate on cryopreserved spermatozoa	34
2. Thesis aims	37
3. Materials and Methods	39
3.1 Materials	39
3.1.1 Equipment	39
3.1.2 Consumables	39
3.1.3 Chemicals, reagents, solutions	40
3.1.4 Other	42
3.1.5 Buffers and solutions	42

3.2	Methods.....	44
3.2.1	Mice.....	44
3.2.2	Sperm collection, cryopreservation and thawing procedures.....	45
3.2.3	D-Asp treatment.....	47
3.2.4	Spermatozoa analyses	47
3.2.5	Data analysis	53
4.	Results.....	55
4.1	Aim I: To characterise the effects of D-aspartate on the fertility and quality of cryopreserved mouse spermatozoa and the mechanisms involved	55
4.1.1	D-Asp treatment does not affect spermatozoa concentration	55
4.1.2	D-Asp treatment for 4 weeks increases the motility of spermatozoa.....	55
4.1.3	D-Asp treatment for 2 weeks decreases sperm abnormalities in young B6N males	57
4.1.4	D-Asp-treatment leads to higher capacitation and acrosome reaction rate.....	58
4.1.5	Oral treatment with D-Asp increases DHE staining and DNA oxidation levels in spermatozoa	60
4.1.6	<i>In vitro</i> D-Asp treatment increases DHE staining and DNA oxidation levels in spermatozoa	62
4.1.7	The beneficial effect of D-Asp on ROS production, capacitation and the acrosome reaction is inhibited by the addition of an antioxidant	64
4.2	Aim II: To evaluate the fertility and quality of mouse spermatozoa cryopreserved and stored at -80°C	67
4.2.1	The fertility rate is stable over time when spermatozoa are cryopreserved and stored at -80°C except in B6J and BALB/c strains	67
4.2.2	The percentage of dead spermatozoa increases in B6J and BALB/c when sperm samples are cryopreserved and stored at -80°C	67
4.2.3	Cryopreservation and storage at -80°C decreases the sperm motility in all strains	70
4.2.4	The percentage of abnormalities is higher in all strains when spermatozoa are cryopreserved and stored at -80°C	70
4.2.5	The sperm ultrastructure is damaged after cryopreservation and storage at -80°C	73
4.2.6	The DNA fragmentation level is higher in spermatozoa cryopreserved at -80°C in all strains.....	73
4.2.7	Summary of significant negative impact of sperm cryopreservation and storage in -80°C compared to LN ₂	77
4.2.8	<i>In vitro</i> D-Asp treatment increases the quality of B6J and BALB/c spermatozoa cryopreserved at -80°C	78
4.2.9	<i>In vitro</i> D-Asp treatment compensates for the decrease of capacitation and acrosome reaction rate in spermatozoa cryopreserved and stored at -80°C	78
5.	Discussion.....	81
5.1	D-Asp improves cryopreserved sperm quality by increasing ROS levels	81

5.2	Influence of cryopreservation and storage temperature on sperm integrity and fertility	86
5.3	Can D-Asp treatment of cryopreserved sperm be of interest for human health?	91
	References	93
	Appendix	104
	Curriculum Vitae	106
	ERKLÄRUNG	107

List of figures and tables

Figure 1	Workflow of principal ARTs in mouse repositories
Figure 2	Mouse cumulus-oocyte complex
Figure 3	Organisation of the testis, spermatogenesis and spermatozoa morphology of the mouse
Figure 4	Hypothalamic-pituitary-testis axis in male mice
Figure 5	Physiological and pathological role of ROS in male fertility
Figure 6	Mouse sperm cryopreservation protocol
Figure 7	Schematic diagram of the detrimental effects of cryopreservation on sperm integrity leading to the decline in sperm function
Figure 8	Sperm concentration after administration of D-Asp
Figure 9	Sperm motility after administration of D-Asp
Figure 10	Sperm morphology after administration of D-Asp
Figure 11	Sperm maturation rates after administration of D-Asp
Figure 12	Measurement of ROS with DHE staining after oral administration of D-Asp
Figure 13	Analysis of DNA oxidation with immunostaining after oral administration of D-Asp
Figure 14	Measurement of ROS with DHE staining after <i>in vitro</i> of D-Asp treatment
Figure 15	Analysis of DNA oxidation with immunostaining after <i>in vitro</i> D-Asp treatment
Figure 16	Inhibition of the beneficial effect of D-Asp with the antioxidant NAC
Figure 17	Effect of cryopreservation and storage temperature on sperm fertility
Figure 18	Effect of cryopreservation and storage temperature on sperm viability
Figure 19	Effect of cryopreservation and storage temperature on sperm total motility

Figure 20	Effect of cryopreservation and storage temperature on sperm morphology
Figure 21	Effect of cryopreservation and storage temperature on sperm ultrastructure
Figure 22	Effect of cryopreservation and storage temperature on sperm DNA fragmentation levels
Figure 23	Sperm quality after <i>in vitro</i> D-Asp treatment of spermatozoa cryopreserved in LN ₂ or at -80°C
Figure 24	Analysis of capacitation and the acrosome reaction after <i>in vitro</i> D-Asp treatment of spermatozoa cryopreserved in LN ₂ or at -80°C
Figure 25	Working model of the effect of D-Asp on cryopreserved spermatozoa
Figure 26	Mouse strain specificities related to sperm cryopreservation and storage at -80°C
Table 1	Principal mouse repositories
Table 2	Overview of the experimental design
Table 3	Summary of significant negative impact of sperm cryopreservation and storage at -80°C compared to LN ₂

Abbreviations

129	129/SvlmJCnrm
3Rs	Replacement, refinement, reduction
ABP	Androgen binding protein
AI	Artificial insemination
Akt	Protein kinase B (previously known as PKB)
ARRIVE	Animal research: reporting of <i>in vivo</i> experiments
ARTs	Assisted reproductive technologies
ATP	Adenosine triphosphate
A.U.	Arbitrary Unit
B6J	C57BL/6JCnrm
B6N	C57BL/6NTacCnrm
BALB/c	BALB/cByJCnrm
BSA	Bovine serum albumin
Ca ²⁺	Calcium
cAMP	Cyclic adenosine monophosphate
CARD	Center of animal resources and development
CD-1	CrI:CD1(ICR)
CECAD	Universty of Cologne's cluster of excellence in ageing research
cGMP	Cyclic guanosine monophosphate
CNR-EMMA	Consiglio nazionale delle ricerche – European mouse mutant archive
CO ₂	Carbon dioxide
COCs	Cumulus-oocyte complexes
CPM	Cryoprotective medium
CTC	Chlortetracycline
DABCO	1,4-Diazabicyclo[2.2.2]octane
DAG	Diacylglycerol
DAP	DMSO-acetamide-propylene glycol
DAPI	4',6-Diamidino-2-phenylindole
D-Asp	D-aspartate or D-aspartic acid
DDO	D-Asp oxidase
DHE	Dihydroethidium
DMSO	Dimethyl sulfoxide
DNA	Deoxyribonucleic acid
DPBS	Dulbecco's phosphate-buffered saline
DTT	DL-Dithiothreitol
EDTA	Ethylenediaminetetraacetic acid
EMMA	European mouse mutant archive
ERK1/2	Extracellular signal-regulated protein kinase 1/2
ETC	Electron transport chain
FACS	Fluorescence-activated cell sorting
FELASA	Federation of European laboratory animal science associations
FSH	Follicle-stimulating hormone

FVB	FVBN/JCnrm
GC	Germ cell
GluA1/A2/A3	Glutamate A1/A2/A3
GnRH	Gonadotropin-releasing hormone
GSH	Reduced L-glutathione
H ₂ O ₂	Hydrogen peroxide
hCG	Human chorionic gonadotrophin
HCl	Hydrogen chloride
HCO ₃ ⁻	Bicarbonate
HEPES	4-(2-Hydroxyethyl)-1-piperazineethanesulfonic acid
HPT	Hypothalamic-pituitary-testis
HTF	Human tubal fluid
ICSI	Intracytoplasmic sperm injection
IMSR	International mouse strain resource
IP ₂	Inositol triphosphate
IU	International unit
IVF	<i>In vitro</i> fertilisation
KCl	Potassium chloride
LH	Luteinizing hormone
LN ₂	Liquid nitrogen
MTG	Monothioglycerol
NAC	N-acetyl-L-cysteine
NaCl	Sodium chloride
NADPH	Nicotinamide adenine dinucleotide phosphate hydrogen
NaOH	Sodium hydroxide
NGS	Normal goat serum
NH ₃	Ammonia
NMDA	N-methyl-D-aspartate
NMDARs	N-methyl-D-aspartate receptors
NO	Nitric oxide
NOXs	NADPH oxidases
O ₂	Dioxygen
O ₂ ⁻	Superoxide anion
PB	Phosphate buffer
PBS	Phosphate buffered saline
PFA	Paraformaldehyde
PKA / PKC	Protein kinase A / C
PI	Propidium iodide
PIP ₂	Phosphatidylinositol 4,5-bisphosphate
PMSG	Pregnant mare's serum gonadotrophin
ROS	Reactive oxygen species
RT	Room temperature
Soat1	Sterol O-acetyltransferase 1
SSC	Spermatogonial stem cells
StAR	Steroidogenic acute regulatory protein

TCA	Tricarboxylic acid
TEM	Transmission electron microscopy
TRITC	Tetramethylrhodamine
ZP	Zona pellucida

1. Introduction

1.1 Reproductive techniques for mouse colony management

1.1.1 The mouse as an animal model for biomedical research

Biomedical research aims to understand human health and disease at the cellular, tissue and systemic levels. It involves the development of tools and techniques to refine diagnostics, find new therapies and create medical devices in order to treat and prevent diseases or improve quality of life. An important research strategy for studying human biology is the use of experimental models. Organoid, tissue or cell cultures are highly valuable in basic research, providing researchers with simplified biological systems in a well-controlled environment [1]. However, these *in vitro* models have the disadvantage that they do not recapitulate the full complexity of a complete organism. In contrast, the use of animal models is more likely to represent biologically relevant mechanisms because the investigations are carried out in a physiological context [2]. Animal models have long been used to advance our understanding of human health with immense benefits in drug development, toxicity studies, surgical experiments and engineering devices for research in various human diseases [3]. Nevertheless, using animals requires ethical considerations, responsibility and human care. The practical strategy of replacement, refinement and reduction, known as the 3Rs, was first published by W.M.S. Russell and R.L. Burch in the book *The Principles of Humane Experimental Technique* (1959) [4]. Replacement refers to all methods that avoid the use of animals, such as *in vitro* approaches and computer models. Refinement means improving animal well-being and reducing or eliminating pain and distress by adapting husbandry or experimental procedures. Finally, reduction encompasses all strategies to use less animals to obtain a comparable level of information. The 3Rs principle is internationally accepted by legislative institutions as well as researchers and applied when animals are used in research studies [5].

Of all the species used, the mouse is the preferred mammalian model due to its small size, relatively short lifespan, ease of breeding and high homology to humans [6, 7]. In addition, 90% of the human genome is conserved in the mouse and most disease symptoms are common to both species, making mouse research applicable to humans [8, 9]. Finally, the development and refinement of genetic engineering technologies in recent decades has dramatically increased the attractiveness of the mouse model [10, 11].

1.1.2 Mouse repositories

The vast expansion of the use of the mouse model quickly created a huge demand for distributors. As the pressure increased, issues of quality control, genetic fidelity and animal health arose, challenging the reproducibility of scientific results [12]. As a result, robust animal infrastructures have emerged with the goal to identify, classify, archive and disseminate mouse lines to the scientific community. In this way, high quality control standards and policies are available to ensure reproducibility and integrity of research [13, 14].

There are several mouse repositories around the world with more than 90,000 mouse lines available for biomedical research (Table 1). The largest in Europe is the European Mouse Mutant Archive (EMMA) [15]. To navigate between all these resources and to help the scientific community find the appropriate mouse model, an online catalogue, the International Mouse Strain Resource (IMSR), was created in 1999 (<https://findmice.org/>) [16].

Table 1: Principal mouse repositories. (Date as of March 14, 2024; source: IMSR)

Repository	Region	No. of mouse lines
Australian Phenome Bank (APB)	Australia	2,111
Center for Animal Resources and Development (CARD)	Japan	2,057
Canadian Mouse Mutant Repository (CMMR)	Canada	1,246
European Mouse Mutant Archive (EMMA)	Germany	7,610
GemPharmatech (GPT)	China	21,329
MRC Harwell (HAR)	UK	2,059
JAX Mice and Services (JAX)	USA	12,593
Korea Mouse Phenotyping Center (KMPC)	Korea	365
Mutant Mouse Regional Resource Centers (MMRRC)	USA	22,168
National Cancer Institute at Frederick (NCIMR)	USA	139
National Institute of Genetics (NIG)	Japan	142
Oak Ridge Collection at JAX (ORNL)	USA	906
RIKEN BioResource Research Center (RBRC)	Japan	6,027
National Applied Research Laboratories (RMRC-NLAC)	Taiwan	351
Shanghai Model Organisms Center, Inc. (SMOC)	China	9,946
Taconic Biosciences (TAC)	USA	2,725
Texas A&M Institute for Genomic Medicine (TIGM)	USA	195
Total		91,969

Effective colony management is essential to use the space, the equipment and the workforce efficiently, and to minimise the cost and the production of surplus animals in compliance with the 3Rs principle. Mouse repositories not only manage mouse lines but also contribute to the development and implementation of technologies to improve their husbandry, in particular through assisted reproductive technologies (ARTs). Indeed, the maintenance of such a large number of mouse lines as live animals would require considerable space and logistics. In contrast, cryopreservation of mouse resources reduces maintenance costs and

the number of mice used. It also protects mouse lines from infection, disease and genetic drift [17, 18]. In addition, it greatly facilitates the distribution of strains within the scientific community, thereby bypassing some of the health and welfare issues associated with live animal transport.

1.1.3 Assisted reproductive technologies in mice

Reproduction is the most important biological function ensuring the continuation of species. Importantly, male reproductive anatomy and function are largely conserved from rodents to humans [19, 20]. Sexual reproduction in mice involves a female germ cell (oocyte) and a male germ cell (spermatozoon). The fusion of the oocyte and the spermatozoon, called fertilisation, results in an embryo that, when developed, will form a new individual.

ARTs include superovulation, assisted reproduction, embryo transfer and cryopreservation of resources for an efficient preservation and production of mouse lines (Figure 1).

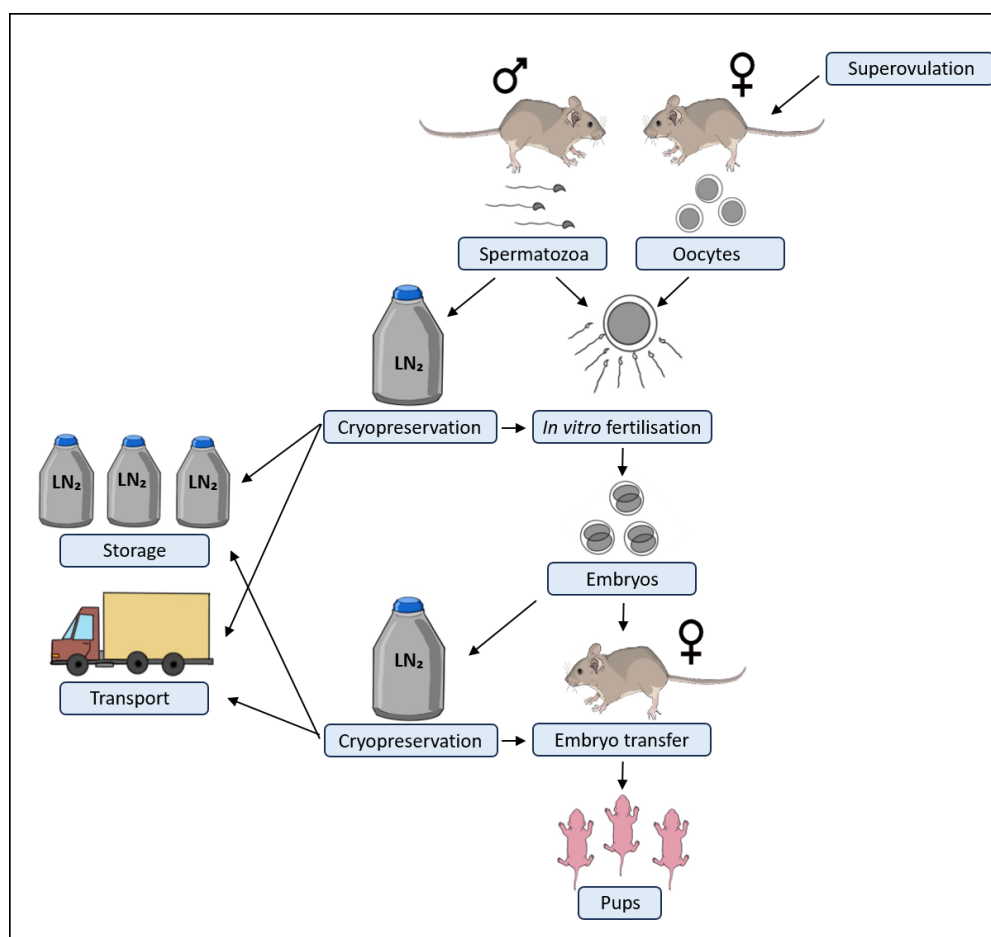


Figure 1: Workflow of principal ARTs in mouse repositories. Cryopreserved spermatozoa and embryos can be archived in LN₂ for an unlimited period of time and distributed within the scientific community as cryopreserved material. *In vitro* fertilisation can be performed with fresh or frozen spermatozoa and oocytes. The 2-cell embryos produced are then implanted into females to reestablish mouse lines or cryopreserved for archiving.

Superovulation

Collecting sufficient oocytes (Figure 2) from females is a critical parameter conditioning the ARTs workflow. Mature female mice usually produce 8-10 oocytes per spontaneous ovulation [21]. To increase this number, an induction of superovulation is required. Females receive a hormonal treatment with pregnant mare's serum gonadotrophin (PMSG) and 48 hours later human chorionic gonadotrophin (hCG). Ovulated oocytes are produced 13-16 hours after hCG. The response to superovulation may vary depending on the dose of hormones, the mouse age and strain [22].

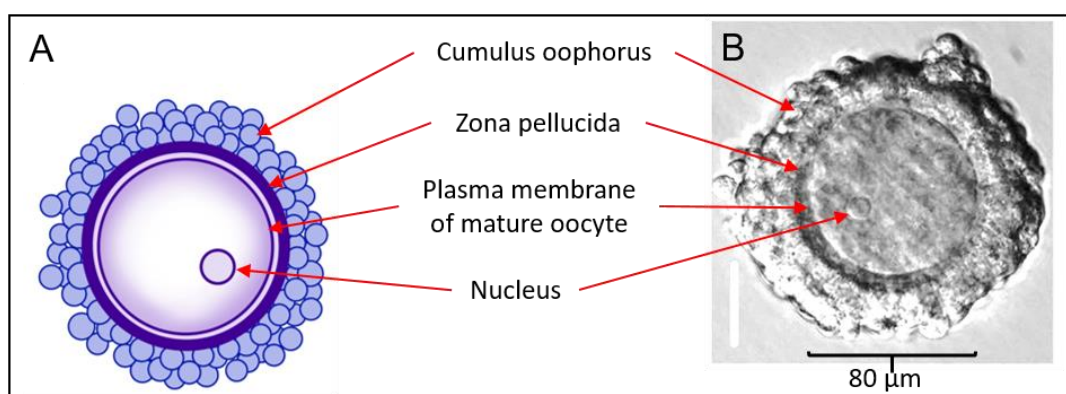


Figure 2: Mouse cumulus-oocyte complex. (A) Schematic representation of an oocyte and (B) microscopic image of an oocyte from [23]. The cumulus oophorus is a mass of granulosa cells that protect the oocyte and support its maturation. The zona pellucida is a thick matrix composed of glycoproteins responsible for species-specific binding of spermatozoa, sperm maturation and prevention of fertilisation by multiple spermatozoa.

Mouse assisted reproduction

These techniques are widely used to revive the mouse lines after cryopreservation of spermatozoa and/or oocytes. They are also necessary to overcome infertility and produce pups in some mouse lines. These techniques correspond to artificial insemination (AI), *in vitro* fertilisation (IVF) and intracytoplasmic sperm injection (ICSI).

AI was first used in mice in 1960 [24]. It involves the direct implantation of sperm into the female reproductive tract. Spermatozoa can be delivered through a needle inserted into the vaginal canal [25]. Alternatively, a surgical technique can be performed under anaesthesia to surgically expose the female reproductive tract and spermatozoa can be injected into the ampulla of the oviduct [26]. Although AI is routinely used in cattle, pigs, sheep and goats, it is not often practiced in mice. However, it may be of interest in certain mouse lines to bypass IVF and embryo transfer [27, 28].

IVF involves the fertilisation of oocytes by sperm in a culture dish (Appendix 1). Since the beginning of mouse IVF in the 1970s, important improvements in fertilisation media and protocols have been made. Nowadays, protocols such as the "Nakagata method" are known

to give a high IVF success rate with most cryopreserved mouse spermatozoa [29]. In the Nakagata method, fresh spermatozoa can be collected or cryopreserved spermatozoa can be thawed (37°C for 10 min) and incubated in a medium that promotes the removal of cholesterol from the plasma membrane to initiate capacitation, an important maturation step (see section 1.2.6. Post-ejaculation sperm maturation). This pre-incubation step is known to increase the success rate of IVF [30, 31]. The sperm suspension is then incubated with oocytes, from superovulated females, in an IVF medium based on the human tubal fluid (HTF) composition, with a high calcium concentration and the antioxidant reduced L-glutathione (GSH) for a duration of 3 to 5 hours. The oocytes are then washed and cultured for 16-18 hours. The resulting 2-cell embryos can then be implanted into recipient for embryo transfer or cryopreserved. The synchronisation of egg fertilisation results in synchronous embryo development, which is a major advantage of IVF in providing age-matched experimental cohorts.

The injection of a single sperm directly into the oocyte, known as ICSI, is an extension of the passive fertilisation used in IVF. It was originally developed in the hamster before being successfully applied to the mouse two decades later [32, 33]. Spermatozoa used for ICSI do not need to be motile, mature or alive, as long as the nucleus is intact in terms of genetic integrity [34]. For these reasons, ICSI is advantageous for bypassing infertility. It is also used to generate transgenic mice with ICSI transgenesis, when large transgenes need to be inserted into the host genome [35]. However, ICSI is often considered as a cumbersome procedure, being extremely time consuming and costly with very low yields compared to IVF.

Embryo transfer

IVF and ICSI must be followed by embryo transfer to rederive a mouse line (Figure 1). Embryos at the 2-cell stage are surgically implanted into the oviduct of a pseudopregnant female (a female becomes pseudopregnant when she mates with a vasectomised male). An average of 10 live pups can result from the transfer of 15 embryos in animals with normal reproductive performance [36]. Alternatively, embryos can be cryopreserved for storage.

Cryopreservation of mouse resources

Spermatozoa, embryos and oocytes are the most common resources cryopreserved in mouse repositories [14, 18, 37].

Cryopreservation of oocytes is mainly performed in order to have access to a large number of oocytes for IVF and requires the preliminary step of superovulation [38]. However, in routine, oocyte cryopreservation is not the privileged method for archiving mouse lines, compared to embryo and spermatozoa, because protocols are limited and not fully reliable. However, oocyte cryopreservation continues to develop rapidly and recent studies with vitrified

oocytes (cryopreservation at a high cooling rate in LN₂) gave excellent results, with 90% of normal morphology and a rate of 89% of oocytes fertilised after warming [38, 39].

Embryo cryopreservation is useful to quickly rederive mutant mouse lines. It has been performed for more than 40 years, with significant improvements and modifications to the method [40]. In mice, excellent results are obtained with embryos cryopreserved by vitrification using 1 M dimethyl sulfoxide (DMSO) and DAP213 (2 M DMSO, 1 M acetamide, and 3 M propylene glycol) [41]. With this method, the survival rate of vitrified embryos can reach 90%, of which 30-50% will develop into pups after embryo transfer. Embryos can be collected after natural mating. However, collecting a sufficient number of embryos with this method is challenging, as typically 200-500 embryos are required to archive a mouse line. In most cases, embryos are collected at the 2-cell stage after *in vitro* fertilisation (IVF), which is the most efficient method [18]. Although the survival rate of cryopreserved embryos is usually high enough for most mouse lines, their ability to develop to term after embryo transfer varies greatly depending on the genetic background [22].

Sperm cryopreservation is the most economical and fastest way to archive a mouse line and appears to be the preferred method over the expensive embryo cryopreservation technique [13, 42, 43]. It also does not require any special treatment unlike in oocyte cryopreservation where females are superovulated. Sperm from 50 mice can be collected and cryopreserved on the same day by only 2 technicians using a very simple technique and without expensive equipment [39]. Another advantage for mouse repositories in disseminating mouse lines as cryopreserved sperm is that the costs of IVF and embryo transfer are shifted to the recipient institute. A limitation is that only half of the genome is preserved, making this method less suitable for strains with multiple mutations. Sperm cryopreservation represents a major improvement in the management of mouse lines. Although this method is very promising, effective sperm cryopreservation protocols have long been difficult to establish. Common cryoprotectants used for other cell types, such as glycerol and DMSO, did not work efficiently with spermatozoa [44]. In particular, a poor IVF success rate was observed with cryopreserved spermatozoa from B6J, the most commonly used mouse strain. Since the 1990s, major improvements have been made to limit cryodamage and reduce the impact of cryopreservation on sperm quality and fertility.

Before introducing the technique of sperm cryopreservation and its impact on sperm integrity, an overview of the male reproductive system is necessary to understand important aspects related to sperm production, maturation and fertility.

1.2 Overview of the male reproductive system in mice

1.2.1 Testis morphology and function

The production of spermatozoa, called spermatogenesis, and the secretion of testosterone are the main functions of the testis, which, in mice, is located in the abdomen [45]. The testis consists of a tubular compartment containing the seminiferous tubules and an intratubular compartment, also known as the interstitial tissue (Figure 3A). Leydig cells are somatic cells located in the interstitial tissue. Their role is to produce testosterone, which regulates spermatogenesis. Spermatogenesis takes place in the epithelium of the seminiferous tubules, which also contains somatic cells called Sertoli cells. Sertoli cells provide structural support for spermatogenesis through cell-cell contact with germ cells [46].

1.2.2 Spermatogenesis

Spermatogonial stem cells (SSC), also known as type A spermatogonia, located in the basal compartment of the seminiferous tubules are capable of self-renewal and differentiation leading to spermatozoa (Figure 3A and 3B) [47]. After various steps of maturation and differentiation, type A spermatogonia develop into type B spermatogonia, move towards the lumen of the seminiferous tubule and become primary spermatocytes. Here, meiosis begins: homologous chromosomes pair and cross over, and the first meiotic division gives rise to secondary spermatocytes containing 20 chromosomes, each with 2 chromatids. During the second meiotic division, the 2 chromatids separate, producing spermatids with a haploid genome. The final phase of spermatogenesis, called spermiogenesis, consists of the maturation of spermatids at the luminal surface with extrusion of cytoplasm, extensive differentiation and release of spermatozoa into the lumen. In addition, chromatin remodelling occurs at this stage, with a histone to protamine transition that allows tight packaging of sperm DNA [48]. In mice, the whole process of spermatogenesis takes about 5 weeks [49].

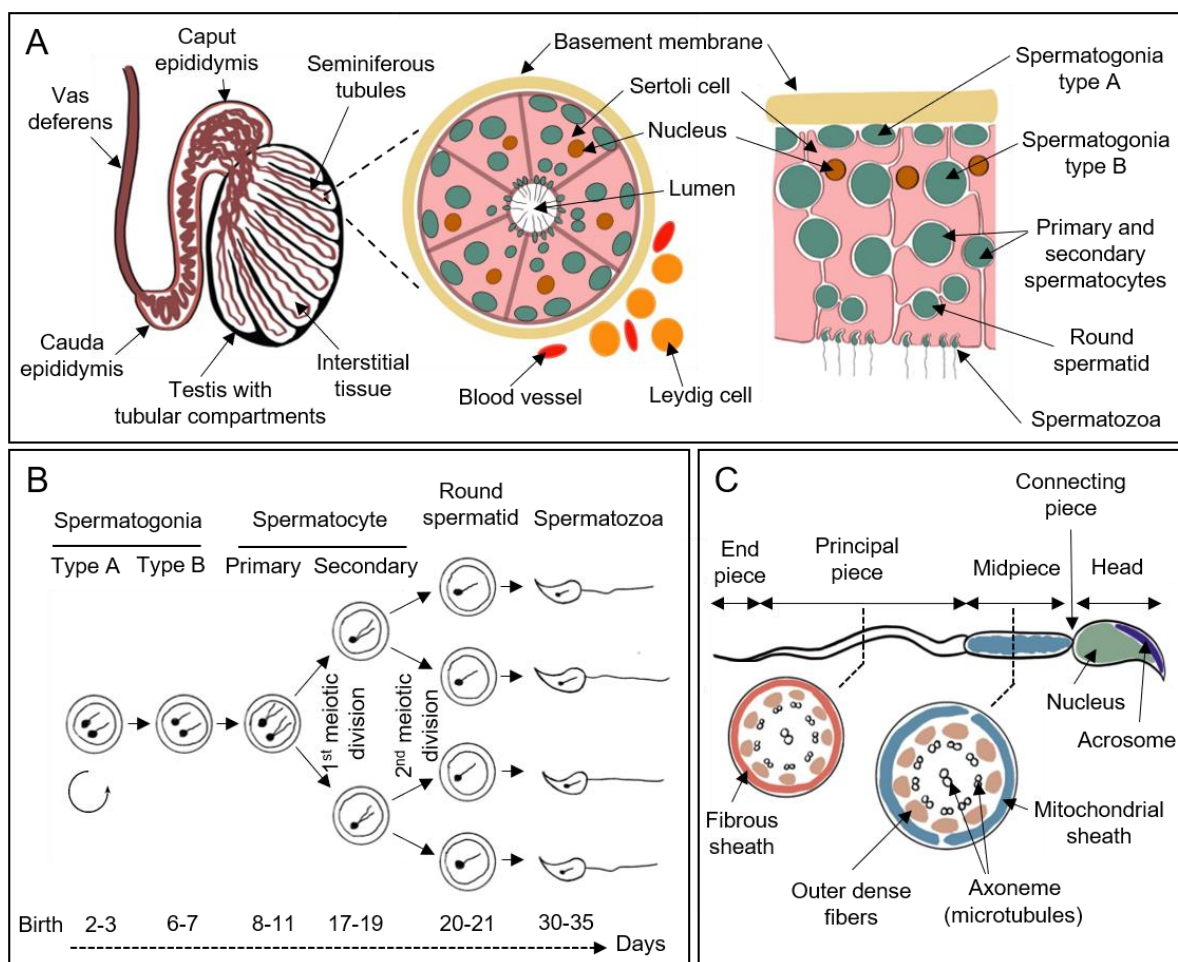


Figure 3: Organisation of the testis, spermatogenesis and spermatozoa morphology of the mouse. (Modified from [45, 50]). A) Schematic representation of the testis (left) which is composed of tubular compartments containing seminiferous tubules (composed of Sertoli cells) and interstitial tissue (with Leydig cells and blood vessels). The testis is extended by the epididymis and then by the vas deferens. The transversal section of a seminiferous tubule (centre) shows the arrangement of Sertoli cells through which spermatozoa transit to reach the lumen. A closer look at the Sertoli cells (right) shows spermatogonia type A cells in the apical region. The germ cells are in close contact with Sertoli cells that support spermatogenesis, which occurs during their transit to the lumen. B) Spermatogenesis is the process by which stem cells (spermatogonia type A, diploid) are transformed to spermatozoa (haploid) through meiosis and differentiation, with stem cell renewal occurring through mitosis. C) Schematic representation of a mature spermatozoon. The sperm head is approximately 8 μm long and the sperm flagellum (connecting piece, midpiece, principal piece and end piece) 122 μm long.

1.2.3 Endocrinology of the male reproductive system

The reproductive axis, also known as the hypothalamic-pituitary-testis axis (Figure 4), controls the secretion of testosterone and spermatogenesis. The hypothalamus is a central nervous system structure located on the ventral side of the third ventricle of the brain. It contains neurons that produce and secrete gonadotropin-releasing hormone (GnRH). GnRH stimulates the secretion of luteinizing hormone (LH) and follicle-stimulating hormone (FSH) by

gonadotropin-secreting cells in the anterior pituitary [51]. LH and FSH circulate in the bloodstream to act on the testis (Figure 4).

LH stimulates the Leydig cells to produce testosterone by increasing the levels of several proteins, in particular the steroidogenic acute regulatory protein (StAR). StAR is part of a complex that transports cholesterol from the outer mitochondrial membrane to the inner mitochondrial membrane where it is converted into testosterone [52].

FSH specifically stimulates Sertoli cells to produce androgen binding protein (ABP) as well as inhibin B, and it increases the sensitivity of Sertoli cells to testosterone. ABP increases testosterone levels by binding to testosterone in the seminiferous tubules when inhibin B acts on the pituitary gland to inhibit FSH secretion. The role of testosterone and FSH is to initiate and maintain spermatogenesis. In addition, testosterone is required for the development of the genital organs [30]. Finally, testosterone acts at the level of the hypothalamus and pituitary gland as a negative feedback to GnRH, LH and FSH secretion [53].

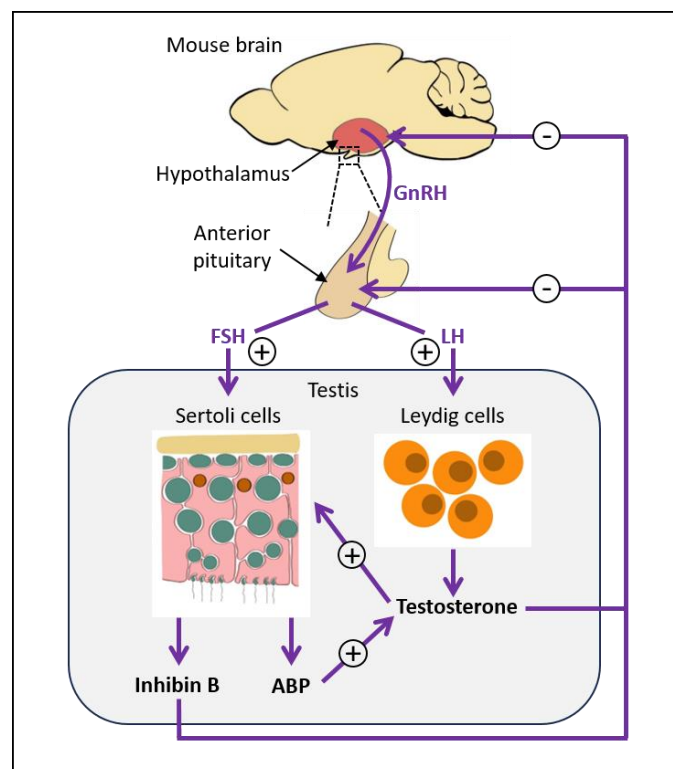


Figure 4: Hypothalamic-pituitary-testis axis in male mice. GnRH: gonadotropin-releasing hormone, LH: luteinizing hormone, FSH: follicle-stimulating hormone, ABP: androgen binding protein.

1.2.4 Spermatozoa morphology

Mouse spermatozoa are composed of two distinct compartments, the head and the tail (flagellum) (Figure 3C) [50]. The head is "hook-shaped" or falciform and consists of the nucleus and the acrosome, which is a secretory vesicle involved in the binding of the sperm to the zona

pellucida of the oocyte (Figure 2). The axoneme is the key component of the flagellar structure as it generates the force for sperm movement. It runs through the entire length of the flagellum as an array of microtubules (2 central singlet microtubules surrounded by 9 doublet microtubules). The sperm tail can be divided into 4 regions: the connecting piece (attached to the sperm head), the midpiece (containing all the sperm mitochondria wrapped in a spiral pattern), the principal piece (important for sperm propulsion) and the end piece (no structural elements other than the axoneme). Mouse spermatozoa are approximately 130 μm long.

Sperm morphology is considered as an important parameter in assessing fertility potential [54]. Therefore, the analysis of sperm morphology is part of the routine evaluation of semen quality, with a particular emphasis on the shape of the head, the straightness of the tail and the presence of a cytoplasmic droplet (residual sperm cytoplasm located on the tail removed during sperm maturation) [55]. Spermatozoa are considered abnormal if the head is amorphous and/or the tail is bent and/or in the presence of a heavy cytoplasmic droplet. In most cases, the cause of semen abnormalities has no medical explanation. However, testicular trauma and exposure to environmental pollutants and toxic agents can cause morphological defects [56, 57]. In addition to basic morphological assessment, ultrastructural analysis with transmission electron microscopy can be performed and provides valuable information about sperm motility and physiology [58].

1.2.5 Epididymal maturation of spermatozoa

Spermatozoa arriving in the lumen of seminiferous tubules are not yet functionally mature. They are transported into the epididymis (Figure 3A) by the testicular fluid secreted by the Sertoli cells and by peristaltic contractions. During their transit from the caput/head region to the cauda/tail region of the epididymis, they acquire motility and undergo important modifications necessary to fertilise the oocyte [59]. The exact mechanisms involved in the acquisition of motility are not well understood. Motility can be acquired by increasing intracellular cyclic adenosine monophosphate (cAMP), suggesting that the cAMP-dependent protein kinase pathway is involved [60]. In parallel with other pathways, sperm disulfide bond formation, which stabilises sperm structure and maintains flagellar straightness, is important for the acquisition of motility [61]. In addition to motility, important modifications of the sperm plasma membrane occur in the epididymis. These include changes in protein composition, particularly in the acrosomal region, and lipid composition, which contribute to an increase in membrane fluidity [62, 63]. Finally, the cauda epididymis is the site where spermatozoa are stored before being transported into the female tract during ejaculation.

Mouse sperm concentration and motility can be measured using a computerised sperm analyser. Normal sperm count varies with the genetic background, but an average of 1.8×10^6 spermatozoa per ejaculate for a volume of 3.2 μL are found in mice [64]. Motility is an important

criterion for assessing sperm quality [65, 66]. The threshold for normal total sperm motility (moving in any direction) is 40% and progressive motility (moving in a straight line) is 32% [30]. Moreover, to get a better idea of the quality of the spermatozoa, the viability assessment can be measured [67]. Immotile and live spermatozoa indicate structural defects in the tail, whereas immotile and dead spermatozoa are more likely to be associated with epididymal dysfunction [68]. Measurement of these parameters provides valuable information about testicular function and the ability of spermatozoa to reach the oocyte and penetrate the zona pellucida [30, 56].

1.2.6 Post-ejaculation sperm maturation

Spermatozoa that are deposited in the female reproductive tract are not yet competent for fertilisation since two final maturation steps are required: capacitation and the acrosome reaction [69]. Capacitation is characterised by hyperactivated motility, changes in sperm membrane architecture and activation of molecular mechanisms necessary for the acrosome reaction [70]. The first step is cholesterol depletion of the plasma membrane, leading to membrane destabilisation. This later leads to an increase in intracellular calcium (Ca^{2+}) and bicarbonate (HCO_3^-). This, in turn, triggers a signalling cascade involving increased generation of the second messenger cAMP, activation of protein kinase A (PKA), and tyrosine phosphorylation of several sperm proteins necessary for flagellum hyperactivity and plasma membrane remodelling. These mechanisms are essential to prepare for acrosomal exocytosis and zona pellucida recognition [71].

The acrosome reaction takes place after capacitation. It consists of fusion between the sperm plasma membrane and the underlying acrosomal membrane to release the acrosomal contents rich in digestive enzymes (e.g. acrosin and hyaluronidase) [72]. The acrosome reaction depends on an increase in intracellular Ca^{2+} concentration and pH, which is initiated during capacitation. A signalling cascade is then activated, in particular, the cleavage of phosphatidylinositol 4,5-bisphosphate (PIP_2) into diacylglycerol (DAG) and inositol triphosphate (IP_3). IP_3 activates actin-severing protein, which induces fusion of the acrosomal and plasma membranes [72]. The timing of the acrosome reaction has been controversial. However, it is now accepted that mouse spermatozoa lose their acrosome before penetrating the cumulus oophorus and reach the zona pellucida without an acrosome.

Sperm capacitation can be induced *in vitro* by placing spermatozoa in a capacitation medium [30]. The *in vitro* assessment of sperm capacitation and the acrosome reaction provides a good predictive analysis of sperm fertility. Among different techniques, detection of capacitated spermatozoa can be performed using the fluorescent probe chlortetracycline (CTC). It is widely used to differentiate between uncapacitated, capacitated-acrosome-intact and capacitated-acrosome-reacted spermatozoa based on the redistribution of the intracellular calcium in sperm head [73, 74]. For the acrosome reaction, basic staining with Coomassie

brilliant blue gave excellent results in identifying the presence of the acrosome (intense blue staining of the acrosome) and acrosome-reacted spermatozoa (absence of staining in the acrosomal region) [75].

1.2.7 Fertilisation

After penetrating the cumulus oophorus, spermatozoa bind to the zona pellucida. The glycoproteins ZP2 and ZP3 in the zona pellucida have been identified as sperm binding proteins [76]. Penetration of the zona pellucida requires the breakdown of this glycoprotein matrix by enzymes released after the acrosome reaction and hyperactivation to have the strength to reach the gamete. When the first spermatozoon penetrates the zona pellucida, its surface changes and becomes harder to inhibit the fusion of additional spermatozoa. The oocyte nucleus completes its meiosis and a nuclear membrane forms around the female and the male pronuclei, which move towards the centre. The membranes of the pronuclei break down and the chromosomes assemble on the spindle. The fertilised oocyte, or zygote, finally begins cell division 17 to 20 hours after fertilisation [30].

1.2.8 Function of reactive oxygen species in male reproduction

Reactive oxygen species, or ROS, are highly reactive molecules derived from oxygen and characterised by having unpaired electrons in their outer shell [77]. They can be divided into non-radical (2 electrons radical) and free radical (at least one free electron) species. The most common ROS are hydrogen peroxide (H_2O_2) and superoxide anion (O_2^-). H_2O_2 is a non-radical oxidant produced from O_2 and is recognised as the most important ROS involved in the redox regulation of biological activities. O_2^- is a free radical, well known to be a major source of H_2O_2 by spontaneous reaction or catalysed by the superoxide dismutase. Endogenous H_2O_2 and O_2^- are mainly produced in mitochondria through 2 mechanisms: 1- the electron transport chain (ETC), where oxygen is used to generate ATP, and 2- activity of NADPH oxidases (NOXs), present in different cellular localisations [77, 78]. Due to their instability and their need to reach a balanced state, ROS react with nearby organic molecules such as proteins, lipids and DNA. An excessive level of ROS induces oxidative stress, which is associated with reduced fertility due to lipid peroxidation of the sperm plasma membrane, cellular damage and apoptosis [79, 80]. However, at physiological concentrations, ROS act as signalling molecules and are crucial for normal sperm function [81]. More specifically, ROS are required for spermatogenesis by supporting spermatogonial stem cells pool self-renewal [82]. ROS are also essential for testicular sperm maturation, for the replacement of histones by protamines involved in chromatin condensation, for sperm motility by acting on disulfide bridges stabilising sperm flagella and for steroidogenesis by acting on Leydig cells [83-86]. Most importantly, ROS

is well known to be involved in capacitation, although the specific ROS implicated in this process are no yet known. ROS are necessary to promote plasma membrane remodelling as cholesterol depletion appears to be increased by capacitation-dependent oxidation of sterol [87]. It also activates adenylyl cyclase activity, which increases cAMP production and regulates tyrosine phosphorylation by activating protein kinase A and deactivating phosphatase [88]. Finally, ROS are involved in the acrosome reaction and sperm-oocyte fusion by increasing sperm membrane fluidity [78]. Therefore, a controlled redox balance is extremely important for normal male reproductive functions (Figure 5).

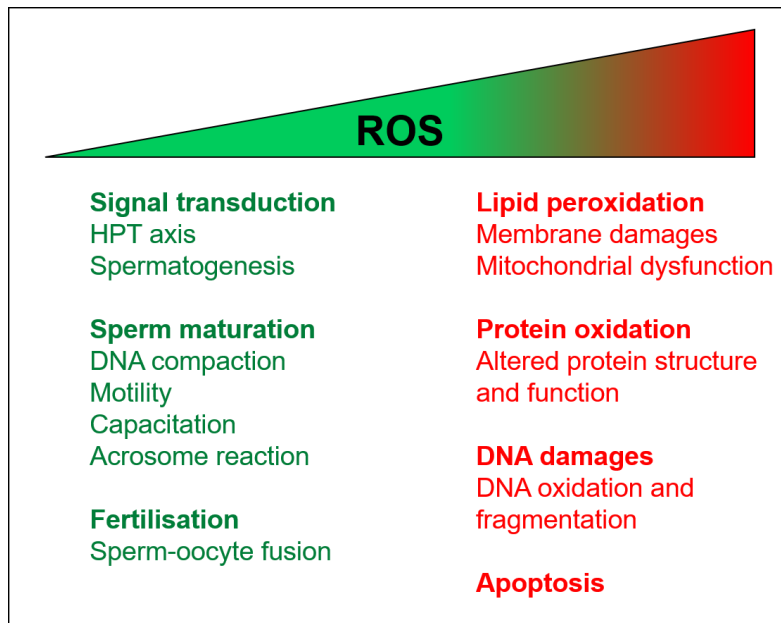


Figure 5: Physiological and pathological role of ROS in male fertility. (modified from [78]). HPT: Hypothalamic-pituitary-testis

1.3 Cryopreservation of spermatozoa

Sperm cryopreservation is the preferred method for archiving mouse lines in repositories. Live mice can be recovered from cryopreserved spermatozoa after IVF and embryo transfer as needed. Protocols for sperm cryopreservation are very recent compared to those for embryo cryopreservation and refinements are still needed to improve the workflow and limit sperm cryodamage.

1.3.1 History and principles of sperm cryopreservation

Cryopreservation is the process by which cells, including spermatozoa, are stored at a temperature below zero. Lazzaro Spallanzani first observed in 1776 that sperm from various

mammalian species cooled in snow could survive and continue swimming after warming. But it was not until 1949, with the discovery of glycerol as a cryoprotectant, that successful cryopreservation protocols emerged using spermatozoa from roosters [89]. Two years later, the first calves conceived by artificial insemination with sperm cryopreserved in dry ice (-80°C) were born. During 1953-1964, Sherman collected evidence of successful cryopreservation and long-term storage of sperm using LN₂ (-196°C) instead of dry ice [90]. In fact, long-term storage is only possible in the absence of cellular reaction and under metabolic arrest, which is achieved at a temperature of -196°C, where no biochemical activity can be detected due to insufficient thermal energy [91]. As a result, LN₂ was adopted for cryopreservation and storage of sperm and the use of cryopreserved sperm for artificial insemination became the norm in the livestock industry. In the 1970s and 1980s, major improvements were made in the cryopreservation of mouse embryos, particularly with the use of DMSO as a cryoprotectant. Unfortunately, the cryoprotective effect of glycerol and DMSO did not work effectively for the cryopreservation of mouse sperm, and for this reason the development of effective cryopreservation methods for mouse sperm took another ten years [44, 92]. Since then, important improvements have been made in the cryoprotectant, leading to the use of 18% raffinose and 3% skim milk [93, 94].

Cell survival during the cryopreservation process is largely dependent on the cooling rate (temperature per minute), which must be adjusted to avoid or minimise ice crystal formation. Slow cooling rate is a step cooling method, usually performed over a period of 2 to 4 hours, where the cooling rate is slow enough to avoid the formation of intracellular ice crystals. Ice occupies a larger volume than liquid water and its expansion causes pressure, which results in damage to intracellular organelles [95]. However, the cooling rate must also be fast enough to avoid extra-cellular ice formation. In fact, the relative reduction of extracellular water due to ice crystals creates a water flow from the inside of the cell to the outside, resulting in cell dehydration [96]. Alternatively, vitrification methods that require a higher cooling rate, such as direct immersion in LN₂, bypass ice formation with the formation of a glass-like structure instead [97].

The use of cryoprotectants helps to protect cells during the cooling process to limit intracellular ice formation [44]. Cryoprotectants have a much higher osmolarity (about 1,500 mOsm) compared to the cell (300 mOsm). This leads to an elimination of water from the cell and uptake of cryoprotectant, which equilibrates the osmotic pressure and eliminates the possibility of intracellular ice formation. As a result, cells undergo osmotic shrinkage, which can also damage the cell [98]. Therefore, the optimal cooling rate and the composition and concentration of cryoprotectants are key factors in the success of sperm cryopreservation.

1.3.2 Sperm cryopreservation protocol

The well-known Ostermeier protocol is widely used for mouse sperm cryopreservation (Figure 6) [99]. Spermatozoa collected from the cauda epididymis and vas deferens are placed in a cryoprotective medium (CPM) consisting of 18% w/v raffinose, 3% w/v skim milk and 477 μL of the antioxidant monothioglycerol (MTG) in water. Spermatozoa are allowed to disperse for 10 minutes, after which 10 μL of sperm+CPM are loaded into a 0.25 mL straw pre-filled with CPM. The straws are sealed and exposed to LN_2 on a floating raft for 10 minutes, resulting in a cooling rate of $37^\circ\text{C}/\text{min}$, before being immersed and stored in LN_2 . Alternatively, another technique of sperm cryopreservation developed by Nakagata laboratory, using cryoprotective medium with L-glutamine which stabilises the plasma membrane instead of the antioxidant MTG, is also commonly used [100].

To obtain optimal sperm concentration and quality, spermatozoa are usually collected from males at 13 weeks of age. In fact, although the first spermatozoa are seen in males as early as 5 weeks of age, they start to become sexually mature at 6-7 weeks [49, 101]. Finally, between 7 and 13 weeks of age, sperm concentration, motility and morphology increase, making the selection of 13-week-old males more appropriate [102, 103].

1.3.3 Sperm thawing protocol

Sperm samples that are cooled quickly by vitrification must be thawed quickly to avoid recrystallisation and cryodamage [104-106]. Therefore, in accordance with this principle, spermatozoa are quickly transferred from -196°C to 37°C , as described in the protocol of Ostermeier (Appendix 1). In brief, cryopreserved straws are removed from the LN_2 -tank, held in the air for 5 seconds and immersed in a water bath at 37°C for 30 seconds. The sperm sample is then transferred to the capacitation medium in a dish and incubated (37°C , 5% CO_2) for 1 hour before performing IVF.

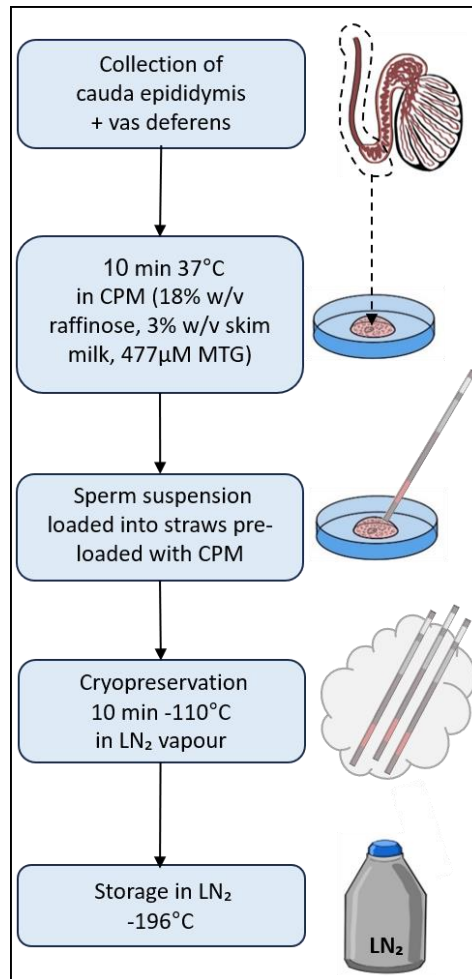


Figure 6: Mouse sperm cryopreservation protocol. Sperm cryopreservation with LN₂ protocol according to [99]. CPM: cryoprotective medium, MTG: monothioglycerol.

1.3.4 Sperm cryodamage

Cryopreserved spermatozoa undergo various morphological and physiological damages leading to reduced cell function or death (Figure 7). Among all the defects reported in cryopreserved spermatozoa, the decrease in motility, plasma membrane function and acrosome integrity are the most important post-thaw damages encountered [107, 108]. In particular, the sperm plasma membrane is exposed to major morphological changes due to the cryoprotectant, which alters the cell volume, and the physical freezing event, which destabilises the membrane and may cause the acrosome to disintegrate [106, 109]. Cryoinjuries to sperm DNA have also been reported such as DNA fragmentation, probably related to an increase in DNA oxidation [91, 106, 110]. Therefore, quantification of ROS and assessment of DNA fragmentation and oxidation can help in the analysis of sperm cryodamage [111]. Mitochondria in the spermatozoa are also susceptible to cryodamage, becoming swollen with a loss of cristae, as previously reported for rams [112] and mice [113]. Furthermore, the combination of high DNA fragmentation and mitochondrial damage is associated with reduced motility after human sperm cryopreservation [114].

Sperm cryodamage is known to be species-dependent and intra-species dependent [115, 116]. Different types and levels of sperm cryodamage are attributed to cellular morphology, membrane lipid content and composition, and cytoskeletal architecture [98, 115, 117]. Mouse strain differences toward sperm cryopreservation are also attributed to the genetic background and the strain-specific ability to undergo capacitation after cryopreservation-thawing procedures [118]. As a result, significant differences in sperm motility and IVF success rate are found between mouse lines after sperm cryopreservation [99, 115, 119].

1.3.5 LN₂-free alternative protocol for mouse sperm cryopreservation

Sperm is classically cryopreserved and archived in LN₂ for a duration of a few days to unlimited time [42]. Several reasons can make the use of LN₂ complicated. Because of its extremely low temperature, it is considered as a health hazard that can cause severe cold burns and permanent eye damage. In addition, LN₂ vapour can displace air and create an oxygen-deficient environment, leading to asphyxiation. Another important limitation is related to the availability of LN₂ in remote areas or during a worldwide crisis [119]. Finally, the limited storage capacity in LN₂ tanks (5 times less than in a freezer of comparable size) and the cost associated with transporting dry shippers make the use of ultra-low freezers and dry ice (-79°C) more appropriate and safer [120].

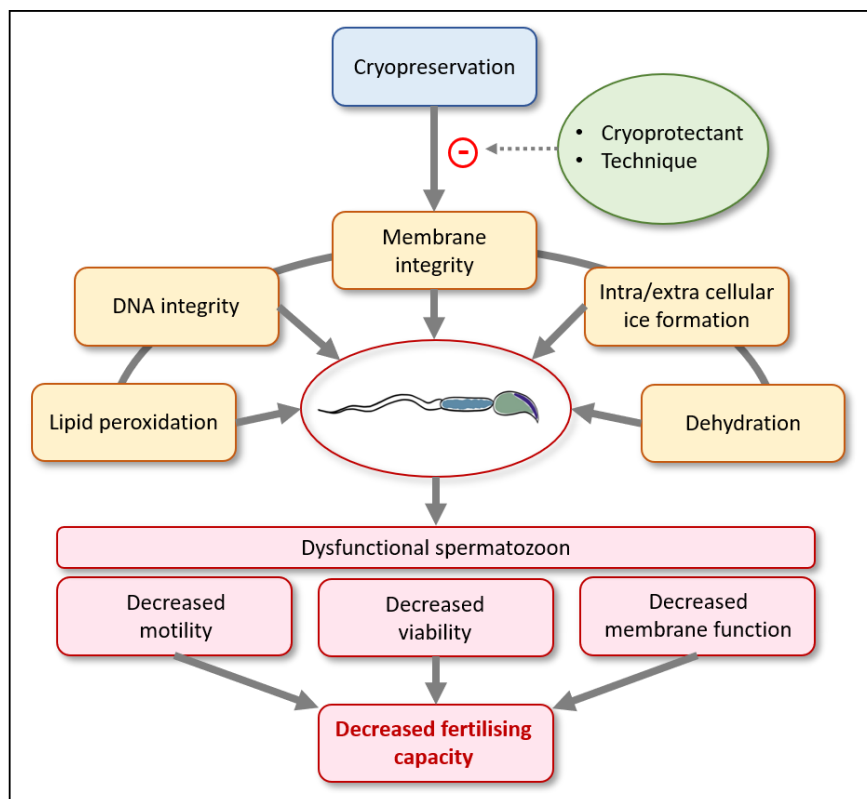


Figure 7: Schematic diagram of the detrimental effects of cryopreservation on sperm integrity leading to the decline in sperm function. (Modified from [121]).

Previous studies have reported successful attempts to cryopreserve and store sperm using -150°C freezers. Zebrafish sperm cryopreserved and stored for 3 months at this temperature maintained their motility, viability and fertility compared to LN_2 [122]. Bull and dog spermatozoa can be cryopreserved and stored at -152°C for up to 6 months and 12 months, respectively, without loss of motility, viability and morphology [123-125]. Successful attempts have also been reported with goat semen, which can be stored at -152°C for up to one year without significant changes in sperm quality and fertility [126, 127]. However, -150°C freezers are much less available on the market than -80°C freezers, their price is three times higher and their electricity consumption is five times higher. Moreover, there is no current means to maintain samples at this specific temperature for transport, unlike -80°C where dry ice can be used [128]. Although the temperature for sperm cryopreservation and storage should be less than -130°C , which corresponds to the glass transition point of water, to substantially slow biological process and minimize cell cryodamage [129, 130], successful attempts of sperm cryopreservation and/or storage at -80°C have been reported in humans [131], dogs [132], bulls [133] and aquaculture fish [134]. In cat, sperm motility, viability, membrane integrity and acrosome reaction were conserved after cryopreservation and storage at -75°C for 4 months [130]. In mice, LN_2 -cryopreserved spermatozoa from 6 different mouse genetic backgrounds were stored in ultra-low freezers (-80°C) for 7 days without affecting the fertilisation rate compared to storage in LN_2 [128]. Following this study, the same authors showed that spermatozoa from C57BL/6N, C57BL/6J and CD-1 mice cryopreserved in LN_2 can be stored at -80°C for 5 years in freezers with minimal effects on viability and no differences in the fertilisation rate [135]. It is also known that spermatozoa from C57BL/6N (control and mutant) can be cryopreserved by placing the samples at -80°C in ultra-low freezers instead of LN_2 and stored up to 12 months at -80°C without affecting the fertility rate [136]. Nevertheless, deeper insights are needed to unravel the potential integrity damage of spermatozoa cryopreserved and stored at -80°C .

1.3.6 Effect of D-aspartate on cryopreserved spermatozoa

Endogenous D-aspartate in male reproduction

The role of the amino acid D-aspartate or D-aspartic acid (D-Asp) on endocrine function and spermatogenesis has been extensively studied in rodents. Like most other amino acids, aspartic acid exists in 2 stereoisomers: the L-form and the D-form [137]. Because only L-aspartate is directly incorporated into protein, it was initially thought that the biological role of D-Asp was negligible [138]. Free D-Asp in vertebrate tissues may come from the diet through protein degradation and consumption of plants that are particularly rich in D-Asp [139]. There is also some evidence that D-Asp can be synthesised from L-Asp, supporting the idea of the

presence of D-Asp racemase in mammalian cells [140, 141]. D-Asp can be oxidised by D-aspartate oxidase, which converts D-Asp to oxaloacetate, NH_3 and H_2O_2 [142]. D-Asp can be methylated by N-methyl-D-aspartate synthase to N-methyl-D-aspartate (NMDA), a well-known and essential neurotransmitter and neuroendocrine regulator [143]. Although D-Asp receptors remain to be characterised, N-methyl-D-aspartate receptors (NMDARs) are known to respond to D-Asp and are found in rodent testis, spermatogonia and Leydig cells [144-146].

D-Asp has been found at high levels in mammalian neuroendocrine tissues, seminal plasma, spermatozoa and testes. The widespread presence of D-Asp in these regions supports the potential beneficial effect on rodent reproduction through hormone release and spermatogenesis [147-151]. D-Asp acts on the hypothalamus to stimulate the synthesis and release of GnRH, which in turn increases the level of LH, and thus the level of testosterone [152, 153]. D-Asp can also act directly on the anterior pituitary gland to stimulate the synthesis and release of LH with the participation of the second messenger cGMP (cyclic guanosine monophosphate) [154]. Leydig cells can also be stimulated directly by D-Asp to promote the production and release of testosterone by increasing the expression of StAR and using cAMP (cyclic adenosine monophosphate) as a second messenger [154-156].

D-aspartate treatment of cryopreserved spermatozoa

Previous studies have reported improvements in IVF success rate and cryopreserved sperm quality with *in vivo* D-Asp treatment in roosters [157], in men [158], in rabbits [159] and in mice [153, 160]. More specifically, Raspa *et al.* showed that D-Asp given orally to sexually immature B6N mice (7 weeks old) for 2 and 4 weeks improved the IVF success rate, the motility and the morphology of cryopreserved spermatozoa. However, it is not clear whether the results were influenced by the duration of D-Asp treatment (2 or 4 weeks) or the age of the animals (9 or 11 weeks, respectively, at the end of the treatment). More recently, Raspa *et al.* showed that oral administration of D-Asp for 2 or 4 weeks to B6N mice, aged 9 weeks and 16 weeks at the end of the treatment, improved the IVF success rate of cryopreserved spermatozoa in both age groups. These results make the use of D-Asp very promising for improving the fertility of cryopreserved mouse spermatozoa, thus increasing the efficiency of mouse lines recovery. D-Asp is also of particular interest for male mice that cannot reach the ideal age (13 weeks) for sperm cryopreservation.

Although the beneficial effect of D-Asp on sperm fertility has been well described, little is known about its mechanisms of action. It can presumably be attributed to the D-Asp effect on endocrine function and spermatogenesis that may lead to a higher IVF success rate. However, a direct effect of D-Asp on sperm quality has also been reported. Indeed, *in vitro* D-Asp treatment of cryopreserved spermatozoa is known to improve sperm parameters in cattle [161, 162], in men [163, 164] and in mice [165]. In particular, D-Asp is known to increase sperm

motility and fertility. These studies suggest a mechanism of action at the cellular level that directly improves the quality of cryopreserved spermatozoa to potentially improve IVF success rates. However, the precise mechanisms are unknown.

Interesting work by Chandrashekar and Muralidhara [166, 167] showed that excessive D-Asp intake in Wistar rats increased oxidative stress in the testes. In particular, they showed an increase in mitochondrial and cytoplasmic ROS and other markers of oxidative stress. This was accompanied by higher levels of lipid peroxidation and antioxidant enzymes (glutathione). In addition, D-Asp is known to increase the levels of nitric oxide, which is a free radical metabolite of L-arginine. This last observation was also found in D-Asp-treated boar testes [168]. All of these findings suggest that D-Asp is involved in the increase of ROS production. As previously mentioned (section 1.2.8), a physiological concentration of ROS supports male reproductive functions. Knowing that a moderate increase in oxidants can improve health and longevity [169-171], it may also be possible that a moderate increase in ROS improves sperm parameters. Therefore, the beneficial effect of D-Asp on sperm quality and fertility may be due to a moderate elevation of ROS.

2. Thesis aims

Mouse assisted reproductive technologies are constantly evolving to provide the most efficient, most cost-effective and safest techniques. Cryopreservation of spermatozoa from laboratory mice has only become efficient in the last two decades due to the poor survival rate of sperm cryopreserved in early attempts. Although much progress has been made, cryopreservation methods need to be further improved and simplified to maximise the affordability and success rate of IVF. My Ph.D. thesis addressed these issues, focusing on two complementary approaches to: 1- increase sperm fertility after cryopreservation with the use of D-Asp and 2- reduce the logistical burden associated with sperm cryopreservation by using a LN₂-free cryopreservation and storage method.

Aim 1: To characterise the effects of D-aspartate on the fertility and quality of cryopreserved mouse spermatozoa and the mechanisms involved

An important gap exists in fertility and quality between fresh and cryopreserved spermatozoa, mainly due to cryoinjury. Therefore, there is still room for improvement in limiting sperm cryodamage and increasing the fertilising ability of cryopreserved spermatozoa. D-Asp treatment given orally to mice has been shown to improve IVF success rates following sperm cryopreservation. However, it is not clear whether this was influenced by the age of the animals and/or the duration of the treatment. In addition, little is known about the mechanisms of action of D-Asp. The first objective of this thesis was to investigate the effect of an oral D-Asp treatment (2 or 4 weeks) on cryopreserved spermatozoa in B6N male that were younger (9 weeks at the end of the treatment) and older (16 weeks at the end of the treatment) than the usual age for sperm cryopreservation (13 weeks).

Then, the possibility that the beneficial effect of D-Asp on cryopreserved spermatozoa relies on a mild increase in oxidants was investigated. To this end, the levels of ROS in cryopreserved spermatozoa following *in vivo* and *in vitro* D-Asp treatment and the level of sperm DNA oxidation were assessed. An antioxidant treatment was also used to quench ROS and functionally test their contribution to the beneficial effects of D-Asp in sperm maturation.

Aim 2: To evaluate the fertility and quality of mouse spermatozoa cryopreserved and stored at -80°C

LN₂ is commonly used for cryopreservation and storage of laboratory mouse spermatozoa. However, the use of an alternative to LN₂ has huge advantages such as simplifying and reducing the cost of sample transport, limiting the risk of accidents to operators and allowing the storage of a higher number of straws at lower costs. Therefore, the possibility to avoid LN₂ and simplify the process of sperm cryopreservation and storage without causing

additional cryodamage would be a major advancement in the field of mouse assisted reproductive technology. The purpose of Aim II was to compare the effects of sperm cryopreservation and long-term storage in LN₂ versus -80°C freezers. As sperm damage can vary between strains, six different mouse strains among the most commonly used in biomedical research, were analysed. Sperm fertility, viability, motility and morphology were assessed. In addition, ultrastructural damages and the level of DNA fragmentation were investigated to provide valuable information about cellular integrity.

Finally, given the potential of D-Asp to improve the quality of LN₂-cryopreserved spermatozoa, D-Asp treatment was also applied to spermatozoa, which were most severely affected by cryopreservation and storage at -80°C. Therefore, the combination of both approaches, increasing sperm fertility and improving logistics, would greatly enhance the efficiency of the sperm cryopreservation workflow for archiving mouse lines.

3. Materials and Methods

3.1 Materials

3.1.1 Equipment

Name	Model/Product no.	Manufacturer
Bright-field microscope	314652	Leica Microsystems, Wetzlar, Germany
Centrifuge	Z216MK	Hermle, Wehingen, Germany
CO ₂ incubator	MCO-20AIC	Sanyo-Biomedical, Ewald Innovationstechnik GmbH, Bad Nenndorf, Germany
Electrophoresis power supply	PowerPac Basic	Bio-Rad, München, Germany
Epifluorescence microscope	Olympus IX83	Olympus, Hamburg, Germany
Flow cytometry system	FACSCanto II	BD Diagnostics, Franklin Lakes NJ, USA
Heating plate	12511	Medax, Olching, Germany
Individually Ventilated Cages (IVCs)	GM500	Tecniplast, Gazzada, Italy
LN ₂ -tank	MVE SC 36/32	Chart industries, Ball Ground GA, USA
pH meter	Doc-pH meter	Sartorius, Goettingen, Germany
Sperm analyzer	Hamilton Thorne IVOS	Hamilton Thorne, Beverly, MA, USA
Stereomicroscope	C-DSS230	Nikon Instruments Inc, Melville NY, USA
Thermoshaker	RH B 2 S000	IKA, Staufen, Germany
Transmission electron microscope	JEM2100PLUS	JOEL, Freising, Germany
Ultra-low temperature freezer	MDF-U73V	Sanyo-Biomedical, Ewald Innovationstechnik GmbH, Bad Nenndorf, Germany
Ultramicrotome	EM UC7	Leica Microsystems, Wetzlar, Germany
Vortex	Vornado	Benchmark scientific, Sayreville NJ, USA
Water bath	Sonorex Super RK 100H	Bandelin, Berlin, Germany

3.1.2 Consumables

Name	Product no.	Manufacturer
Counting chamber 100 micron	SC 100-01-02-B-CE	Leja Products BV, Nieuw-Venep, The Netherlands
81 place polypropylene freezer boxes	88520011	Sigma-Aldrich, Taufkirchen, Germany

Materials and Methods

Cassettes for spermatozoa	16980/0601	MTG Medical Technology, Bruckberg, Germany
Coverslip	LH26.1	Carl Roth, Karlsruhe, Germany
Disposable wipes KIMTECH	P502.4	Carl Roth, Karlsruhe, Germany
Electrophoresis chamber	Mini-Sub Cell GT	Bio-Rad, München, Germany
Falcon 15 mL tube	352096	Corning, Glendale AZ, USA
Falcon 50 mL tube	352070	Corning, Glendale AZ, USA
Fine scissors	FSCI14095-11	VWR, Radnor PA, USA
Forceps	232-0188	VWR, Radnor PA, USA
Forceps, straight	232-0094	VWR, Radnor PA, USA
Metal Sealing Ball 0.25 mL	13400/9970	Minitube, Tiefenbach, Germany
Needle 27G x 3/4"	4657705	Braun, Melsungen, Germany
Pipette 0.5-10µl	3123000020	Eppendorf, Hamburg, Germany
Pipette 10-100µl	3123000047	Eppendorf, Hamburg, Germany
Pipette 20-200µl	3123000055	Eppendorf, Hamburg, Germany
Pipette 100-1000µl	3123000063	Eppendorf, Hamburg, Germany
Pipette tips 0.1-10µl	613-1093	VWR, Radnor PA, USA
Pipette tips 1-200µl	613-1092	VWR, Radnor PA, USA
Pipette tips 100-1250µl	613-1087	VWR, Radnor PA, USA
Poly-lysine-coated glass slides	631-0107	VWR, Radnor PA, USA
Serological Pipette 2 mL	75816-104	VWR, Radnor PA, USA
Serological Pipette 10 mL	75816-100	VWR, Radnor PA, USA
Serological Pipette 25 mL	75816-090	VWR, Radnor PA, USA
Serological Pipette 50 mL	75816-088	VWR, Radnor PA, USA
Straw, EcoPaillette transparent 0.25 mL	13407/3010	Minitube, Tiefenbach, Germany
Syringe 1 mL	300013	BD Diagnostics, Franklin Lakes NJ, USA
Tissue culture dish 35 mm	734-2317	VWR, Radnor PA, USA
Tissue scissors, micro	HAMMHSB556-18	VWR, Radnor PA, USA
Tube 0.5 mL	7060.1	Carl Roth, Karlsruhe, Germany
Tube 1.5 mL	7805 00	BRAND, Wertheim, Germany
Tube 2 mL	EA85.1	Carl Roth, Karlsruhe, Germany
Tube 5 mL	30119401	Eppendorf, Hamburg, Germany

3.1.3 Chemicals, reagents, solutions

Name	Product no.	Manufacturer
Ammonium acetate	CC585416	Merck, Darmstadt, Germany
Acetic acid	3738.4	Carl Roth, Karlsruhe, Germany
Acetone	179124	Sigma-Aldrich, Taufkirchen, Germany
Aqueous anti-fading mounting medium with DABCO	10981	Sigma-Aldrich, Taufkirchen, Germany
BSA	A4503	Sigma-Aldrich, Taufkirchen, Germany

Materials and Methods

CARD FERTIUP PM 0.5 mL - CARD MEDIUM Set	KYD-005-EX	Cosmo Bio USA, Carlsbad CA, USA
Citric acid	251275	Sigma-Aldrich, Taufkirchen, Germany
Cook's medium	K-RVFE-50	Cook Medical, Brisbane, Australia
Coomassie brilliant blue G- 250, ready-to-use	786-497	VWR, Radnor PA, USA
CTC-HCl	C4881	Sigma-Aldrich, Taufkirchen, Germany
DAPI	D9542	Sigma-Aldrich, Taufkirchen, Germany
D-Aspartic acid	219096	Sigma-Aldrich, Taufkirchen, Germany
DHE	D7008	Sigma-Aldrich, Taufkirchen, Germany
DMSO	D8418	Sigma-Aldrich, Taufkirchen, Germany
DPBS	D8537	Sigma-Aldrich, Taufkirchen, Germany
DTT	D9779	Sigma-Aldrich, Taufkirchen, Germany
Ethanol 70	T913.2	Carl Roth, Karlsruhe, Germany
Ethanol absolute	34852	Sigma-Aldrich, Taufkirchen, Germany
hCG (Ovogest 300 IU/mL)	A265A01	MSD, Rahway NJ, USA
HCl 1N	1.09057.1000	Merck, Darmstadt, Germany
HEPES	25245.03	Serva, Heidelberg, Germany
Hoechst 33342	62249	ThermoFisher Scientific, Waltham, Germany
HTF	MR-070-D	Merck, Darmstadt, Germany
KCl		
L-cystein	168149	Sigma-Aldrich, Taufkirchen, Germany
L-glutathione reduced	G4251	Merck, Darmstadt, Germany
M16 medium	M7292	Sigma-Aldrich, Taufkirchen, Germany
M2 medium	M7167	Sigma-Aldrich, Taufkirchen, Germany
Methanol	1.00837.1000	Merck, Darmstadt, Germany
Monothioglycerol (MTG)	M6145	Sigma-Aldrich, Taufkirchen, Germany
Mounting medium Roti- Histokitt	6638.1	Carl Roth, Karlsruhe, Germany
N-Acetyl-L-Cysteine	A7250	Sigma-Aldrich, Taufkirchen, Germany
NaCl powder	S9888	Sigma-Aldrich, Taufkirchen, Germany
NaOH pellets	221465	Sigma-Aldrich, Taufkirchen, Germany
Normal Goat Serum	S26	Sigma-Aldrich, Taufkirchen, Germany
Paraffin oil	76235	Sigma-Aldrich, Taufkirchen, Germany
PFA 4% (roti-histofix 4%)	P087.4	Carl Roth, Karlsruhe, Germany
PMSG	OPPA01037	Aviva systems biology, San Diego CA, USA
Proteinase K	1.24568.0100	Sigma-Aldrich, Taufkirchen, Germany
Raffinose	R7630	Sigma-Aldrich, Taufkirchen, Germany
Skim milk	232100	BD Diagnostics, Franklin Lakes NJ, USA
Sodium phosphate dibasic	S9763	Sigma-Aldrich, Taufkirchen, Germany
Sodium phosphate monobasic monohydrate	S9638	Sigma-Aldrich, Taufkirchen, Germany
Tris-EDTA buffer solution	93302	Sigma-Aldrich, Taufkirchen, Germany
Tris-HCl	9090.2	Carl Roth, Karlsruhe, Germany
Triton X-100	X100	Sigma-Aldrich, Taufkirchen, Germany

3.1.4 Other

Antibodies

Name	Product no.	Manufacturer
biotin mouse monoclonal [15A3] to DNA/RNA Damage	ab183395	Abcam, Cambridge, UK
Streptavidin Alexa Fluor 555 conjugated	S21381	ThermoFisher Scientific, Waltham, Germany

Kits

Name	Product no.	Manufacturer
LIVE/DEAD® Sperm Viability Kit from Molecular Probe	L7011	ThermoFisher Scientific, Waltham, USA
Single cell gel electrophoresis (comet Assay)	ab238544	Abcam, Cambridge, UK

Mouse diet

Name	Product no.	Manufacturer
Standardized diet	4RFN and Emma 23	Mucedola, Settimo Milanese, Italy

Software

Name	Manufacturer
FlowJo	BD Diagnostics, Franklin Lakes NJ, USA
ImageJ	Open source, National Institutes of Health, Bethesda, Maryland, USA
GraphPad Prism 7	Graphpad Software, Inc., La Jolla, USA
Excel 2010	Microsoft, Redmont, USA

3.1.5 Buffers and solutions

Cryoprotective medium 100 mL	
Raffinose	18% (18 g)
Skim milk	3% (3 g)
Monothioglycerol	477 μ M (5.16 mg)
in sterile water	

CTC solution 100 mL	
CTC-HCl	750 μ M (38.65 mg)
NaCl	130 mM (759.7 mg)
L-cystein	5 mM (61 mg)
Tris-HCl	20 mM (315 mg)
in distilled water	
pH 7.8	

Flow cytometry: HEPES-buffered saline solution 100 mL

HEPES	10 mM (238.3 mg)
NaCl	150 mM (876.6 mg)
BSA	2% (2 g)
in distilled water	
pH 7.4	

Immunostaining: saturation buffer 50 mL

NGS	1.5% (750 µL)
Triton X-100	0.1% (50 µL)
in PBS 1X	

Immunostaining: decondensation buffer 100 mL

DTT	0.2 mM (3.1 mg)
Triton X-100	0.5% (500 µL)
in PBS 1X	

Comet: lysis buffer 100 mL

NaCl	14.6 g
EDTA solution (provided in the kit)	20 mL
10X lysis solution (provided in the kit)	10 mL
DMSO	10 mL
in distilled water	
pH 10	

Comet: alkaline solution 500 mL

NaOH	6 g
EDTA solution (provided in the kit)	1 mL
in distilled water	

PBS 10X, 1 L

Sodium phosphate monobasic monohydrate ($\text{NaH}_2\text{PO}_4 \cdot \text{H}_2\text{O}$)	0.02 M (3.2 g)
Sodium phosphate dibasic (Na_2HPO_4)	0.08 M (14.24 g)
NaCl	9% (90 g)
in distilled water	
pH 7.4	

PBS 1X, 1 L

PBS 10X	100 mL
Distilled water	900 mL

PB 10X, 1 L

Sodium phosphate monobasic monohydrate ($\text{NaH}_2\text{PO}_4 \cdot \text{H}_2\text{O}$)	0.02 M (3.2 g)
Sodium phosphate dibasic (Na_2HPO_4)	0.08 M (14.24 g)
in distilled water	
pH 7.4	

PB 1X, 1 L

PB 10X	100 mL
Distilled water	900 mL

3.2 Methods

3.2.1 Mice

Males from six mouse strains were used: C57BL/6NTacCnrm (B6N), C57BL/6JCnrm (B6J), BALB/cByJCnrm (BALB/c), Crl:CD1(ICR) (CD-1), FVBN/JCnrm (FVB) and 129/SvImJCnrm (129). All mice were housed under controlled environmental conditions (temperature $20 \pm 2^\circ\text{C}$, 12 h light period: 7am-7pm, relative humidity of $55 \pm 15\%$) in individually ventilated cages. They were bred at the Consiglio Nazionale delle Ricerche - European Mouse Mutant Archive (CNR-EMMA) (Monterotondo Scalo, Rome, Italy), fed a standardised diet *ad libitum* and given free access to chlorinated filtered water. Every 3 months, 6- to 8-week-old B6N sentinels were examined for infectious agents according to the FELASA recommendations [172]. The Animal Care and Use Committee of the CNR-EMMA approved these animal studies (protocol number 0000079 of 18 January 2016). Protocols and experiments followed general guidelines approved by the Italian Ministry of Health (Legislative Decree 26/2014 and 116/1992) and ARRIVE guidelines [173]

Experimental Design

All information on the number of mice used and the summary of analyses are presented in Table 2.

In Aim I, a total of 18 B6N males were used for *in vivo* D-Asp treatment. For each of the two age groups of 9 or 16 weeks, 3 males were used per group (i.e. control, 2 weeks or 4 weeks of D-Asp treatment). Sperm concentration, motility, morphology, capacitation rate, acrosome reaction rate, ROS production and DNA oxidation were determined using these samples.

For the *in vitro* part of Aim I, 5 B6N males were sacrificed at the age of 9 or 16 weeks, giving a total of 10 B6N mice used. Sperm was collected individually from each male. After *in vitro* D-Asp treatment, ROS production and DNA oxidation were determined. In addition, co-

incubation of D-Asp and the antioxidant NAC was performed, followed by analysis of capacitation and acrosome reaction.

In Aim II, B6N, B6J, BALB/c, CD-1, FVB and 129 male mice at the age of 3 months were used. The spermatozoa from 3 males from each strain were pooled during sperm collection, for a total of 18 mice used for this experiment. Spermatozoa were cryopreserved either using the standard method (LN₂) or at -80°C. After 1, 3, 6, 9 or 12 months of storage in LN₂ or at -80°C, *in vitro* fertilisation and viability analysis were performed. Sperm motility, morphology, ultrastructural damage and DNA fragmentation were also determined after 1, 6 or 12 months in LN₂ or at -80°C.

Finally, B6N, B6J and BALB/c spermatozoa cryopreserved and stored in LN₂ or at -80°C for 9 months were treated with D-Asp. Motility, morphology, capacitation rate and acrosome reaction rate were assessed.

3.2.2 Sperm collection, cryopreservation and thawing procedures

Sperm collection

After cervical dislocation, the cauda epididymis and the vas deferens of each male were collected, cleaned of fat and placed into a sperm collection dish containing 120 µL of cryoprotective medium (CPM: 18% raffinose, 3% skim milk, 477 µM MTG in water [99] warmed up to 37°C on a heating plate. Using a small pair of scissors, the cauda epididymis was incised 6 times to release the spermatozoa. After 10 min at 37°C on the heating plate, drops of 10 µL of sperm suspension were placed in a new dish. Each drop was aspirated into a 0.25 mL straw pre-filled with CPM. The straws were then sealed with a metal ball.

Cryopreservation: standard method using LN₂ (-196°C)

After sealing, straws containing the sperm suspension were exposed to LN₂ vapour for 10 min, collected in cassettes, immersed in LN₂ and stored in a LN₂-tank until used.

Cryopreservation: alternative (-80°C)

After sealing, straws were collected in cassettes and placed directly in an ultra-low freezer at a temperature of -80°C. After 1, 3, 6, 9 or 12 months at -80°C, the straws were thawed and used for analysis or placed in a LN₂-tank for longer storage without degradation.

Table 2: Overview of the experimental design

Mice					Treatment			Analyses
Strain	Age	Number	Total number	Type	Duration	Groups		
Aim I								
B6N	9-week-old	9	18	D-Asp <i>in vivo</i>	2 or 4 weeks	Control 2 weeks D-Asp 4 weeks D-Asp	Sperm concentration Motility Morphology Capacitation rate Acrosome reaction rate ROS production DNA oxidation	
B6N	16-week-old	9						
B6N	9-week-old	5	10	D-Asp <i>in vitro</i>	1 h or 5 h	Control 1 h D-Asp 5 h D-Asp	ROS production DNA oxidation Co-incubation D-Asp + NAC	
B6N	16-week-old	5						
Aim II								
B6N		3						
B6J		3						
BALB/c	13-week-old	3	18	Cryopreservation and storage in LN ₂ or at -80°C	1 month 3 months 6 months 9 months 12 months	1 month LN ₂ / -80°C 3 months LN ₂ / -80°C 6 months LN ₂ / -80°C 9 months LN ₂ / -80°C 12 months LN ₂ / -80°C	IVF Viability Motility Morphology Ultrastructure damages DNA fragmentation	
CD-1		3						
FVB		3						
129		3						
B6N		Same mice as above						
B6J	13-week-old	(LN ₂ or -80°C, 9 months)		D-Asp <i>in vitro</i>	1h	LN ₂ Control LN ₂ 1 h D-Asp -80°C Control -80°C 1 h D-Asp	Motility Morphology Capacitation rate Acrosome reaction rate	
BAL/c								

Thawing procedure

For thawing, straws were removed from the LN₂-tank or the ultra-deep freezer depending on the storage method, held in the air for 5 seconds and placed into a 37°C water bath for 30 sec. The contents were then transferred into a pre-warmed 1.5 mL sample tube. The spermatozoa were kept at 37°C in a CO₂ incubator (moisture-saturated atmosphere of 5% CO₂ and 95% air) for 10 min to allow dispersion of the spermatozoa. The samples were then transferred to a pre-warmed 1.5 mL tube containing 200 µL of IVF medium (Cook's medium) and incubated for 1 h at 37°C in a CO₂ incubator, except for samples that received an *in vitro* D-Asp treatment (see section 3.2.3. below).

3.2.3 D-Asp treatment

In vivo D-Asp treatment

A solution of 1 M D-Asp was first prepared and diluted in drinking water to give a concentration of 20 mM of D-Asp with a final pH of 6.6 - 7.5 in the drinking bottle. Male mice 7 or 5 weeks old (young) were treated for 2 or 4 weeks, respectively, so that they were 9 weeks old at the end of the treatment. Male mice aging 14 or 12 weeks (adult) were also treated for 2 or 4 weeks, respectively, so that they were 16 weeks old at the end of the treatment. Control mice received D-Asp-free drinking water.

In vitro D-Asp treatment

A solution of 4 mM of D-Asp (pH of 7.5 - 7.8) in Cook's medium was prepared the day before and incubated overnight at 37°C in a CO₂ incubator. After thawing and 10 minutes incubation at 37°C in a CO₂ incubator, half of the spermatozoa was transferred into a 1.5 mL tube with 200 µL of Cook's medium and used as the control group. The other half was transferred into a 1.5 mL tube with 200 µL of 4 mM D-Asp and designated as the D-Asp-treated group. Both tubes were incubated at 37°C for 1 h corresponding to the capacitation period or for 5 h corresponding to the period for co-incubation of the oocytes and spermatozoa used for the IVF procedure.

3.2.4 Spermatozoa analyses

In vitro fertilisation

Four-week-old female mice were superovulated with 5 IU PMSG 72 h before sacrifice and with 5 IU hCG 12 h before sacrifice. Straws containing spermatozoa were removed from the LN₂-tank, held 5 sec in LN₂ vapour, held at RT for 5 sec and then placed in a water bath at

37°C for 10 min. The straws were then carefully dried with a disposable wipe and the spermatozoa were placed in a dish containing 90 µL of IVF medium (250 µL HTF with 1 mM reduced L-glutathione and 5.14 mM Ca²⁺) covered with paraffin oil prepared the day before (kept overnight at 37°C in a CO₂ incubator). During capacitation for 1 h at 37°C in a CO₂ incubator, the COCs were collected from the females and placed in the CARD medium. A volume of 5 µL of sperm was added to the dish with the COCs. After incubation of the oocytes with the spermatozoa for 5 h at 37°C in a CO₂ incubator, the oocytes were washed 3 times in drops of 100 µL of M2 medium and then transferred to M16 medium for an overnight incubation at 37°C in a CO₂ incubator. The IVF success rate is given as the percentage of 2-cell embryos developing from the total number of oocytes co-incubated.

Viability assessment – Flow cytometry with SYBR-14 and PI

The viability of mouse spermatozoa was assessed by FACSCanto II flow cytometry. SYBR-14 is a permeable DNA-binding dye that emits at 516 nm when bound to DNA. It stains the nuclei of living cells green, whereas propidium iodide (PI) is an impermeable DNA-binding dye that stains cells red (maximum emission at 617 nm) when they have lost their membrane integrity. Cryopreserved spermatozoa were thawed as previously described. The sperm samples were then diluted in HEPES-buffered saline to a concentration of 1x10⁶ cells/mL and incubated with 1 µg/mL Hoechst 33342 at 37°C for 10 min. The samples were then centrifuged at 1,000 g for 6 min, and the pellet was re-suspended in HEPES-buffered saline (1x10⁶ cells/mL). A volume of 5 µL of diluted SYBR-14 dye was added to a final concentration of 100 nM. After 5 min incubation at 37°C, 5 µL PI was added to a final concentration of 12 µM. After 3 min incubation, the sample was analysed by flow cytometry. A 488 nm blue laser was used for SYBR 14 and PI excitation and a 405 nm violet laser for Hoechst 33342. FlowJo software was used to analyse the data (10,000 events analysed, 3 replicates). Hoechst 33342-negative cells were excluded from the analysis. Only SYBR 14-negative and PI-positive spermatozoa are considered dead. Results are expressed as percentage of dead cells in the population analysed.

Sperm concentration and motility

Spermatozoa were thawed and allowed to disperse with or without D-Asp for 1 h at 37°C as described previously. After gentle mixing of the sample, a 2 µL aliquot of the sperm suspension was diluted with 98 µL pre-warmed Cook's medium. A volume of 30 µL of the diluted sample was loaded on each chamber of a two-chamber slide, and sperm motility patterns were analysed using the Hamilton Thorne IVOS computerised sperm analyzer operating at 30 video frames per second (60 Hz). The concentration was reported as millions of spermatozoa per millilitre. Total motility (motile spermatozoa moving at a velocity > 7.4 µm/s

in any direction), progressive motility (spermatozoa with a path velocity > 50 $\mu\text{m/s}$ and a straightness ratio > 80%) and sperm velocity categorized into rapid (mean velocity > 50 $\mu\text{m/s}$), medium (7.4 $\mu\text{m/s}$ < mean velocity \leq 50 $\mu\text{m/s}$), slow (0 $\mu\text{m/s}$ < mean velocity \leq 7.4 $\mu\text{m/s}$) and static (mean velocity = 0 $\mu\text{m/s}$) were reported as percentages of spermatozoa showing the respective trait from the total number of spermatozoa analysed.

Sperm morphology

For morphological investigation, 10,000 spermatozoa were collected and centrifuged at 300 g for 5 min. The pellet was then washed with PBS 1X and centrifuged again at 300 g for 5 min. The supernatant was removed, and 10 μL of PBS 1X was added to re-suspend the pellet. The sample was smeared onto a glass slide, air dried for 1 h, covered with mounting medium and examined under a bright field microscope at a magnification of 40 X. The morphology of the head and the tail was examined from 200 spermatozoa. They were classified as normal (normal head and normal tail), abnormal head with normal tail, abnormal tail with normal head, abnormal head and abnormal tail and finally head detached.

Capacitation rate – Chlortetracycline (CTC) staining

The capacitation rate is the percentage of spermatozoa that are capacitated. Chlortetracycline (CTC) fluorescence staining was used to assess whether spermatozoa had undergone capacitation. After spermatozoa were thawed and allowed to disperse with or without D-Asp for 40 min at 37°C, 10 μL of Hoechst 33342 (9 $\mu\text{g/mL}$) was added to an aliquot of 60,000 spermatozoa. The sample was then returned to the incubator for a further 20 min, for a total incubation time of 1 h. The sample was then centrifuged at 2,000 g for 5 min, the supernatant was removed and the pellet was mixed with 30 μL of Cook's medium. An equal volume of CTC solution (30 μL) was added, and the sample was gently mixed for 20 sec. Then 10 μL of 4% paraformaldehyde was added. After 10 min at RT, the sample was centrifuged at 2,000 g for 5 min, the pellet was suspended in 30 μL of Cook's medium and transferred to 3 glass slides (10 μL sperm suspension per slide). When the slide was dried, a coverslip was added with an aqueous anti-fading mounting medium with DABCO. Images were taken with an epifluorescence microscope at 100X using a FITC filter (excitation 491 nm / emission 516 nm) and a DAPI filter (excitation 359 nm / emission 457 nm). The pattern of fluorescence given with a CTC staining depends on the localization of the intracellular calcium in sperm head that changes during capacitation [74]. Cells with a uniform green fluorescent head were considered as not capacitated, and cells with a non-fluorescent band in the post-acrosomal region were considered as capacitated. At least 200 spermatozoa were counted per assay.

Acrosome reaction rate – Coomassie brilliant blue staining

The acrosome reaction is the second step in sperm maturation, after capacitation. Because the acrosome reaction corresponds to the fusion between the acrosome membrane and the plasma membrane, spermatozoa are losing their acrosome during acrosome reaction, resulting in a loss of staining [133]. The acrosome reaction rate represents the percentage of spermatozoa without their acrosome. After the spermatozoa were thawed and allowed to disperse with or without D-Asp for 1 h at 37°C, 60,000 spermatozoa were collected and centrifuged at 1,500 g for 2 min. The supernatant was removed, and the pellet was suspended in 200 µL of 4% paraformaldehyde. After 10 min of incubation at RT, the sample was centrifuged again at 1,500 g for 2 min. The pellet was suspended in 500 µL ammonium acetate (0.1 M, pH = 9), gently mixed and centrifuged at 1,500 g for 2 min. Finally, the pellet was mixed with 30 µL of ammonium acetate (0.1 M, pH = 9), and 10 µL of the cell suspension was smeared onto a poly-lysine-coated slide (3 slides in total per sample) and air dried for 1 h at RT. When the slides with fixed spermatozoa were ready, they were stained two at a time in a 50 mL Falcon tube containing the Coomassie brilliant blue G-250 at 0.22%. After 2 min of incubation, the slides were removed individually, and the excess Coomassie solution was absorbed by an absorbent paper. The slides were then placed two at a time in another 50 mL Falcon tube containing distilled water for 1 min. The slides were gently removed to eliminate the excess water. They were placed on a heating plate at 37°C for 20 min to dry and then mounted with mounting medium. A bright field microscope was used to examine the spermatozoa at 40X magnification. The acrosome is stained dark blue before the acrosome reaction (acrosome present and intact), and no staining is seen after the acrosome reaction (loss of acrosome). A minimum of 200 spermatozoa was counted per assay.

Production of reactive oxygen species – Dihydrodethyidium staining

ROS level was assessed using a dihydrodethyidium (DHE) staining. DHE staining is a simple and effective fluorescence dye-based detection method widely used to measure ROS level in cells [174]. DHE reacts with ROS to give a red fluorescent signal so the level of fluorescence is linked to the presence of ROS. After thawing and appropriate incubation at 37°C, aliquots containing 20,000 spermatozoa were centrifuged at 300 g for 5 min, the supernatant was removed, and 200 µL of warm (30°C) PBS 1X was added to the pellet to wash the spermatozoa. They were centrifuged again at 300 g for 5 min, and the pellet was re-suspended in 1 mL of a 5 µM DHE solution. The spermatozoa were incubated at 37°C for 10 min and then centrifuged at 300 g for 5 min. The pellets were then washed 3 times with warm PBS 1X before spermatozoa were fixed with 4% paraformaldehyde in PBS 1X. After 5 min of incubation at RT, the spermatozoa were washed 3 times with warm PBS 1X. The final pellet was re-suspended in 20 µL of PBS 1X, and 10 µL of spermatozoa were applied to each of 2

poly-lysine-coated glass slides. Slides were air-dried for 20 min and mounted with DABCO anti-fading mounting medium. Images were taken with an epifluorescence microscope at 60X using a TRITC filter (excitation 488-532nm / emission 576nm). The mean grey intensity, corresponding to the average grey intensity within the selection of the sperm head, was calculated using ImageJ software. For this purpose, 50 spermatozoa were randomly selected per slide (100 spermatozoa in total). The result of the *in vivo* study is presented as the mean grey intensity of 100 spermatozoa (pooled spermatozoa from 3 males) for each age group. The results of the *in vitro* study correspond to the average of the mean grey intensity of 100 spermatozoa each from 5 individual experiments.

DNA oxidation – Immunostaining

The biotin mouse monoclonal antibody [15A3] to DNA/RNA Damage was used to detect oxidised guanine (8-hydroxy-2'-desoxyguanosine). After thawing and appropriate incubation at 37°C, an aliquot containing 50,000 spermatozoa was centrifuged at 300 g for 5 min, and the supernatant was then removed. The pellet was re-suspended in decondensation buffer and incubated for 1 h at RT. After further centrifugation at 300 g for 5 min, the spermatozoa were washed in PBS 1X, and the final pellet was re-suspended in 20 µL of PBS 1X, and 10 µL of spermatozoa were smeared on each of 2 poly-lysine-coated glass slides. Slides were air-dried for 1 h, incubated in a fixative solution (ethanol 95 / acetone 1:1) for 30 min at 4°C and air-dried again for at least 20 min. They were then hydrated (ethanol 90, ethanol 70 and distilled water for 1 min each) and washed in 0.1% Triton X-100 in PBS 1X for 5 min. After 2 h of incubation in the saturation buffer at RT, the slides were incubated with primary antibody (1:200 dilution in saturation buffer) overnight at 4°C. Slides were then washed 3 times for 5 min each with 0.1% Triton X-100 in PBS 1X. The secondary antibody was applied for 1 h at RT in the dark (1:1000 dilution in 0.1% Triton X-100 in PBS 1X). The slides were washed 3 times for 5 min each with PBS 1X and incubated 5 min at RT in the dark with 500 µL of 3 µM DAPI to stain the nucleus. Finally, the slides were washed 3 times for 2 min each in PBS 1X, air-dried and mounted with an aqueous anti-fading mounting medium containing DABCO. Images were taken with an epifluorescence microscope at 60X using an AF555 filter (excitation 488-532nm / emission 580nm) and a DAPI filter (excitation 359nm / emission 457nm). Results are given as a mean grey intensity calculated using ImageJ software, corresponding to the mean grey intensity using AF555 filter (oxidised DNA) within the nucleus. The nucleus areas were based on DAPI fluorescent signals, using an automatic selection to define individual regions of interest, visualised by a grey line on images. A total of 50 spermatozoa was randomly selected per slide (100 spermatozoa in total). The result of the *in vivo* study is presented as the mean grey intensity of 100 spermatozoa (pooled from 3 males) for each age

group. The results of the *in vitro* study correspond to the average of the mean grey intensity of 100 spermatozoa from 5 individual experiments.

DNA fragmentation – Comet assay

Sperm DNA fragmentation analysis can be performed by single cell gel electrophoresis (comet) assay under alkaline conditions to detect single-strand and double-strand DNA breaks [175]. A comet assay kit from Abcam was used. After thawing and incubation at 37°C for 1h, an aliquot containing 10,000 spermatozoa was centrifuged at 300 g for 5 min. The pellet was washed in ice-cold DPBS and combined with agarose (provided in the kit) according to the comet kit protocol. The mixture was then applied to agarose pre-coated slides (provided in the kit) and incubated at 4°C for 15 min in the dark. The first lysis step was performed with pre-chilled lysis buffer (provided in the kit) for 1 h at 4°C in the dark. The second lysis step was performed with the same lysis buffer warmed to 37°C with the addition of proteinase K (0.1 mg/ml) overnight at 37°C. The next day, the electrophoresis was performed in alkaline solution at a voltage of 1 volt/cm and a current of 300 mA for 15 min. The slides were then washed 3 times for 10 min each in 0.4 M Tris-HCl pH 7.4 and in cold H₂O 3 times for 2 min each. Finally, the slides were dehydrated in 70% ethanol for 5 min and air-dried in the dark at RT. When the agarose was completely dry, 100 µL/well of diluted Vista Green DNA Dye (provided in the kit) was added. After 15 min at RT, the slides were washed twice with DiH₂O and mounted with anti-fading aqueous mounting medium. Spermatozoa were observed under an epifluorescence microscope at 60X magnification. The tail moment of 50 spermatozoa was calculated as follows: tail moment = tail length x tail DNA% where the tail DNA% = 100 x (1 – (total comet circularity / circularity of the comet head)), according to the comet kit protocol. Tail length, total circularity and head circularity were measured using ImageJ software.

Co-incubation of spermatozoa with D-Asp and/or N-acetyl-L-cysteine (NAC)

NAC is an antioxidant used to determine whether the reactive oxygen species produced by D-Asp are necessary for its beneficial role in sperm maturation. After thawing, each sample, corresponding to 1x10⁶ spermatozoa, was divided into 4 groups: Control, D-Asp only, D-Asp + NAC and NAC only. The control group contained spermatozoa in 200 µL Cook's medium. In the D-Asp group, spermatozoa were mixed with 200 µL of 4 mM D-Asp in Cook's medium. In the D-Asp + NAC group, the spermatozoa were incubated in 200 µL of Cook's medium containing 4 mM D-Asp and 2.5 mM NAC. Finally, the remaining group corresponded to spermatozoa in 200 µL Cook's medium containing 2.5 mM NAC. All samples were incubated for 1 h at 37°C in the same incubator. CTC staining and Coomassie brilliant blue staining were then performed to analyse sperm maturation.

Ultrastructural damage – Transmission electron microscopy

To visualise and analyse the ultrastructural damage, spermatozoa were prepared for transmission electron microscopy in collaboration with the CECAD imaging facility. After thawing and incubation for 1h at 37°C in an incubator, 800,000 spermatozoa were collected and washed with 200 µL PB 1X. The samples were then centrifuged at 1,500 g for 2 min, and the pellets were re-suspended in 100 µL of PB 1X. This step was repeated 2 more times. To the final pellets, 60 µL of PB 1X was added and mixed with an equal volume of fixative provided by the CECAD imaging facility (2% formaldehyde, 2% glutaraldehyde, 3 mM CaCl₂ in 0.1 M sodium cacodylate buffer). The sample were then processed according to the CECAD imaging facility protocol. Briefly, the samples were incubated at 4°C for 48 h, washed with 0.1 M sodium cacodylate buffer and centrifuged at 1,500 g for 10 min. The pellets were then mixed with 3% low melting agarose (1:1) and incubated at 37°C for 10 min then at 4°C for 30 min. The pellets were washed with 0.1 M sodium cacodylate buffer and post-fixed at 4°C for 2 h (1% OsO₄, 1.25% sucrose, 1% potassiumferrocyanide in 0.1 M sodium cacodylate buffer). After 4 washing steps in 0.1 M sodium cacodylate buffer and dehydration in ethanol, samples were incubated in a mix of ethanol/propylenoxide (1:1) for 15 min, then pure propylenoxide 2 times 15 min, following by infiltration with epon/propylenoxide (1:1) and epon/propylenoxide (3:1) for 2 h at 4°C each. The samples were incubated overnight in pure epon at 4°C and then for 2 h at RT in a new pure epon bath. Finally, the samples were mounted onto epon blocks. Ultramicrotome was used for ultrathin sections of 70 nm of blocks. The sections were then stained with 1.5% uranyl acetate at 37°C for 15 min and 3% citrate solution for 4 min. A minimum of 25 images of different sperm heads and 25 images of different sperm mid-pieces were acquired using a JEM-2100 Plus Transmission Electron Microscope (JEOL) operating at 80 kV equipped with a OneView 4K camera (Gatan) for analysis. Spermatozoa were classified as Class I if the plasma membrane was intact (slightly wavy membrane accepted), and the mitochondria did not show any specific abnormality. They were classified as Class II if the plasma membrane was strongly rippled without interruption or had minor abnormalities in the mitochondria (diminution of cristae or roundness deviation, for example). Class III spermatozoa showed significant disturbances, damages and breaks in the plasma membrane, spots on the nucleus or major abnormalities of the mitochondria.

3.2.5 Data analysis

Statistical analyses and graphical representations of the data were performed using GraphPad Prism 7 software. The Gaussian distribution of the data was tested with a Shapiro-Wilk normality test when the sample size was equal to or below five, and a D'Agostino-Pearson normality test when the sample size was higher than five. In all figures, data are presented as

mean \pm standard error of the mean (SEM) with individual values where applicable. The significance levels are: $***p < 0.001$; $0.001 < ***p < 0.01$; $0.01 < *p < 0.05$.

In Aim I, a two-by-two table chi-square test (Fisher-test) was performed to analyse the association between D-Asp treatment and sperm morphology in the two age groups independently (Figure 10B). The D-Asp treatment effect on capacitation and acrosome reaction as well as the comparison between age groups were analysed with a logistic regression (Figure 11B and 11D). The concentration and the total and progressive motility were measured in duplicate, hence no statistical analysis was performed (Figure 8 and 9). A non-parametric unpaired t-test (Mann-Whitney test) was applied to analyse the level of ROS (Figure 12B) and DNA oxidation (Figure 13B) since the values were not normally distributed. Parametric unpaired t-tests were performed on the level of ROS (Figure 14B, 14C and 16B), DNA oxidation (Figure 15B and 15C), capacitation rate (Figure 16C) and acrosome reaction rate (Figure 16D), as values were normally distributed with equal variance (controlled with a F test).

Regarding the Aim II, statistical analysis of the IVF success rate (Figure 17) between sperm cryopreserved in LN₂ and at -80°C was performed with a two-by-two table chi-square tests (Fisher-tests) in all six mouse strains and at the five different storage times (1, 3, 6, 9 or 12 months). Dunnett's multiple comparisons tests were performed in the six mouse strains to compare the percentage of dead spermatozoa (Figure 18) between the control condition (sperm in LN₂) and the storage duration of spermatozoa at -80°C for 1, 3, 6, 9 or 12 months. For assessment of the effect of the storage temperature on sperm morphology (Figure 20) and the ultrastructure (Figure 21B), Chi-Squared tests were conducted. Finally, we used a non-parametric unpaired t-test (Mann-Whitney test) to compare the level of DNA fragmentation (Figure 22B) in spermatozoa cryopreserved in LN₂ versus those cryopreserved at -80°C (1, 6 or 12 months of storage). The total motility (Figure 19, Figure 23A) was measured in duplicate, hence no statistical analysis was possible. Ultimately, a 2x2-Table Wald-ChiSquare-Test, which is approximately equivalent to Fisher's exact test, was performed on the morphology analysis, capacitation and the acrosome reaction rate (Figure 23B, 24A and 24B) using usual binomial assumption for counts and considering the counts of the capacitation and the counts of the acrosome reaction, each among total spermatozoa.

4. Results

4.1 Aim I: To characterise the effects of D-aspartate on the fertility and quality of cryopreserved mouse spermatozoa and the mechanisms involved

The results presented in this section (Figures 8, 9, 10 and 11) are part of the publication Raspa et al. 2022 [160] and correspond to my personal and exclusive research work. The effect of oral administration of D-Asp on the quality of cryopreserved spermatozoa was investigated. Spermatozoa from B6N mice at 2 different stages of sexual maturation were used: 9 weeks old (young) and 16 weeks old (adult). To determine whether the observed D-Asp effect was influenced by the duration of treatment, mice received 20 mM D-Asp for 2 or 4 weeks before sacrifice. Spermatozoa were collected from 3 males and pooled for cryopreservation in LN₂, as routinely done by repositories. The spermatozoa were then thawed for downstream analyses of sperm concentration, motility, morphology and maturation.

4.1.1 D-Asp treatment does not affect spermatozoa concentration

The concentration of spermatozoa from 9-week-old and 16-week-old B6N males that received D-Asp for 2 or 4 weeks or from controls is shown in Figure 8. In 9-week-old mice, the concentration of spermatozoa treated with D-Asp for 2 or 4 weeks was $13.0 \times 10^6/\text{mL}$ or $9.1 \times 10^6/\text{mL}$, respectively, vs. $10.6 \times 10^6/\text{mL}$ in the control. In 16-week-old mice, the concentration of spermatozoa treated with D-Asp for 2 or 4 weeks was $22.4 \times 10^6/\text{mL}$ or $21.7 \times 10^6/\text{mL}$, respectively, vs. $28.1 \times 10^6/\text{mL}$ in the control. The concentration of spermatozoa was higher at each time point for the 16-week-old males compared to the 9-week-old males. Statistical analysis was not performed because measurements were possible from only 2 straws of the pooled spermatozoa.

4.1.2 D-Asp treatment for 4 weeks increases the motility of spermatozoa

Total motility, which includes all spermatozoa movements, and progressive motility, which is the ability of the spermatozoa to move in a straight line, were analysed using the Hamilton Thorne IVOS computerized semen analyzer (Figure 9). The total motility was higher after 4 weeks of oral D-Asp treatment compared to the control (23.3% vs. 17.9% in 9-week-old males and 28.5% vs. 19.8% in 16-week-old males). Concerning progressive motility, after 4 weeks of oral D-Asp treatment compared to the control, these values were 10.3% vs. 6.3% in 9-week-old males and 10.3% vs. 7.6% in 16-week-old males.

Results

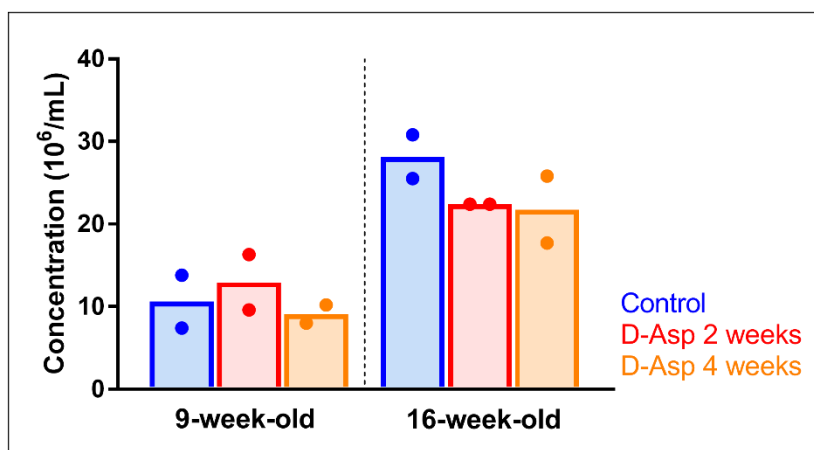


Figure 8: Sperm concentration after administration of D-Asp. (Modified from [160]). The concentration of spermatozoa in 9- and 16-week-old B6N males that received D-Asp in the drinking water for 2 or 4 weeks was measured using the Hamilton Thorne IVOS sperm analyzer. Control mice received water without D-Asp. Data are shown as the mean of two measurements of a pool of spermatozoa collected from 3 males.

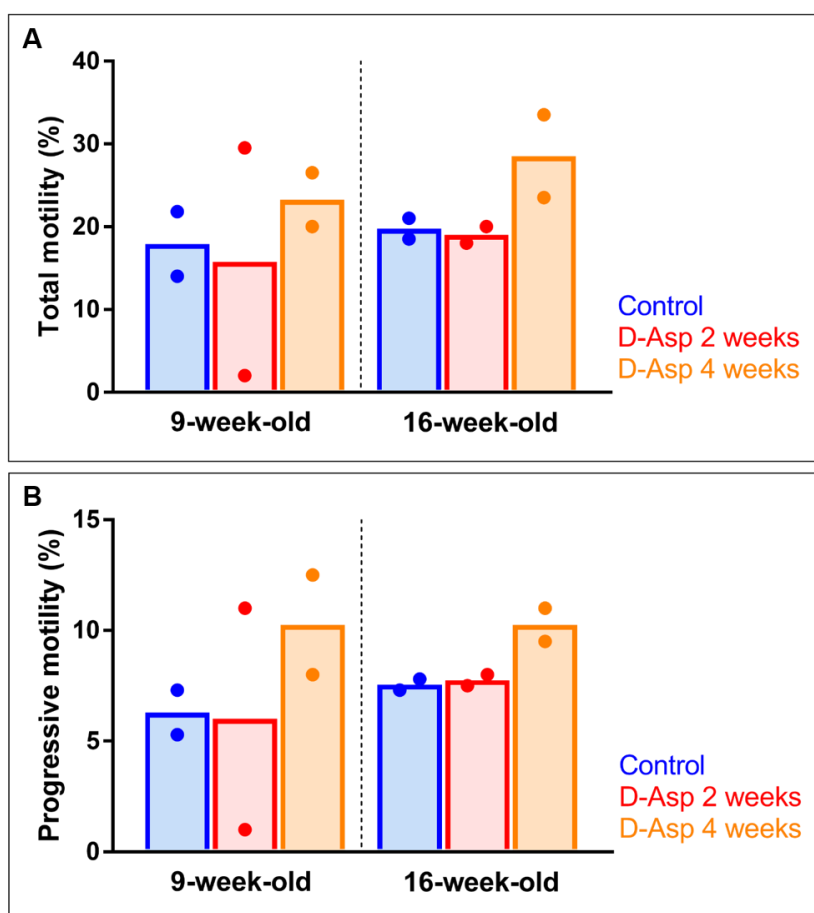


Figure 9: Sperm motility after administration of D-Asp. (Modified from [160]). Analysis of the total motility (A) and the progressive motility (B) of spermatozoa from 9- and 16-week-old B6N males that received D-Asp in the drinking water for 2 or 4 weeks using the Hamilton Thorne IVOS sperm analyzer. Control mice received water without D-Asp. Data are shown as the mean of two measurements of a pool of spermatozoa collected from 3 males.

Results

Treatment with D-Asp for 2 weeks resulted in a total motility of 15.8% in 9-week-old males and 19.0% in 16-week-old males. The progressive motility of spermatozoa after 2 weeks of D-Asp was 6.0% in 9-week-old males and 7.8% in 16-week-old males. Statistical analysis was not performed because measurements were possible from only 2 straws of the pooled spermatozoa.

4.1.3 D-Asp treatment for 2 weeks decreases sperm abnormalities in young B6N males

Spermatozoa from 9- and 16-week-old B6N males treated with D-Asp for 2 or 4 weeks were classified depending on the presence of morphological abnormalities (Figure 10A).

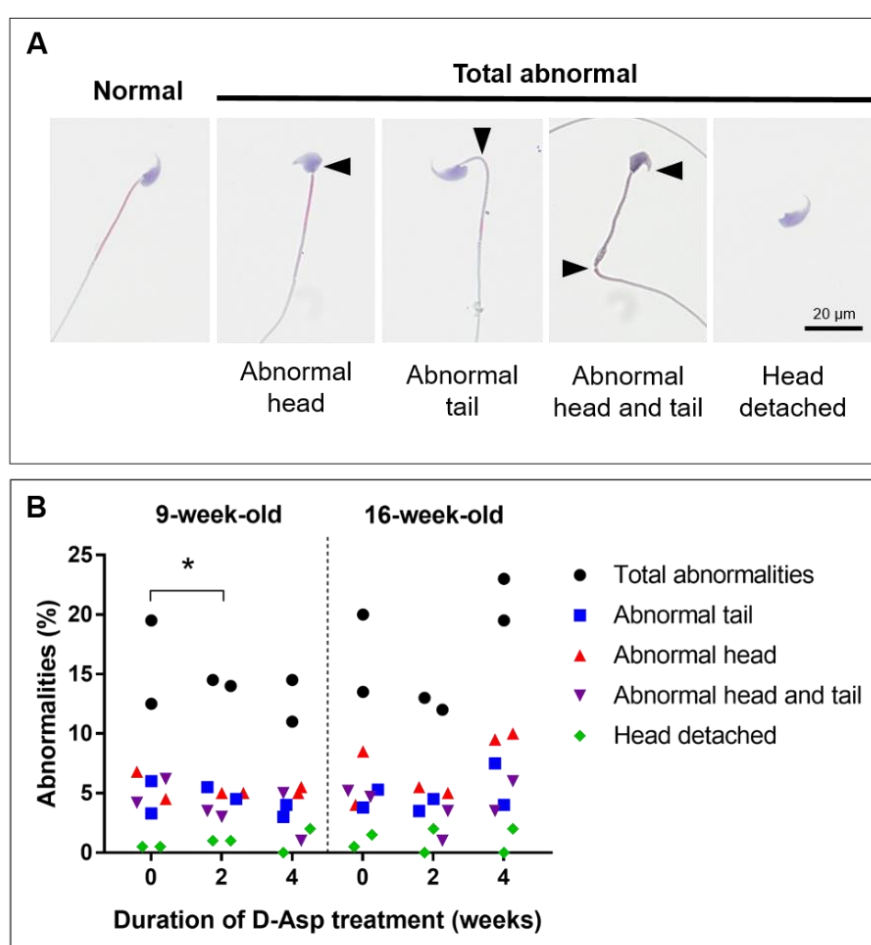


Figure 10: Sperm morphology after administration of D-Asp. (Modified from [160]).

(A) Representative images of spermatozoa: on the left is a spermatozoon with a normal shape, then a spermatozoon with an abnormal head, a spermatozoon with an abnormal tail, a spermatozoon with both abnormal head and abnormal tail, and head detached. Black arrows point to abnormalities (abnormal head morphology or tail bent). (B) Percentage of spermatozoa from 9- and 16-week-old B6N males that received D-Asp in the drinking water for 0 (control), 2 or 4 weeks with abnormal morphology. Data are shown as 2 counts per category (200 spermatozoa from a pool of spermatozoa collected from 3 males per counting). * $p < 0.05$.

Results presented in Figure 10B correspond to the total abnormal spermatozoa, abnormal head, abnormal tail, abnormal head and tail, and head detached. Spermatozoa from 9-week-old males that received D-Asp for 2 weeks showed significantly less abnormalities than those in the control (14.3% vs. 16.0%). In 16-week-old mice, after 2 weeks of D-Asp treatment, sperm abnormalities were 12.5% vs. 16.8% in the control. In contrast, 4 weeks of D-Asp treatment resulted in a non-significantly higher level of abnormalities of spermatozoa compared to the control (21.3% vs. 16.8%).

4.1.4 D-Asp-treatment leads to higher capacitation and acrosome reaction rate

Sperm capacitation was visualised by CTC staining (Figure 11A). Figure 11B represents the capacitation rate, which corresponds to the percentage of spermatozoa that underwent capacitation. Concerning the 9-week-old mice, the capacitation rate was significantly higher in spermatozoa treated with D-Asp for 2 or 4 weeks compared to the control: $72.4 \pm 2.8\%$ ($p < 0.01$) or $70.3 \pm 3.1\%$ ($p < 0.001$), respectively, vs. $61.3 \pm 1.3\%$. Similarly, in 16-week-old males, D-Asp treatment for 2 or 4 weeks significantly increased the capacitation rate compared to the control: $88.6 \pm 0.9\%$ or $81.3 \pm 1.7\%$, respectively, vs. $74.0 \pm 1.4\%$ ($p < 0.001$). A comparison between age groups shows a significant increase of the capacitation rate in 16-week-old males compared to 9-week-old males at all timepoints.

The acrosome reaction was visualised by Coomassie brilliant blue staining (Figure 11C). Figure 11D represents the acrosome reaction rate, which corresponds to the percentage of spermatozoa without an acrosome (right panel in Figure 11C). The acrosome reaction rate was significantly increased in spermatozoa from 9-week-old males treated with D-Asp for 2 or 4 weeks compared to the control: $38.4 \pm 0.9\%$ ($p < 0.05$) or $46.3 \pm 0.7\%$ ($p < 0.001$), respectively, vs. $32.6 \pm 1.1\%$. Similarly, in 16-week-old males, the acrosome reaction rate was significantly higher in spermatozoa treated with D-Asp for 2 or 4 weeks compared to the control: $48.8 \pm 0.9\%$ ($p < 0.01$), or $50.2 \pm 0.6\%$ ($p < 0.001$), respectively, vs. $42.7 \pm 0.2\%$. A comparison between age groups indicates a significant increase of the acrosome reaction rate in 16-week-old males compared to 9-week-old males at all timepoints.

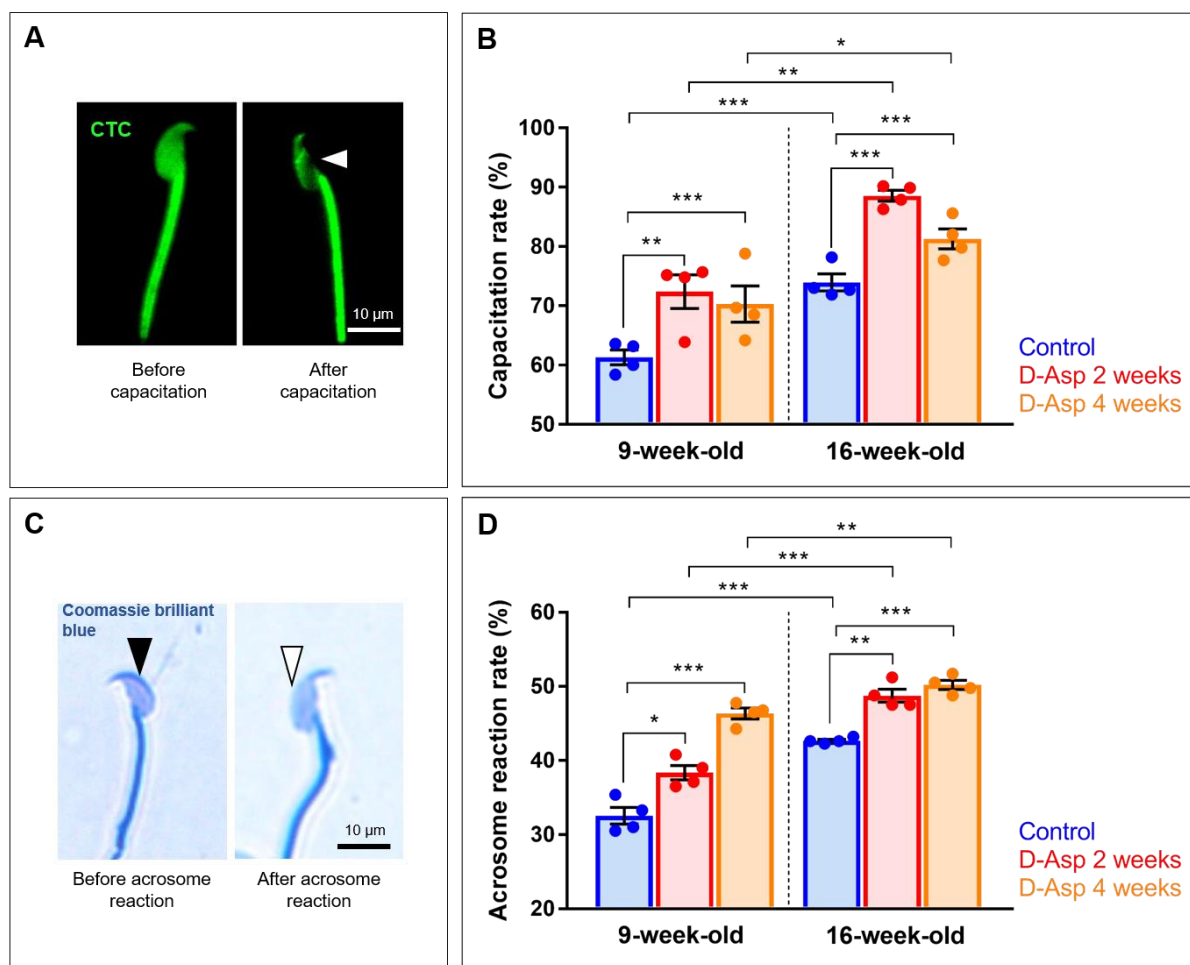


Figure 11: Sperm maturation rates after administration of D-Asp. (Modified from [160]). (A) Representative images of spermatozoa stained with chlortetracycline (CTC): left image before capacitation (green fluorescence signal in the whole sperm head) and right image after capacitation (no staining band in the basal area of the sperm head marked with a white arrowhead). (B) Percentage of spermatozoa that underwent capacitation in control mice (not treated with D-Asp) and in mice treated with D-Asp for 2 or 4 weeks. Data are shown as the mean of 4 analyses (200 spermatozoa from a pool of spermatozoa collected from 3 mice per analysis). (C) Representative images of spermatozoa stained with Coomassie brilliant blue: left image before acrosome reaction (blue band staining in the acrosome region marked with a black arrowhead) and right image after acrosome reaction (no staining in the acrosome region marked with a white arrowhead). (D) Percentage of spermatozoa that underwent the acrosome reaction in control mice (not treated with D-Asp) and in mice treated with D-Asp for 2 or 4 weeks. Data are shown as the mean of 4 analyses (200 spermatozoa from a pool of spermatozoa collected from 3 males per analysis). * $p < 0.05$, ** $p < 0.01$ and *** $p < 0.001$.

The next section (Figures 12, 13, 14, 15 and 16) explores the hypothesis that the production of ROS by D-Asp treatment is implicated in the improvement of sperm quality. The level of ROS in cryopreserved spermatozoa following *in vivo* (oral) or *in vitro* D-Asp treatment as well as the level of sperm DNA oxidation were evaluated. Then, the production of ROS was quenched with an antioxidant to provide information on the role of D-Asp-generated ROS in the maturation of spermatozoa.

4.1.5 Oral treatment with D-Asp increases DHE staining and DNA oxidation levels in spermatozoa

Dihydroethidium (DHE) staining was performed as an indirect measurement of the level of ROS in spermatozoa from 9- and 16-week-old B6N mice that received D-Asp orally for 0, 2 or 4 weeks. Figure 12A presents representative images obtained. The mean grey intensity, corresponding to DHE fluorescence intensity, was measured with ImageJ in 100 spermatozoa in each condition (Figure 12B). The mean grey intensity was significantly increased in spermatozoa collected from 9-week-old mice treated with D-Asp for 2 or 4 weeks compared to the control: 369.8 ± 7.7 A.U. or 421.7 ± 8.5 A.U., respectively, vs. 276.2 ± 5.8 A.U. ($p < 0.001$).

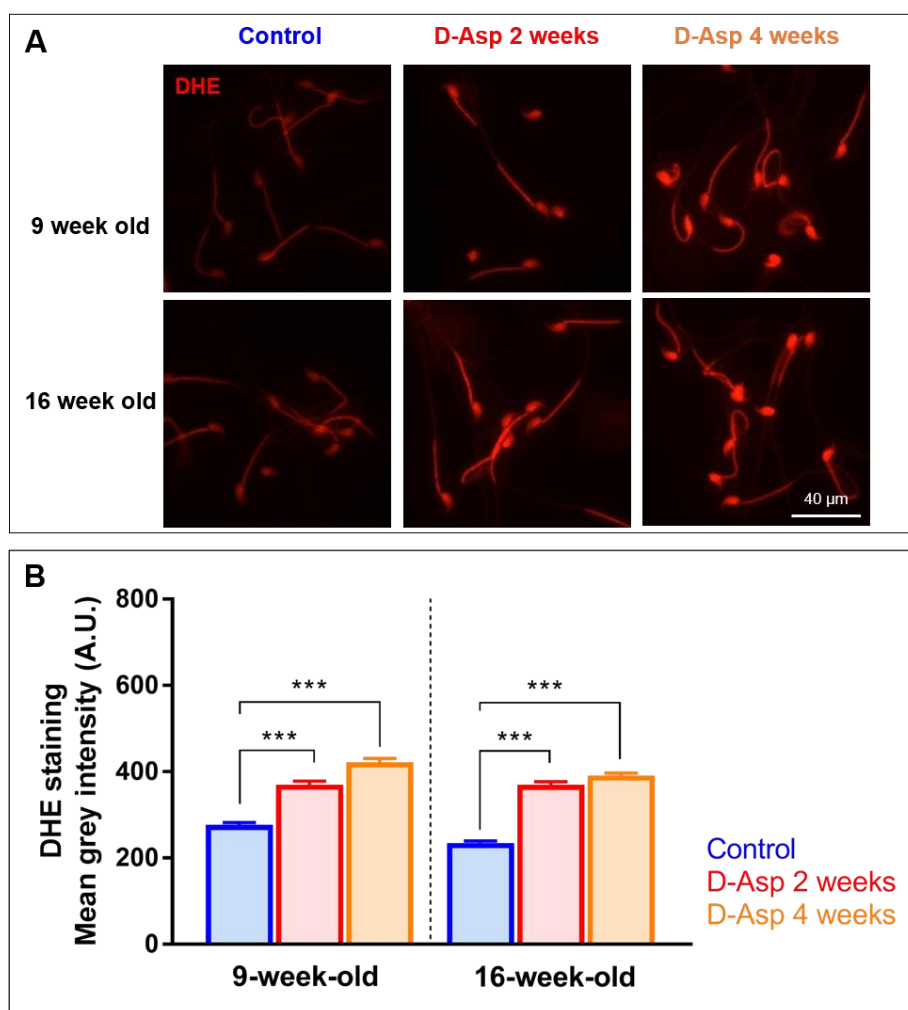


Figure 12: Measurement of ROS with DHE staining after oral administration of D-Asp. (A) Representative images of DHE staining of spermatozoa from 9- and 16-week-old B6N males that received D-Asp in the drinking water for 2 or 4 weeks. Control mice received water without D-Asp. (B) Level of DHE fluorescence, given as the mean grey intensity (arbitrary unit in ImageJ), of 100 spermatozoa from a pool of spermatozoa collected from 3 males. *** $p < 0.001$.

Similar results were obtained in 16-week-old mice: 368.7 ± 7.4 A.U. or 390.8 ± 5.4 A.U., respectively, vs. 234.4 ± 4.4 A.U. ($p < 0.001$). No statistical difference of the mean grey

intensity between spermatozoa from 9-week-old males and 16-week-old males was observed at all timepoints ($p > 0.05$).

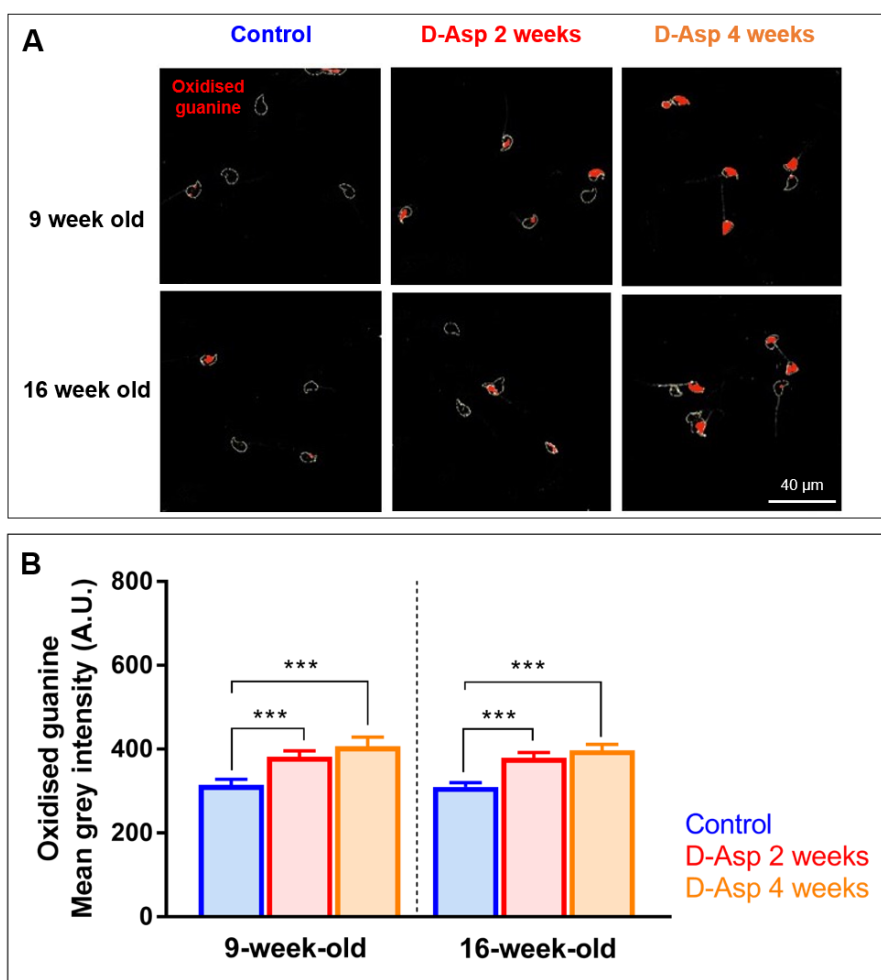


Figure 13: Analysis of DNA oxidation with immunostaining after oral administration of D-Asp. (A) Representative images of DNA oxidation of spermatozoa from 9- and 16-week-old B6N males that received D-Asp in the drinking water for 2 or 4 weeks. Control mice received water without D-Asp. The red staining corresponds to oxidised guanine (AF555 filter), and the grey lines correspond to the automatic detection of the sperm nucleus. (B) Level of DNA oxidation, given as the mean grey intensity (arbitrary unit in ImageJ), of 100 spermatozoa from a pool of spermatozoa collected from 3 males. *** $p < 0.001$.

DNA oxidation was measured by performing immunostainings using an antibody against oxidised guanine and counterstained with DAPI (nuclear staining). In Figure 13A, representative images of samples show oxidised DNA with a red fluorescent signal. DAPI staining was used to automatically select the nucleus region (grey lines on images), and the mean grey intensity, corresponding to oxidised DNA, was measured in these regions. In Figure 13B, the mean grey intensity was significantly higher in spermatozoa from 9-week-old males that received D-Asp for 2 or 4 weeks compared to the control: 381.9 ± 13.8 A.U. or 406.2 ± 21.9 A.U., respectively, vs. 314.6 ± 12.9 A.U ($p < 0.001$). Similar results were obtained in 16-

week-old males: 378.7 ± 12.9 A.U. or 397.2 ± 13.7 A.U., respectively, vs. 310.0 ± 9.80 A.U. ($p < 0.001$). No statistical difference of the mean grey intensity between spermatozoa from 9-week-old males and 16-week-old males was observed at all timepoints ($p > 0.05$).

4.1.6 *In vitro* D-Asp treatment increases DHE staining and DNA oxidation levels in spermatozoa

The *in vivo* results showed that D-Asp treatment in drinking water increased the level of DHE staining and DNA oxidation in spermatozoa. To test whether D-Asp could act directly on spermatozoa to induce ROS production and oxidative stress, cryopreserved spermatozoa from 9-week-old and 16-week-old B6N males were thawed and incubated *in vitro* with 4 mM D-Asp for 1 or 5 hours. First, the level of ROS was measured with DHE staining (Figure 14A).

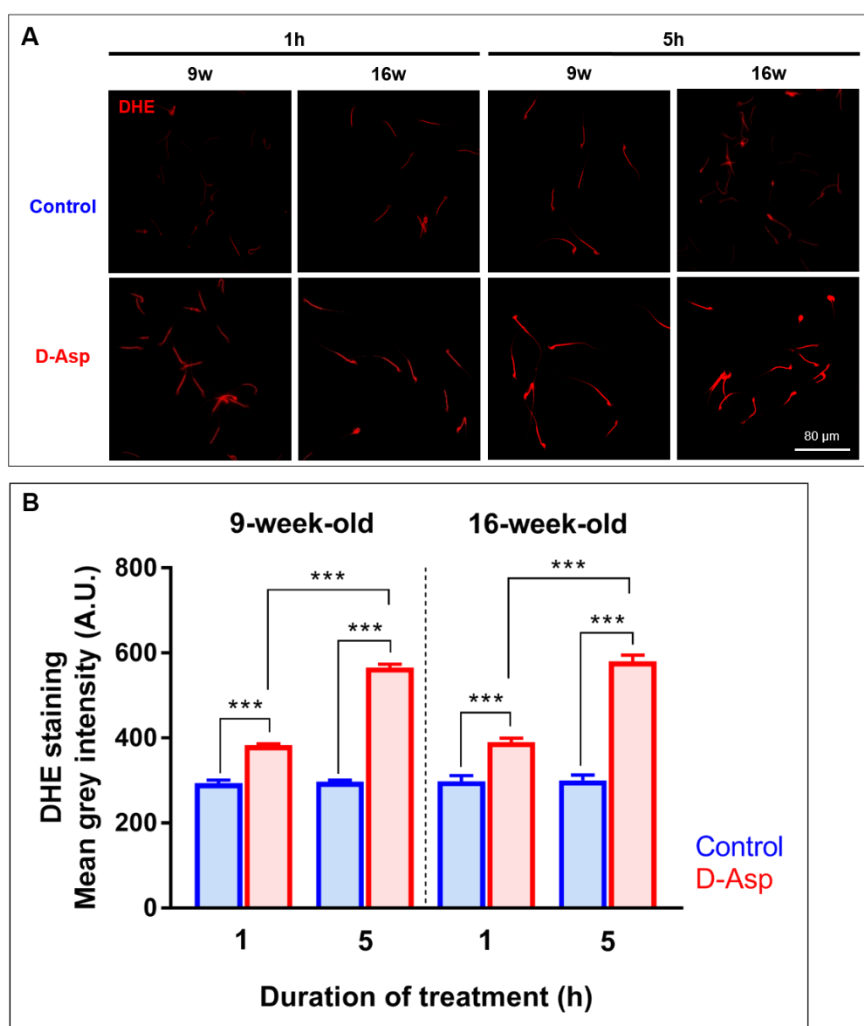


Figure 14: Measurement of ROS with DHE staining after *in vitro* D-Asp treatment. (A) Representative images of DHE staining of spermatozoa without D-Asp (control) or treated *in vitro* with D-Asp for 1 or 5 hours. (B) The level of DHE fluorescence after 1 or 5 hours of treatment, given as the mean grey intensity (arbitrary unit in ImageJ), from 100 spermatozoa per male ($n = 5$ males). *** $p < 0.001$.

Results

Figure 14B represents the mean grey intensity of DHE staining after 1 or 5 hours of incubation with or without D-Asp. After 1 hour, the mean grey intensity was significantly higher in D-Asp-treated spermatozoa compared to the control in 9-week-old males: 382.9 ± 3.6 vs. 293.6 ± 7.7 A.U. ($p < 0.001$) and 16-week-old males: 390.1 ± 4.1 A.U. vs. 298.6 ± 5.8 A.U. ($p < 0.001$). Similar results were found after 5 hours of D-Asp treatment in spermatozoa from 9-week-old males: 565.4 ± 8.2 A.U. vs. 297.2 ± 3.8 A.U. in the control ($p < 0.001$) and from 16-week-old males: 580.4 ± 6.7 A.U. vs. 300.6 ± 5.4 A.U. in the control ($p < 0.001$). A significant increase of the mean grey intensity is observed between 1 and 5 hours of D-Asp treatment ($p < 0.001$). No statistical difference of the mean grey intensity between spermatozoa from 9-week-old males and 16-week-old males was observed at all timepoints ($p > 0.05$).

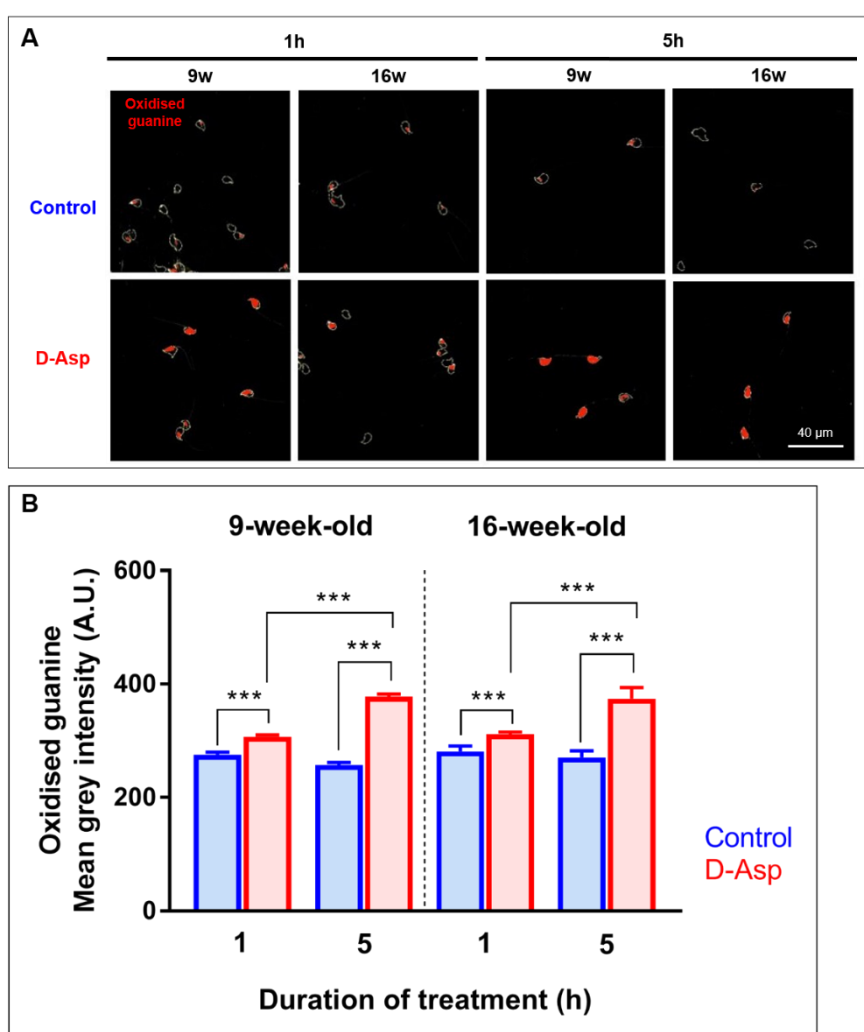


Figure 15: Analysis of DNA oxidation with immunostaining after *in vitro* D-Asp treatment. (A) Representative images of the DNA oxidation immunostaining targeting oxidised guanine of spermatozoa without D-Asp (control) or treated *in vitro* with D-Asp for 1 or 5 hours. The red staining corresponds to oxidised guanine (AF555 filter), and the grey lines correspond to the automatic detection of the sperm nucleus. (B) The level of fluorescence corresponding to oxidised guanine after 1 or 5 hours of treatment, given as the mean grey intensity (arbitrary unit in ImageJ), from 100 spermatozoa per male ($n = 5$ males). *** $p < 0.001$.

Then, immunostaining to measure oxidised guanine was performed, as described previously. Figure 15A shows representative images of the staining. In Figure 15B, after 1 hour of incubation, the mean grey intensity was significantly higher in D-Asp-treated spermatozoa than in the control from 9-week-old males (306.8 ± 3.2 A.U. vs. 275.2 ± 4.5 A.U., $p < 0.001$) and from 16-week-old males (311.2 ± 2.0 A.U. vs. 281.2 ± 4.2 A.U., $p < 0.001$). The increase was even higher after 5 hours of *in vitro* D-Asp treatment in spermatozoa from 9-week-old males (377.6 ± 4.5 A.U. vs. 257.0 ± 4.5 A.U., $p < 0.001$) and from 16-week-old males (374.6 ± 8.6 A.U. vs. 270.7 ± 5.0 A.U., $p < 0.001$). A significant increase of the mean grey intensity is observed between 1 and 5 hours of D-Asp treatment ($p < 0.001$). No statistical difference of the mean grey intensity between spermatozoa from 9-week-old males and 16-week-old males was observed at all timepoints ($p > 0.05$).

4.1.7 The beneficial effect of D-Asp on ROS production, capacitation and the acrosome reaction is inhibited by the addition of an antioxidant

D-Asp given in drinking water increased both sperm quality and markers of oxidative stress (Figures 9 to 13). In addition, the *in vitro* studies confirmed the *in vivo* effect of D-Asp on the ROS level and DNA oxidation (Figures 14 and 15). Thus, we hypothesized that D-Asp increases sperm quality by increasing the ROS level. To test this hypothesis, spermatozoa were treated simultaneously with D-Asp and N-acetyl-L-cysteine (NAC), a widely-used antioxidant [176].

First, to validate the decrease of ROS in the presence of NAC, DHE staining was performed and Figure 16A shows representative images of the staining. In Figure 16B, spermatozoa treated with 4 mM of D-Asp showed a higher level of DHE staining compared to the control (392.2 ± 4.6 A.U. vs. 274.8 ± 4.3 A.U., $p < 0.001$). The DHE staining was weaker when 2.5 mM of NAC was added in combination with D-Asp compared to D-Asp alone (286.5 ± 4.2 A.U., $p < 0.001$). With NAC alone, the DHE level was similar to that of the control (285.4 ± 2.6 A.U., $p > 0.05$). This staining confirmed that the presence of NAC decreased the level of ROS with the D-Asp treatment.

The capacitation rate (Figure 16C) was then analysed. Considering the 9-week-old males, the capacitation rate was significantly higher in D-Asp-treated spermatozoa compared to the control ($63.0 \pm 1.9\%$ vs. $37.0 \pm 1.8\%$, $p < 0.001$). When spermatozoa were treated with D-Asp and co-incubated with NAC, the capacitation rate was significantly lower ($36.9 \pm 1.3\%$, $p < 0.001$) compared to D-Asp treatment alone and was comparable to that of the control. Finally, NAC alone did not impact the sperm capacitation rate ($38.7 \pm 2.0\%$). Similarly, in 16-week-old males, the capacitation rate was significantly higher in D-Asp-treated spermatozoa compared to the control (89.8 ± 1.9 vs. $68.8 \pm 1.8\%$, $p < 0.001$). When spermatozoa were

Results

treated with D-Asp and co-incubated with NAC, the capacitation rate was significantly lower ($75.0 \pm 2.3\%$, $p < 0.001$) compared to D-Asp treatment alone and was comparable to that of the control. Finally, NAC alone did not impact the sperm capacitation rate ($75.3 \pm 2.3\%$). The capacitation rate was significantly higher in spermatozoa from 16-week-old males compared to 9-week-old males in all groups ($p < 0.001$).

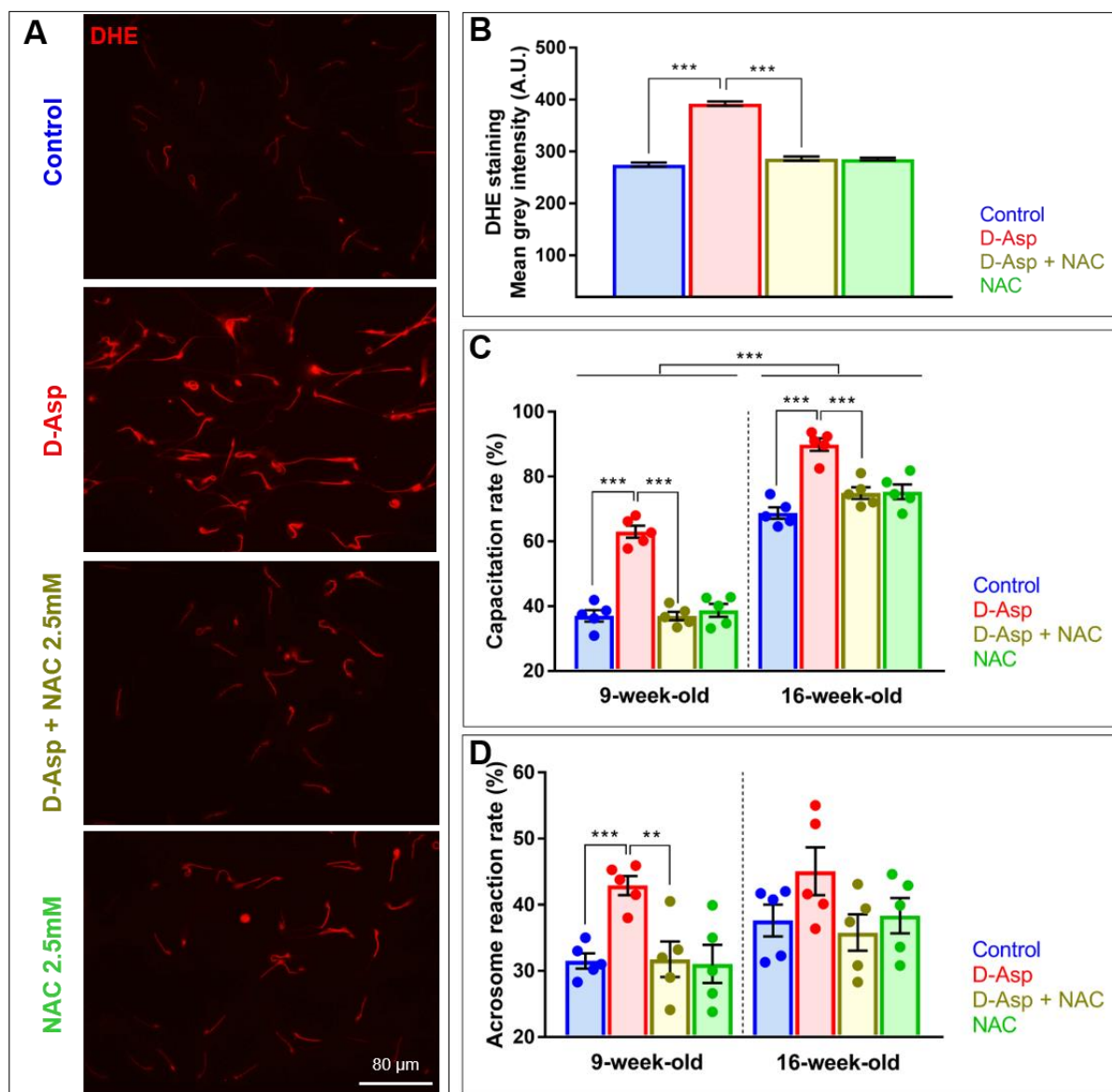


Figure 16: Inhibition of the beneficial effect of D-Asp with the antioxidant NAC. (A) Representative images obtained after DHE staining to visualize the level of ROS in spermatozoa untreated (control) or treated *in vitro* with 4 mM D-Asp or 2.5 mM NAC or both. (B) The level of DHE fluorescence after 1 hour of treatment given as the mean grey intensity (arbitrary unit in ImageJ), 100 spermatozoa from a pool of spermatozoa collected from 3 males (C) Analysis of the capacitation rate of spermatozoa from 9-week or 16-week-old B6N males that were untreated (control) or treated *in vitro* with 4 mM D-Asp or 2.5 mM NAC or both (200 spermatozoa per dot ($n = 5$ males)). (D) Analysis of the acrosome reaction rate of spermatozoa from 9-week or 16-week-old B6N males that were untreated (control) or treated *in vitro* with 4 mM D-Asp or 2.5 mM NAC or both (200 spermatozoa per dot, 5 males). ** $p < 0.01$, *** $p < 0.001$.

Results

The acrosome reaction was also measured (Figure 16D). In 9-week-old males, the acrosome reaction rate was significantly higher in spermatozoa treated with D-Asp compared to the control ($42.9 \pm 1.4\%$ vs. $31.5 \pm 1.2\%$, $p < 0.001$). The addition of NAC to D-Asp-treated spermatozoa significantly reduced the rate of the acrosome reaction compared to that of D-Asp-treated spermatozoa ($31.8 \pm 2.7\%$, $p < 0.01$). Co-incubation with NAC alone had no impact on the acrosome reaction rate compared to that of the control ($31.1 \pm 2.9\%$). Even though it was not significant, similar results were obtained in spermatozoa from 16-week-old males: the acrosome reaction rate was higher in spermatozoa treated with D-Asp compared to the control ($45.1 \pm 3.6\%$ vs. $37.6 \pm 2.4\%$). The addition of NAC to D-Asp-treated spermatozoa reduced the rate of the acrosome reaction compared to that of D-Asp-treated spermatozoa ($35.8 \pm 2.7\%$). Co-incubation with NAC alone had no impact on the acrosome reaction rate compared to that of the control ($38.4 \pm 2.7\%$). The acrosome reaction rate was non-significantly higher in spermatozoa from 16-week-old males compared to 9-week-old males in all groups.

4.2 Aim II: To evaluate the fertility and quality of mouse spermatozoa cryopreserved and stored at -80°C

The purpose of Aim II is firstly to compare the effects of the standard LN₂ method with those of the ultra-low freezer (-80°C) method for sperm cryopreservation and storage over a period of 1 to 12 months in 6 different mouse strains. The latter represent the genetic backgrounds of the genetically engineered mice that are most commonly used for biomedical research. Spermatozoa from 3 males of each strain were collected, pooled and loaded into straws. Half of the straws was cryopreserved using the standard LN₂ method and the other half was cryopreserved by placing straws directly in an ultra-low freezer at -80°C. In all analyses except fertility, the control straw in LN₂ was thawed after 12 months of storage. In contrast, the -80°C straws were thawed at the appropriate time points within the 1-12 month storage period. We assumed that spermatozoa would remain stable over time when cryopreserved and stored in LN₂ in all mouse strains.

4.2.1 The fertility rate is stable over time when spermatozoa are cryopreserved and stored at -80°C except in B6J and BALB/c strains

Sperm fertility was analysed by performing *in vitro* fertilisation (IVF). Figure 17 represents the IVF success rate depending on the cryopreservation method and the storage duration. At 1 month, no difference of the IVF success rate was found in all mouse strains when comparing LN₂ and the -80°C conditions. Regarding the storage duration, no decline of fertility was observed in spermatozoa from B6N, CD-1, FVB and 129 mice when they were stored at -80°C compared to LN₂. However, concerning B6J and BALB/c, sperm fertility significantly decreased when spermatozoa were stored at -80°C compared to LN₂ (B6J at 6 months: 49.0 ± 3.0% vs. 66.4 ± 4.1%, $p < 0.001$, BALB/c at 3 months: 54.8 ± 3.0% vs. 66.2 ± 4.9%, $p < 0.01$). Moreover, the IVF success rate of spermatozoa from BALB/c stored in LN₂ decreased from 74.8 ± 3.3% at 1 month to 48.4 ± 2.6% at 12 months.

4.2.2 The percentage of dead spermatozoa increases in B6J and BALB/c when sperm samples are cryopreserved and stored at -80°C

Sperm viability was examined by flow cytometry with two DNA-binding dyes, SYBR 14, which stains the nuclei of living cells and propidium iodide, which stains the nuclei of dead cells. The results are shown as percentages of dead spermatozoa (Figure 18). The percentage of dead spermatozoa remained relatively stable over time at -80°C compared to LN₂ in B6N, CD-1, FVB and 129. However, the percentage of dead spermatozoa was significantly higher at -80°C compared to LN₂ in samples from B6J (after 6 months: 67.7% vs. 52.5%, $p < 0.01$)

Results

and BALB/c (after 3 months: 43.6% vs. 31.5%, $p < 0.05$). In addition, the percentage of dead spermatozoa negatively correlates with the success of IVF in B6J and BALB/c (Appendix 2).

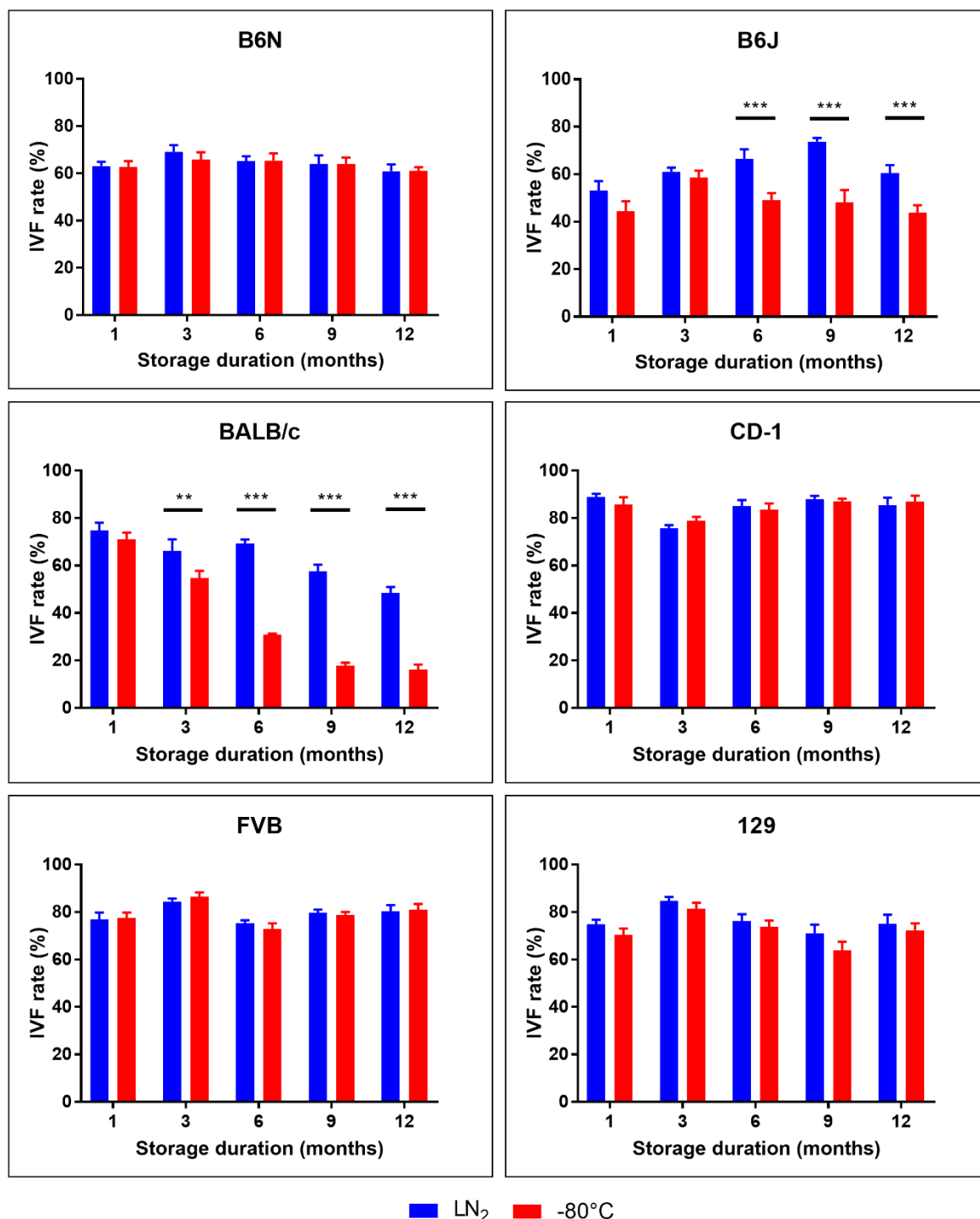


Figure 17: Effect of cryopreservation and storage temperature on sperm fertility. Sperm suspensions from B6N, B6J, BALB/c, CD-1, FVB and 129 mice cryopreserved in LN₂ or at -80°C and then stored for 1 to 12 months were co-incubated with oocytes. The IVF success rate corresponds to the resulting 2-cell embryos (considered as fertilised oocytes) in 6 assays using a pool of spermatozoa from 3 males. ** $p < 0.01$, *** $p < 0.001$.

Results

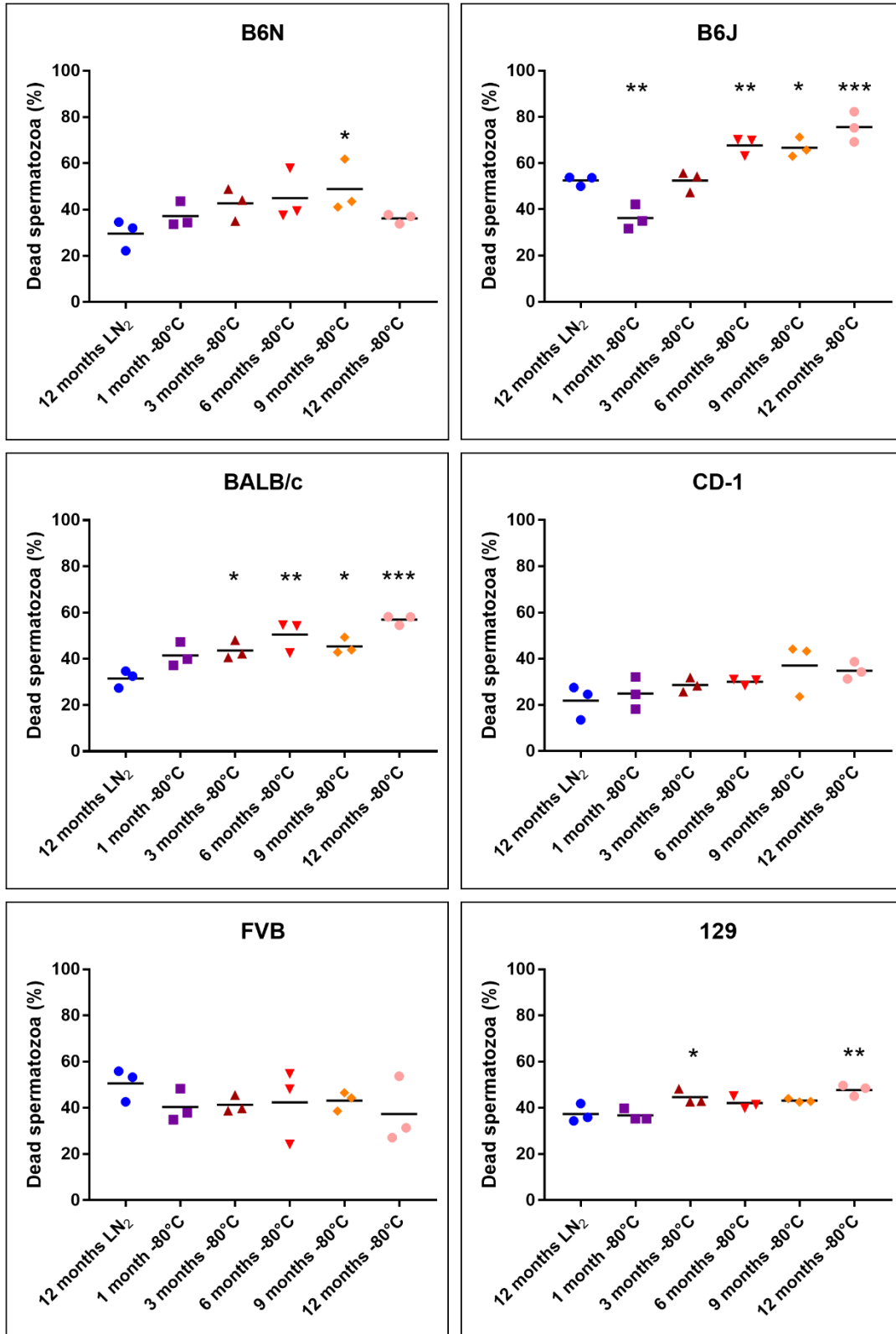


Figure 18: Effect of cryopreservation and storage temperature on sperm viability. Sperm suspensions from B6N, B6J, BALB/c, CD-1, FVB and 129 mice cryopreserved in LN₂ and then stored for 12 months or cryopreserved at -80°C and then stored for 1 to 12 months were analysed by flow cytometry to detect dead spermatozoa (10,000 events per assay, 3 assays using a pool of spermatozoa from 3 males). * $p < 0.05$, ** $p < 0.01$ and *** $p < 0.001$.

4.2.3 Cryopreservation and storage at -80°C decreases the sperm motility in all strains

The total motility of the sperm samples was measured using the Hamilton Thorne IVOS semen analyzer. In Figure 19, the total motility of spermatozoa cryopreserved and stored for one year in LN₂ (blue bars) was the highest in B6N and 129 compared to the other mouse strains, where more than 20% of spermatozoa had a velocity above 7.4 µm/s. Spermatozoa from BALB/c showed the lowest total motility (less than 10% of spermatozoa had a velocity above 7.4 µm/s). The total motility was always lower in the -80°C groups (storage for 1, 6 and 12 months) compared to LN₂ (storage for 12 months). Notably, when spermatozoa were cryopreserved and stored for 1 month at -80°C compared to LN₂, we obtained a 2-fold decrease of B6N sperm motility (from 24% to 12%). Similarly, we obtained a 1.25-fold decrease in B6J (from 10% to 8%), a 1.17-fold decrease in BALB/c (from 7% to 6%), a 1.63-fold decrease in CD-1 (from 13% to 8%), a 1.25-fold decrease in FVB (from 15% to 12%) and a 1.77-fold decrease in 129 (from 23% to 13%). However, the total motility was maintained over time (from 1 to 12 months) at -80°C except in B6J (from 8% at 1 month/-80°C to 4% at 12 months/-80°C).

4.2.4 The percentage of abnormalities is higher in all strains when spermatozoa are cryopreserved and stored at -80°C

Spermatozoa were classified depending on the nature of abnormalities (of the head and/or the tail and head detached, see Figure 10A) and the results are shown in Figure 20. Regarding the LN₂ condition after 1 year of storage, the percentage of total abnormalities was approximately 20% in all mouse strains except in B6J and BALB/c, where 29.2% and 41.6%, respectively, of spermatozoa had at least one morphological abnormality. For all strains except BALB/c, the total abnormality is increased but not significant between 12 months in LN₂ and 1 month at -80°C (from 18.8% to 25.6% in B6N, from 29.2% to 35.7% in B6J, from 22.5% to 27.7% in CD-1, from 24.9% to 28.5% in FVB and from 20.8% to 28.4% in 129). However, a prolonged period of storage of 12 months at -80°C significantly increased the percentage of total abnormalities in spermatozoa in all strains. Spermatozoa from BALB/c showed a significant increase in total abnormalities as soon as after 1 month of storage at -80°C compared to LN₂ (from 41.6% to 53.3%, $p < 0.05$). Also, specifically in BALB/c, most of the abnormalities were found in the head of the spermatozoa (above 20%, represented by the red triangles) compared to the tail (less than 15%, represented by the blue squares). In all other strains, most of the abnormalities were found in the tail of the spermatozoa.

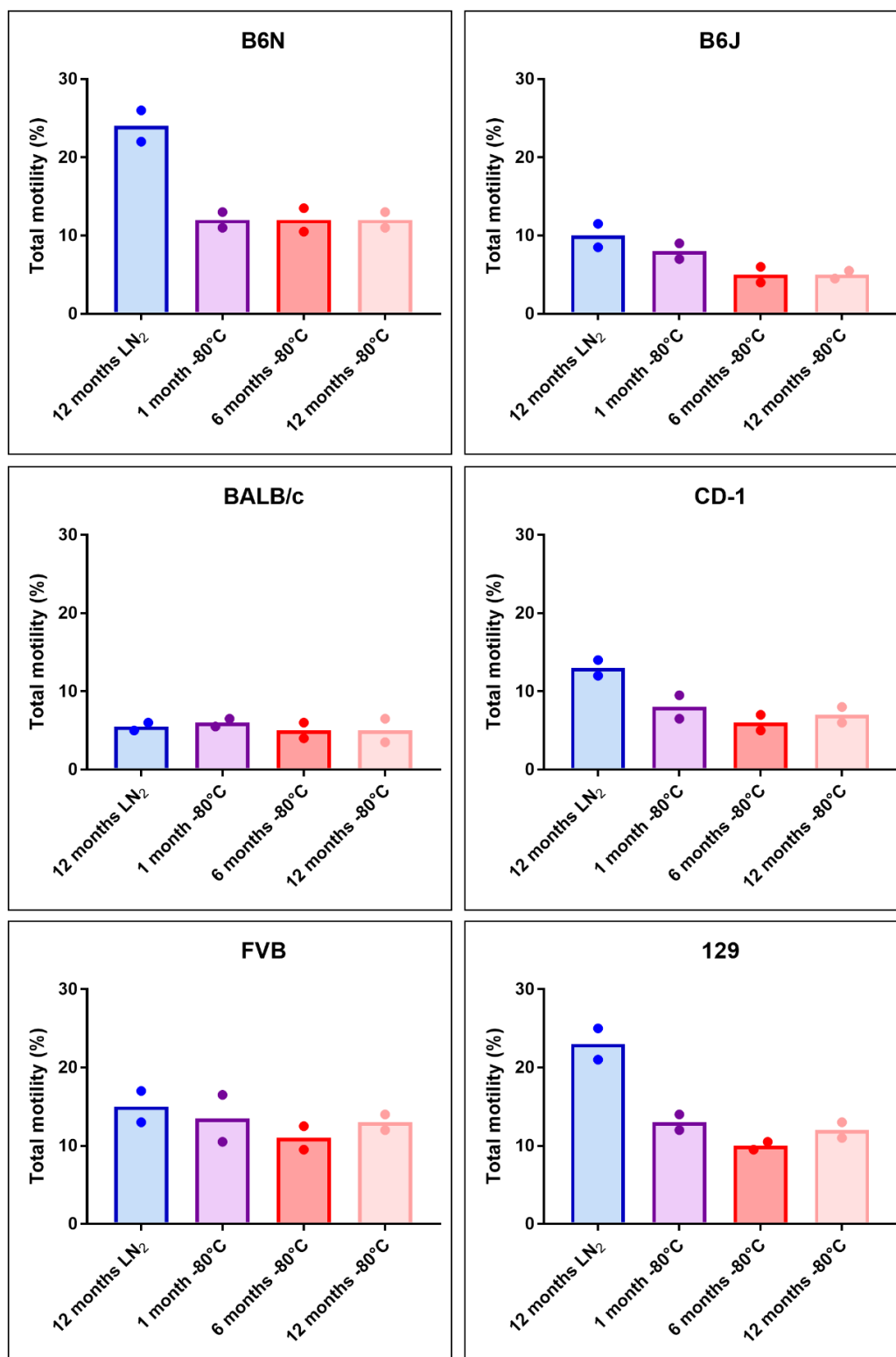


Figure 19: Effect of cryopreservation and storage temperature on sperm total motility. Total motility of spermatozoa from B6N, B6J, BALB/c, CD-1, FVB and 129 mice cryopreserved in LN₂ and then stored 12 months or cryopreserved at -80°C and then stored for 1 to 12 months was measured using the Hamilton Thorne IVOS sperm analyzer (mean of 2 measurements from a pool of 3 males). Spermatozoa are considered motile when their velocity is above 7.4 μm/s in any direction.

Results

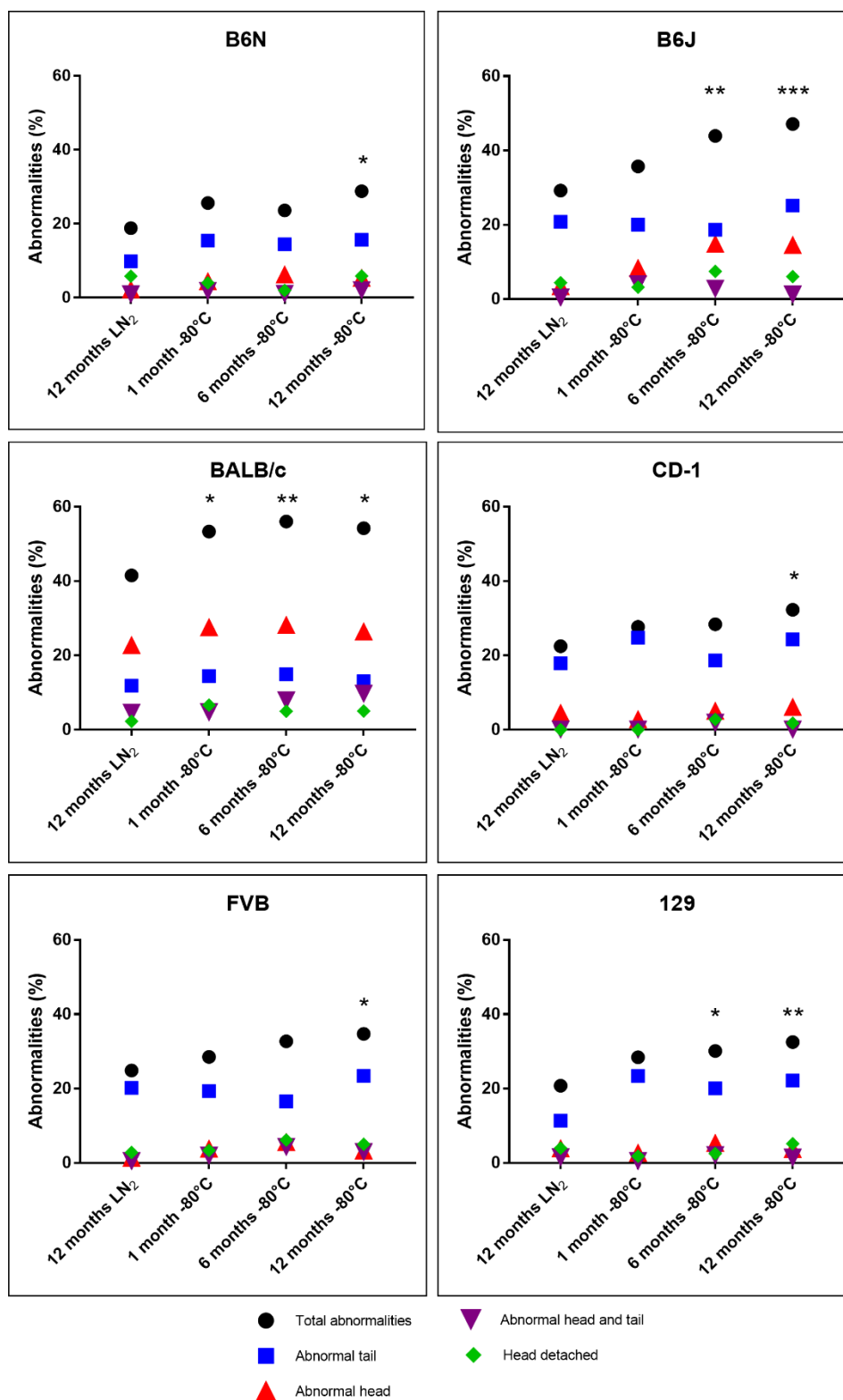


Figure 20: Effect of cryopreservation and storage temperature on sperm morphology. Spermatozoa from B6N, B6J, BALB/c, CD-1, FVB and 129 mice cryopreserved in LN₂ and then stored for 12 months or cryopreserved at -80°C and then stored for 1 to 12 months were classified depending on their morphology (see images Figure 2A). Results are shown as percentage of abnormal spermatozoa found in each condition and strain. A total of 200 spermatozoa was examined from a pool of 3 males. * $p < 0.05$, ** $p < 0.01$ and *** $p < 0.001$.

4.2.5 The sperm ultrastructure is damaged after cryopreservation and storage at -80°C

Ultrastructural damage was analysed based on transmission electron microscopy images. Spermatozoa were classified into class I (intact), class II (lightly damaged) and class III (heavily damaged) as shown in Figure 21A. Two different organelles were examined, the nucleus and mitochondria, as well as the plasma membrane. On the representative images, the nucleus of the spermatozoa is black. The plasma membrane around the nucleus was considered intact (class I), waved (class II, orange arrow) or broken (class III, red arrow). Mitochondria were also visible with transversal section of the midpiece of the spermatozoa. They were considered as intact (class I), lightly damaged with loss of cristae and roundness (class II, orange arrow) or heavily damaged with considerable loss of cristae and roundness (class III, red arrow).

Figure 21B represents the classification of spermatozoa from each strain depending on the cryopreservation method and storage duration. The percentage of heavily damaged spermatozoa (class III) significantly increased when spermatozoa were cryopreserved at -80°C and stored for 1 month at this temperature compared to LN₂ in all mouse strains. We also observed a gradual increase of class III spermatozoa over time at -80°C for most of the strains. The opposite effect was seen concerning intact (class I) spermatozoa. Finally, the highest rate of sperm ultrastructural damage in LN₂ and at -80°C was found in BALB/c. Notably, 71.4% of BALB/c spermatozoa were damaged (class II + class III) after 1 year at -80°C, in contrast to only 20.0% in B6N.

4.2.6 The DNA fragmentation level is higher in spermatozoa cryopreserved at -80°C in all strains

The comet assay detects DNA breaks at the level of individual cells. When DNA is fragmented, it migrates out of the nucleus under electrophoresis to form a comet tail visible with a DNA binding dye, as seen in Figure 22A. The tail moment, corresponding to the level of DNA fragmentation, of spermatozoa from each strain and condition is presented in Figure 22B. In all strains, the level of DNA fragmentation was significantly higher when spermatozoa were cryopreserved and stored at -80° compared to LN₂. In B6N males, the tail moment increased 15.7-fold in spermatozoa stored for 1 year at -80°C compared to 1 year in LN₂ (1.1 ± 0.2 A.U. vs. 17.9 ± 3.4 A.U.). In BALB/c, the level of DNA fragmentation of the spermatozoa was the highest, with values of tail moment being more than thirty times higher than that in B6N (163.1 ± 11.7 A.U. vs. 4.5 ± 0.8 A.U.) when they were cryopreserved and stored for 1 month at -80°C.

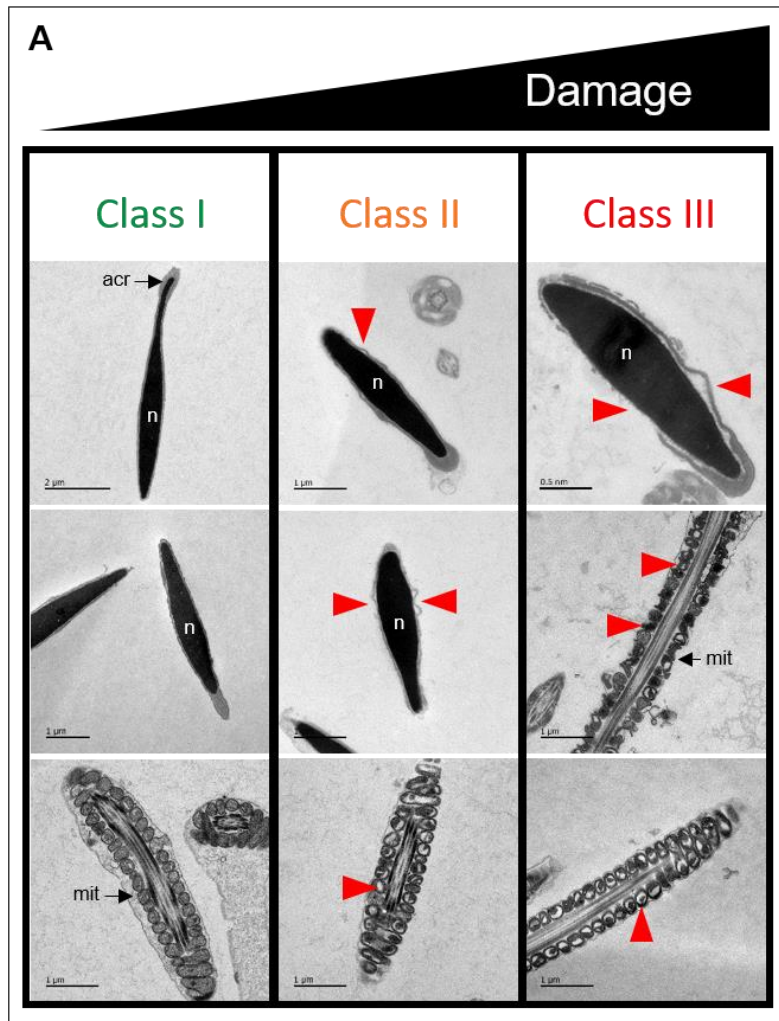


Figure 21A: Effect of cryopreservation and storage temperature on sperm ultrastructure. Transmission electron microscopy images of longitudinal sections of spermatozoa from B6N, B6J, BALB/c, CD-1, FVB and 129 males cryopreserved in LN₂ and then stored 12 months or cryopreserved at -80°C and then stored for 1 to 12 months were obtained, focusing on the head of the spermatozoa and the midpiece that contains mitochondria. Spermatozoa were classified depending on the ultrastructural damage found: class I have an intact or slightly waved plasma membrane and intact mitochondria, class II have heavily waved plasma membrane (arrowhead) without breaks and/or mitochondria with minor abnormalities (arrowhead showing loss of cristae), and class III have significant disturbances, damages and breaks of the plasma membrane (arrowhead) and/or major abnormalities of the mitochondria (arrowhead for abnormal shape and loss of cristae); n: nucleus, acr: acrosome, mit: mitochondria.

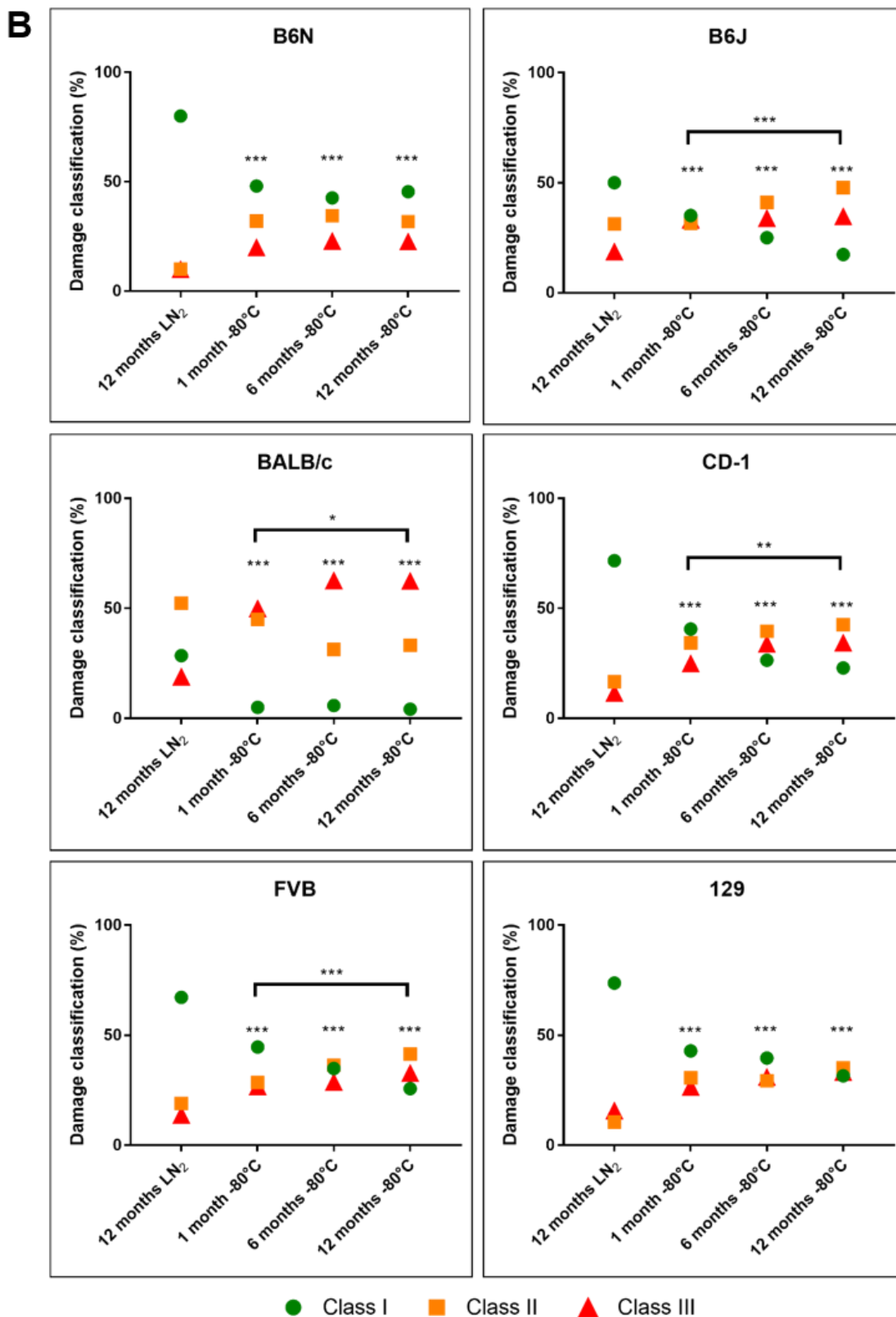


Figure 21B: Effect of cryopreservation and storage temperature on sperm ultrastructure. Percentage of class I, class II and class III spermatozoa depending on the cryopreservation method in each strain, 50 to 70 spermatozoa were examined from a pool of 3 males. * $p < 0.05$, ** $p < 0.01$ and *** $p < 0.001$.

Results

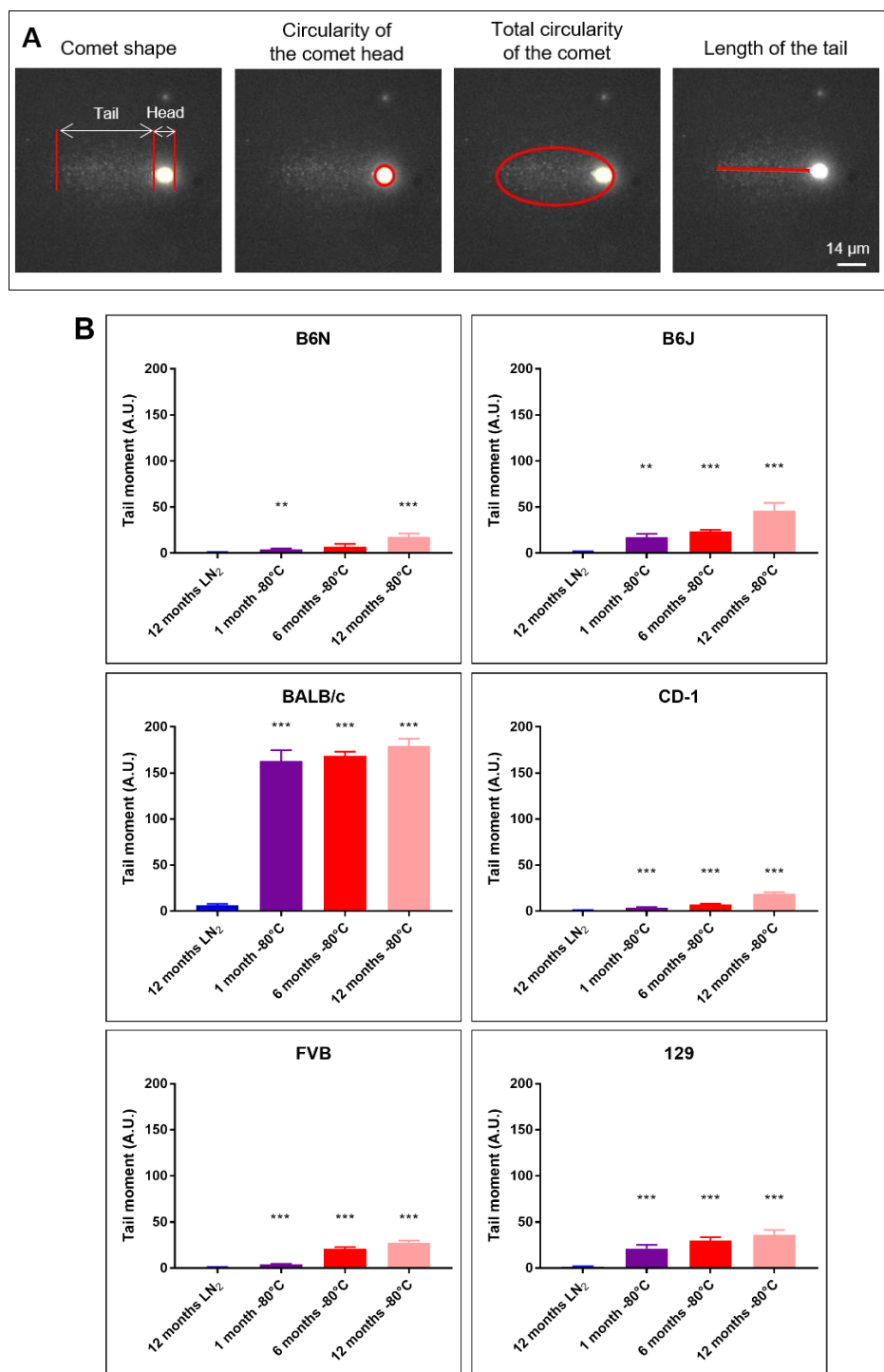


Figure 22: Effect of cryopreservation and storage temperature on sperm DNA fragmentation levels. DNA fragmentation of spermatozoa from B6N, B6J, BALB/c, CD-1, FVB and 129 mice cryopreserved in LN₂ and then stored for 12 months or cryopreserved at -80°C and then stored for 1 to 12 months was analysed with the comet assay and quantified with the calculation of the tail moment, which corresponds to the extent of DNA damages in individual spermatozoon. (A) Visualisation of a spermatozoon with DNA fragmentation following the comet assay. The comet shape can be divided in 2: the tail and the head of the comet. Then, measurements used to calculate the tail moment (circularity of the head, total circularity of the comet and length of the comet tail) were performed with the ImageJ software. (B) Tail moment of 30 spermatozoa from a pool of 3 males in each group. * $p < 0.05$, *** $p < 0.001$.

4.2.7 Summary of significant negative impact of sperm cryopreservation and storage in -80°C compared to LN_2

Table 3 summarises the results of Figures 17, 18, 19, 20, 21 and 22. The data showed that spermatozoa from B6N, CD-1, FVB and 129, in contrast to B6J and BALB/c, can be cryopreserved and stored for up to one year at -80°C without negatively impacting the IVF success rate and viability. However, a decrease of sperm motility and morphology, and an increase of ultrastructural damage and DNA fragmentation, were observed in spermatozoa cryopreserved and stored at -80°C compared to LN_2 in all strains.

Table 3: Summary of significant negative impact of sperm cryopreservation and storage at -80°C compared to LN_2 .

Strain	Months at -80°C	IVF	Viability	Motility	Morphology	Ultrastructural damage	DNA fragmentation
B6N	1			●●●		●●●	●●
	6			●●●		●●●	
	12			●●●	●	●●●	●●●
B6J	1		●●	●		●●●	●●
	6	●●●	●●	●●●	●●	●●●	●●●
	12	●●●	●●●	●●●	●●●	●●●	●●●
BALB/c	1			●	●	●●●	●●●
	6	●●●	●●	●	●●	●●●	●●●
	12	●●●	●●●	●	●	●●●	●●●
CD-1	1			●●		●●●	●●●
	6			●●●		●●●	●●●
	12			●●	●	●●●	●●●
FVB	1			●		●●●	●●●
	6			●		●●●	●●●
	12			●	●	●●●	●●●
129	1			●●		●●●	●●●
	6			●●●	●	●●●	●●●
	12		●●	●●	●●	●●●	●●●

IVF, viability, morphology and DNA fragmentation: ●: $p < 0.05$, ●●: $p < 0.01$, ●●●: $p < 0.001$

Motility: ●: ratio $\text{LN}_2/-80^{\circ}\text{C} < 1.4$, ●●: $1.4 \leq \text{ratio } \text{LN}_2/-80^{\circ}\text{C} < 2$, ●●●: ratio $\text{LN}_2/-80^{\circ}\text{C} \geq 2$

Ultrastructural damage: ●: damaged spermatozoa $< 65\%$, ●●: $65\% \leq$ damaged spermatozoa $< 80\%$, ●●●: damaged spermatozoa $\geq 80\%$

Studies in Aim 1 showed that in vitro D-Asp treatment increases the quality and the fertility of B6N spermatozoa cryopreserved in LN_2 . In the next section, we investigated whether D-Asp is beneficial in increasing the quality of spermatozoa cryopreserved and stored at -80°C . Hence, spermatozoa from B6N, B6J and BALB/c cryopreserved in LN_2 or at -80°C and stored

for 9 months were treated *in vitro* with D-Asp. Sperm motility, morphology, capacitation and the acrosome reaction were investigated to evaluate the impact of D-Asp on sperm quality.

4.2.8 *In vitro* D-Asp treatment increases the quality of B6J and BALB/c spermatozoa cryopreserved at -80°C

Figure 23A presents the motility of spermatozoa from B6N, B6J and BALB/c which were cryopreserved and stored for 12 months in LN₂ or cryopreserved and stored for 9 months at -80°C. D-Asp treatment, compared to the control, increased the motility of spermatozoa from B6N (26.0% vs. 22.0%), B6J (13.3% vs. 9.0%) and BALB/c (10.5% vs. 8%) when cryopreserved and stored in LN₂. Similar results were obtained when spermatozoa were cryopreserved and stored at -80°C in B6N (15.3% vs. 11.8%), in B6J (8.8% vs. 5.0%) and BALB/c (8.3% vs. 5.8%). A global decrease of sperm motility was seen between -80°C and LN₂ conditions, especially in B6N spermatozoa.

Concerning sperm morphology (Figure 23B), no significant differences were found between D-Asp and control but D-Asp treatment tended to decrease the level of abnormalities of spermatozoa from B6N (14.3% vs. 18.9%), B6J (25.9% vs. 28.6%) and BALB/c (37.4% vs. 40.3%) when cryopreserved and stored in LN₂. Similar results were obtained when spermatozoa were cryopreserved and stored at -80°C in B6N (21.8% vs. 26.6%), in B6J (38.4% vs. 44.1%) and BALB/c (49.8% vs. 55.3%). A global increase of sperm abnormalities was seen between -80°C and LN₂ conditions, especially in BALB/c spermatozoa, that is statistically significant.

4.2.9 *In vitro* D-Asp treatment compensates for the decrease of capacitation and acrosome reaction rate in spermatozoa cryopreserved and stored at -80°C

The capacitation rate (Figure 24A) was measured in D-Asp-treated spermatozoa from B6N, B6J and BALB/c that were cryopreserved and stored for 12 months in LN₂ or cryopreserved and stored for 9 months at -80°C. Controls were not treated with D-Asp. Compared to the controls, in B6N mice, the capacitation rate slightly increased when LN₂-cryopreserved spermatozoa were treated with D-Asp (62.4% vs. 58.6%, $p = 0.2458$). Similar results were obtained with spermatozoa cryopreserved and stored at -80°C (62.5% vs. 58.5%, $p = 0.6403$). In B6J and BALB/c, D-Asp treatment increased the capacitation rate at both temperatures without being significant. Notably, the capacitation rate of B6J spermatozoa cryopreserved at -80°C and treated with D-Asp was comparable to that of B6J spermatozoa, which were cryopreserved in LN₂ and untreated (55.6% vs. 56.8%). The same observation was made in spermatozoa from BALB/c (53.9% vs. 54.6%).

Results

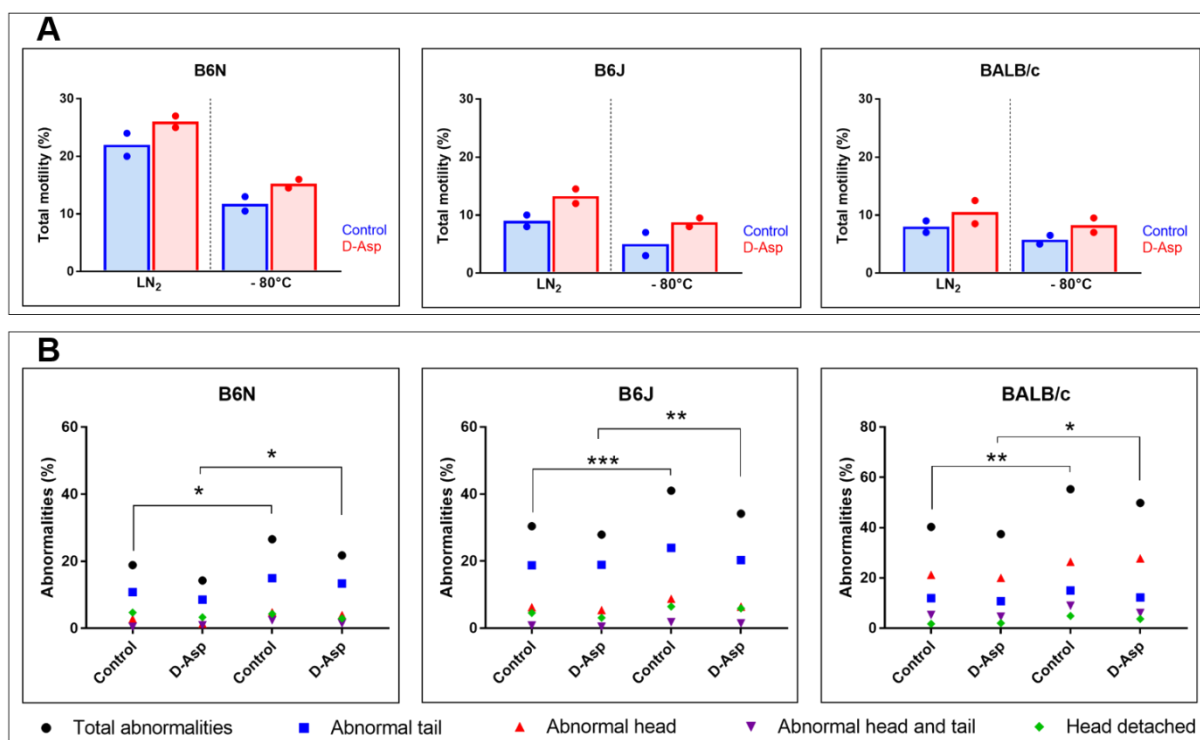


Figure 23: Sperm quality after *in vitro* D-Asp treatment of spermatozoa cryopreserved in LN₂ or at -80°C. Analysis of (A) total motility and (B) morphology of spermatozoa from B6N, B6J and BALB/c males cryopreserved and stored for 9 months in LN₂ or at -80°C, untreated (control) and treated *in vitro* with D-Asp for 1 h, data are shown as 2 counts per category (200 spermatozoa from a pool of spermatozoa collected from 3 males per counting).

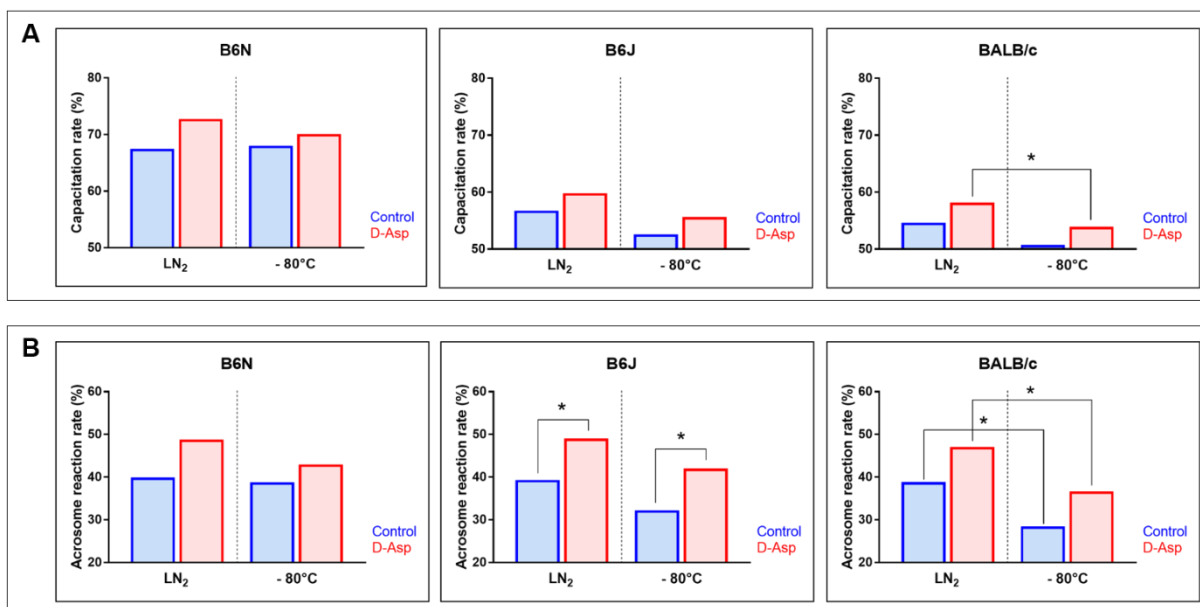


Figure 24: Analysis of capacitation and the acrosome reaction after *in vitro* D-Asp treatment of spermatozoa cryopreserved in LN₂ or at -80°C. Analysis of the capacitation rate (A) and the acrosome reaction rate (B) of spermatozoa from B6N, B6J and BALB/c males cryopreserved and stored for 9 months in LN₂ or at -80°C, untreated (control) or treated *in vitro* with D-Asp for 1 h (200 spermatozoa from a pool of 3 males analysed), * $p < 0.05$

Results

Concerning the difference between LN₂ and -80°C, in control B6N spermatozoa, the capacitation rate was similar at both cryopreservation temperatures (58.6% vs. 58.5%) as well as in D-Asp-treated groups (62.4% vs. 62.5%). However, in B6J control groups, the capacitation rate of spermatozoa cryopreserved and stored at -80°C was lower than that of spermatozoa cryopreserved and stored in LN₂ (52.6% vs. 56.8%, $p = 0.0762$) as well as in D-Asp groups (55.6% vs. 59.8%, $p = 0.1652$). Similar results were obtained in BALB/c control groups (50.7% vs. 54.6%, $p = 0.0859$) and D-Asp groups (53.9% vs. 58.1%, $p = 0.0259$).

Similar results to those regarding the capacitation rate were obtained concerning the acrosome reaction (Figure 24B). In B6N, B6J and BALB/c mice, the acrosome reaction rate increased following D-Asp treatment at both cryopreservation temperatures but was only significant in B6J mice (49.0% vs. 39.3%, $p < 0.05$ in the LN₂ group and 42.0% vs. 32.2% in the -80°C group, $p < 0.05$). In B6J and BALB/c, the acrosome reaction rate was lower in spermatozoa kept at -80°C than in LN₂ in the control groups (in B6J: 32.2% vs. 39.3% and in BALB/c: 28.4% vs. 38.8%, $p < 0.05$) as well as in D-Asp-treated groups (in B6J: 42.0% vs. 49.0% and in BALB/c: 36.7% vs. 47.1%, $p < 0.05$). Finally, the acrosome reaction rate of B6J spermatozoa cryopreserved at -80°C and treated with D-Asp was comparable to B6J spermatozoa, which were cryopreserved in LN₂ and untreated (42.0% vs. 39.3%). The same observation was made in spermatozoa from BALB/c (36.7% vs. 38.8%).

5. Discussion

5.1 D-Asp improves cryopreserved sperm quality by increasing ROS levels

Cryopreservation is the most efficient way to archive the large number of mouse lines that are available in mouse repositories. Sperm cryopreservation appears to be the preferred method as it is easier, faster and cheaper than embryo or oocyte cryopreservation. Combined with IVF and embryo transfer, it allows the reestablishment of mouse lines on demand, thus reducing the number of live animals used in biomedical research. However, the success rate of IVF with cryopreserved spermatozoa is still limited by cryoinjury and poor survival rate of these cells compared to IVF with fresh spermatozoa [44, 113]. The recent introduction of D-Asp treatment gave very promising results to easily improve the fertility of cryopreserved mouse spermatozoa [158]. However, the mechanisms by which D-Asp supports sperm function after cryopreservation remain poorly understood. Our initial hypothesis was that D-Asp treatment increases spermatogenesis, which in turn would increase IVF success rates after sperm cryopreservation. However, D-Asp administered orally for 2 or 4 weeks to 9-week-old and 16-week-old B6N males had no effect on sperm concentration (Figure 8). Therefore, D-Asp did not influence spermatogenesis under our conditions, in contrast to previous studies claiming that D-Asp improves spermatogenesis by increasing testosterone levels [152-154, 156, 160]. This discrepancy could be explained by the duration of D-Asp treatment in our experimental setup, which was maybe too short to increase sperm concentration. Spermatogenesis is a 5-week process, while we treated animals for 2 or 4 weeks. A longer treatment period may be needed to observe a significant increase in sperm concentration. However, 2 weeks of D-Asp enhanced the morphology and increased the capacitation and acrosome reaction rate of cryopreserved spermatozoa (Figures 10 and 11). Total and progressive motility were increased in both age groups after 4 weeks of D-Asp treatment (Figure 9). For the analysis of concentration and motility, 2 measurements were performed from the same sample (Figures 8 and 9). This limits the ability to perform statistical analyses, but our results are robust because the samples correspond to a pool of spermatozoa collected from 3 different males, which reduces the effect of individual variation when performing analyses. Collectively, our results show that D-Asp improves the quality of cryopreserved spermatozoa. Therefore, the increased fertility rate previously reported with D-Asp treatment may be due to an improvement in sperm quality, rather than in spermatogenesis [153, 165] (Figure 25). In this sense, it is well established that sperm quality is a major factor influencing fertility. For example, poor motility and structural defects affect fertility [57, 177, 178]. Moreover, maturation steps (capacitation and acrosome reaction) are absolutely necessary for

fertilisation [69]. The present results suggest that the improvement of motility, morphology, capacitation and acrosome reaction rate by D-Asp contributes to the better IVF success observed in cryopreserved spermatozoa treated with this compound. Therefore, the addition of 20 mM of D-Asp in the drinking water is a simple and inexpensive protocol (less than 1€/male/week) to improve the reproductive performance of B6N mice, even before they reach 13 weeks, the ideal age for sperm cryopreservation. This method would improve ARTs methodology and can be easily implemented in mouse repositories. It has the advantages of limiting the number of oocyte donors for embryo production and facilitating sperm cryopreservation in sexually but not fully mature males.

D-Asp is known to act on peripheral tissues via endocrine signalling but little is known about its direct effect on spermatozoa. Therefore, we treated spermatozoa directly with D-Asp. Interestingly, *in vitro* D-Asp treatment increased the capacitation and the acrosome reaction rate of cryopreserved spermatozoa in both age groups (Figure 11). We conclude that D-Asp can enhance sperm quality in a cell-autonomous manner not related to the endocrine signalling. Previous studies have reported an increase in oxidative stress markers and ROS levels in the testis following *in vivo* and *in vitro* D-Asp treatment in rats [166, 167]. We could recapitulate these observations since *in vivo* and *in vitro* D-Asp treatments increased the level of DHE staining and DNA oxidation in cryopreserved spermatozoa and no difference was found between age groups (Figures 12, 13, 14 and 15). Therefore, D-Asp seems to stimulate the production of ROS regardless of the age of the males. This led us to the hypothesis that D-Asp improves sperm function by inducing mild oxidative stress. The addition of the antioxidant NAC decreased the level of D-Asp-induced DHE staining and suppressed the beneficial effect of D-Asp on sperm capacitation and the acrosome reaction (Figure 16). NAC alone had no deleterious effect on capacitation and acrosome reaction, showing that the reduction in capacitation and acrosome reaction rate seen in animals treated simultaneously with D-Asp and NAC was not due to a toxic effect of the latter. In conclusion, this work supports a model in which D-Asp enhances sperm quality by increasing ROS levels, thereby contributing to a higher fertilisation rate.

Possible mechanisms by which D-Asp increases ROS levels in spermatozoa

D-Asp can be metabolised by the D-Asp oxidase (DDO or D-AspO), which converts it to oxaloacetate, NH_3 and H_2O_2 [142]. The concentration of DDO is known to be increased following D-Asp treatment in the testes of wild-type animals and rats [166, 179]. Therefore, D-Asp may be a direct source of ROS (H_2O_2) through the activity of DDO (Figure 25).

Another possibility is the elevation of ROS through the activation of NMDA receptors (NMDARs). Indeed, D-Asp is known to activate NMDARs in rat testis [146, 158]. Moreover, NMDARs are found on spermatogonia adjacent to the basement membrane and in the

membrane of rat spermatozoa [145]. Several studies have reported that NMDARs activation leads to an increase in hydrogen peroxide (H_2O_2), superoxide anion (O_2^-) and nitric oxide (NO) levels via NADPH oxidase (NOX2), which is involved in the NMDARs signalling pathway [180-182]. Thus, D-Asp may act through NMDARs to increase the concentration of ROS such as H_2O_2 , O_2^- and NO in spermatozoa (Figure 25).

Further experiments are therefore needed to understand the precise mechanism by which D-Asp increases ROS production and to identify which ROS are generated by D-Asp. The DHE staining used in this study reveals the presence of ROS without distinguishing their nature, as the fluorescent products are formed by a non-specific redox reaction [174]. However, ROS form a complex group, in which radicals such as O_2^- and non-radicals such as H_2O_2 have different targets and different purposes. The effect of NAC shows that at least one ROS corresponds to H_2O_2 because NAC promotes the synthesis of glutathione (GSH), which is involved in the cellular removal of H_2O_2 [176]. However, NAC is also a substrate of several antioxidant enzymes that remain to be defined. Identification of specific ROS with kits targeting individual ROS or, although much more expensive, electron-spin resonance spectroscopy would be preferable compared to an analysis of DHE staining [183, 184].

ROS may improve cryopreserved sperm quality

ROS are well known to contribute to physiological and pathological conditions. Low levels of ROS, considered as oxidative eustress, can activate signalling pathways and participate in biological processes. High levels of ROS referred to as oxidative stress, induce significant damage to DNA, proteins and lipids and are ultimately associated with cell death [185]. In the field of reproductive biology, the impact of oxidative stress on male fertility has been studied since the mid-20th century [186]. There are many reports indicating that spermatozoa are vulnerable to oxidative stress, particularly due to lipid peroxidation in their membrane. The latter is responsible for male infertility problems in humans and many other different species [187-192]. Recently, the essential physiological function of ROS in reproduction and sperm function has been of interest regarding testosterone production, spermatogenesis, sperm DNA condensation, sperm motility, capacitation, acrosome reaction and sperm-oocyte fusion [78, 82-88]. ROS are therefore actively involved in promoting sperm quality under physiological conditions. A mild increase in ROS may improve these processes and contribute to better sperm recovery after sperm cryopreservation (Figure 25).

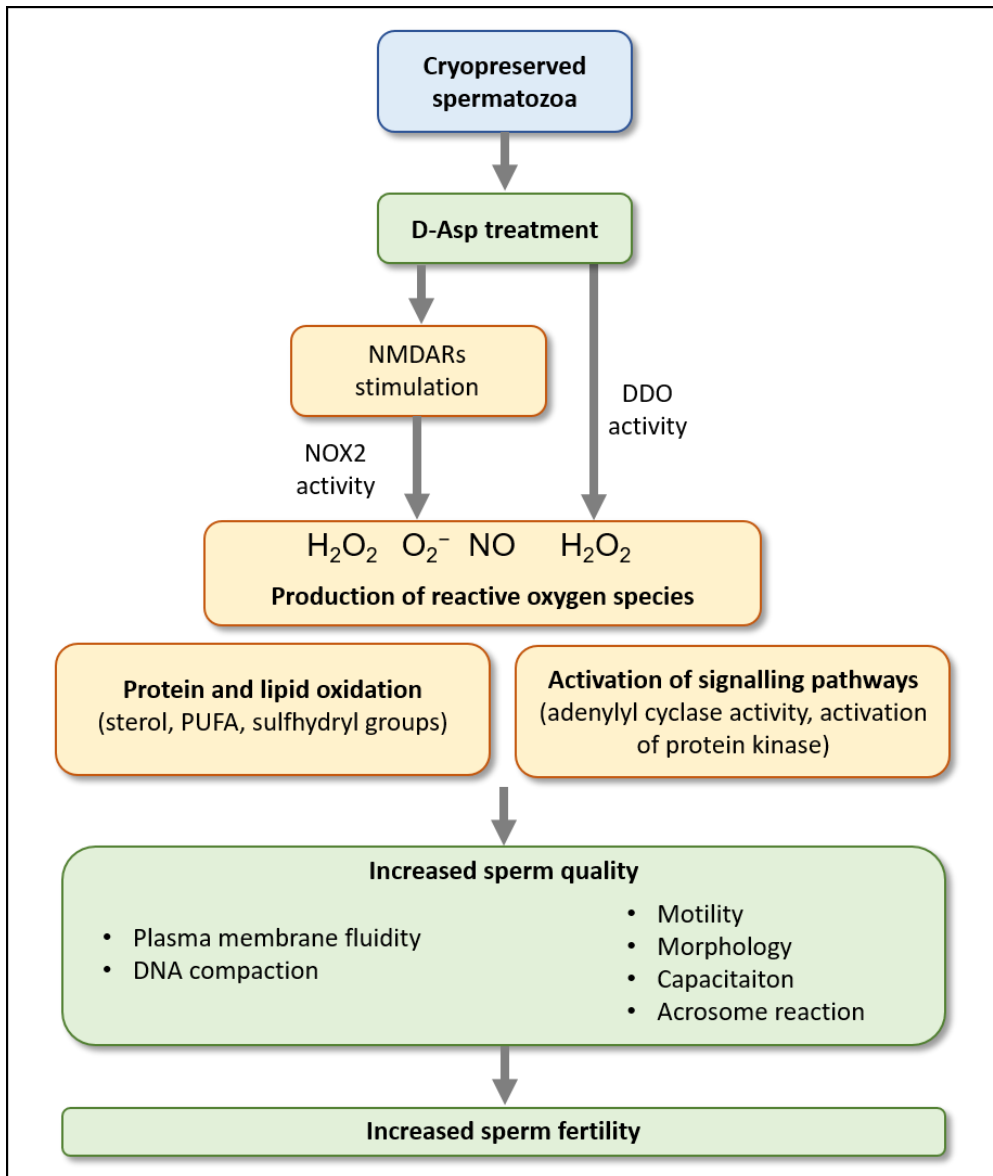


Figure 25: Working model of the effect of D-Asp on cryopreserved spermatozoa. D-Asp treatment of cryopreserved and thawed spermatozoa may increase the levels of reactive oxygen species through the activation of NMDARs and via its metabolism by DDO. Activation of redox signalling pathways and the oxidation of targeted proteins and lipids may result in increased membrane fluidity and DNA compaction. This process may contribute to better recovery of spermatozoa after cryopreservation, thereby improving overall sperm quality. As a result, higher sperm quality would have a greater chance of fertilising oocytes. (DDO: D-Asp oxidase; NOX: NADPH oxidase; NMDARs: NMDA receptors; PUFA: polyunsaturated fatty acids).

The majority of cryodamage observed in sperm cryopreserved in LN₂ corresponds to defects in plasma membrane integrity, decreased sperm motility and DNA fragmentation [106, 108]. More specifically, the cryopreservation and thawing procedures are known to harden the plasma membrane, thereby leading to a loss of integrity [193]. The ability of spermatozoa to resist cryopreservation-induced stress is associated with a higher plasma membrane fluidity, which is notably dependent on membrane composition, such as the level of cholesterol, the

degree of fatty acid unsaturation, as well as protein and phospholipid composition [193-195]. Interestingly, H_2O_2 and O_2^- are known to increase the activity of phospholipase A2 by activating kinases such as PKC and inhibiting phosphatase, resulting in higher plasma membrane fluidity of spermatozoa [78, 196, 197]. Therefore, ROS-dependent increase in plasma membrane fluidity may protect it from cryodamage. In addition, H_2O_2 participates in the sulfhydryl oxidation (or sulfoxidation) that regulates the formation of disulfide bridges of sperm protamine, which is required for DNA compaction, and flagellar proteins, which are required for the acquisition of progressive motility [78]. A slight increase in ROS may result in higher motility, promoting sperm fertility, and higher DNA compaction, protecting against cryoinjury and DNA fragmentation.

Limitations of D-Asp treatment duration and age-related differences in sperm quality

D-Asp treatment for 4 weeks, as opposed to 2 weeks, gave in some aspects ambivalent results. It improved total and progressive sperm motility in both age groups and increased the acrosome reaction rate, especially in 9-week-old males (Figures 9 and 11). However, it had a negative effect on sperm morphology and decreased the capacitation rate in 16-week-old males (Figures 10 and 11). The reason for this phenomenon is not clear, but one possible explanation is that the beneficial effects of D-Asp reach a maximum between 2 and 4 weeks of treatment, after which D-Asp could be detrimental due to excessive ROS production. Using *in vitro* assays, the duration of D-Asp incubation impacted the production of ROS: five hours of treatment produced a much higher level of ROS and DNA oxidation than one hour. A detrimental effect of D-Asp was also reported after *in vitro* D-Asp treatment of mouse germ cells by Tomita *et al.* [198]. This study reported a detrimental effect on mitosis in pre-meiotic germ cells following an *in vitro* D-Asp treatment at 10 mM, whereas 1 mM and 5 mM supported this process. This strengthens the hypothesis that prolonged D-Asp treatment leads to higher ROS production, which may negatively affect sperm quality. The age of the males also seems to be important in this phenomenon, as the deleterious effect of D-Asp is specific to older males. Under physiological conditions, D-Asp synthesis, transport and degradation vary with age to modulate D-Asp levels and its physiological role in the testis [198]. Endogenous D-Asp levels in mouse testes increase from 2 to 10 weeks of age and reach a plateau at 10 weeks. The adult mice used in this study were 16 weeks old. At this age, endogenous D-Asp levels have already reached their maximum level. It is possible that 4 weeks of D-Asp supplementation at this age may have exposed the animals to excessive D-Asp, which in turn would be detrimental to spermatozoa. Therefore, the recommendation for mouse repositories would be to treat males with 20 mM D-Asp for 2 weeks regardless of the age, while a 4-week treatment could be used for males younger than 10 weeks. Alternatively, cryopreserved spermatozoa can be incubated with 4 mM of D-Asp for 1 hour prior to IVF.

Finally, sperm quality was not similar in 9- and 16-week-old males. Sperm concentration, motility and maturation are higher in 16-week-old mice compared to 9-week-old mice. This is consistent with previous studies that also reported an increase in these parameters with age [102, 103]. Therefore, sexual development is still ongoing in 9-week-old males. In this context, D-Asp may have a greater beneficial effect on immature spermatozoa, as its range of action is higher at this age than in older males.

5.2 Influence of cryopreservation and storage temperature on sperm integrity and fertility

Advancing the knowledge in the field of IVF involves not only the improvement of cryoprotectants and fertilisation media for oocytes and spermatozoa, but also the development of new cryopreservation methods. Sperm cryopreservation has traditionally been performed using LN₂. However, the use of LN₂ can be challenging for reasons of safety, cost and availability. Available alternatives to LN₂ would be the use of ultra-low temperature freezers. Several studies on sperm cryopreservation and storage at -80°C by Raspa *et al.* have already shown promising results in B6N mice [128, 135, 136, 199]. Therefore, to expand our knowledge on the use of sperm cryopreservation and storage at -80°C, the study was extended to diverse mouse genetic backgrounds, with a focus on sperm quality and integrity, in order to identify potential strain specificity. Finally, the possibility that D-Asp compensates for the impairment of sperm quality caused by cryopreservation and storage at -80°C was investigated.

B6N, CD-1, FVB and 129 spermatozoa can be cryopreserved and stored at -80°C for up to one year without loss of fertility

Cryopreservation and long-term storage at -80°C for up to one year can be considered for spermatozoa from B6N, CD-1, FVB and 129 mouse strains as no decline in fertility was observed (Figure 17). The study also showed that the viability of spermatozoa from these strains was maintained for up to one year at -80°C (Figure 18). However, changes in sperm motility, morphology, ultrastructure and DNA damage were detected in all these mouse strains.

An initial decrease of 40% (on average) in total sperm motility was found when spermatozoa were cryopreserved at -80°C compared to LN₂ (Figure 19). However, the total motility was maintained from 1 to 12 months. This suggests that defects in motility are due to the initial cryopreservation procedure but not to long-term storage at -80°C. Changes in the ultrastructure of the sperm flagella may occur at an early stage of cryopreservation, especially during the cooling phase since mouse sperm motility is known to depend on the cooling rate [104].

A prolonged storage period of 12 months at -80°C significantly increased the percentage of abnormalities (Figure 20). In contrast to motility, our results suggest that the duration of storage but not the initial cryopreservation at -80°C damages sperm morphology in these strains. Studies of sperm cryopreservation and storage at -80°C in other species have not reported an increase in sperm abnormalities. However, the duration of storage was limited to 5 days in mandarin fish [134], 1 month or 3 months in humans [131, 200], and 4 months in dogs and cats [130, 132]). Therefore, it is possible that prolonged storage period at -80°C affects sperm morphology in these species. In addition to morphological abnormalities, increased ultrastructural damage was found already after 1 month of storage at -80°C and continued over time, except for spermatozoa from B6N and 129, where it remained stable from 1 to 12 months (Figure 21). Thus, the ultrastructural damage of spermatozoa seems to depend not only on the cryopreservation temperature, but also on storage duration. Similar cryodamage has been reported in spermatozoa cryopreserved in LN_2 from mice [113], chickens [201] and rams [202]. Thus, a higher cryopreservation temperature may lead to the same type of ultrastructural cryoinjury. Higher DNA fragmentation was also found in spermatozoa cryopreserved and stored at -80°C already after 1 month of storage (Figure 22), which is consistent with a previous study realised in B6N spermatozoa [119]. Since DNA fragmentation is a late-stage marker of apoptosis [121], it is surprising that we did not observe an increase in the percentage of dead spermatozoa with PI and SYBR-14 dual staining. This method detects rupture in plasma membrane integrity of dead cells. However, DNA fragmentation may not always be associated with damaged plasma membrane as membrane-intact spermatozoa can exhibit DNA fragmentation [203].

In conclusion, B6N, CD-1, FVB and 129 spermatozoa can be cryopreserved and stored at -80°C without affecting their fertility but this procedure compromises their quality and integrity (Figure 26).

A decline in sperm quality is not necessarily associated with a decline in IVF success rate

The reason why the decline in sperm motility and integrity observed in B6N, CD-1, FVB and 129 spermatozoa is not associated with loss of fertility is unclear. Considering sperm motility, conflicting results about its association with IVF success rate are found in the literature. Some studies indicate a correlation between sperm motility and IVF success in humans and mice [66, 204, 205]. However, there are also studies in mice where sperm motility did not correlate with the fertilisation rate [118]. Sperm morphology is also considered an important parameter to assess fertility potential [54]. But fertilisation is still possible even in the case of abnormal sperm morphology [206]. Finally, DNA breaks detected by comet assay have been associated with loss of fertility [207].

One possible explanation for the maintenance of the IVF success rate despite sperm abnormalities would be that the remaining intact (or less damaged) gametes are sufficient to support a normal fertilisation rate. Therefore, the concentration of spermatozoa used for IVF would play an important role to compensate for the loss of sperm function due to cryodamage. However, it cannot be excluded that damaged spermatozoa are still capable of fertilising oocytes. In this context, the consequences of altered sperm integrity on offspring are largely unknown. Further analysis is needed to determine the potential consequences of sperm cryodamage on embryo development, birth rate and/or offspring survival and health.

B6J and BALB/c spermatozoa are the most sensitive to temperature

The use of a -80°C freezer for sperm cryopreservation and storage affects the fertility and integrity of mouse spermatozoa in a strain-dependent manner. Indeed, B6J and BALB/c spermatozoa behaved differently from the B6N, CD-1, FVB and 129 strains for most of the parameters studied. First, a decrease in fertility was observed in relation to the duration of storage at -80°C, starting at 6 months for B6J and 3 months for BALB/c (Figure 17). The storage duration at -80°C also affected sperm viability in B6J and BALB/c and the timing corresponded to the decline in sperm fertility (Figure 18). In addition, a correlation was found between IVF success rate and sperm viability for these two strains (Appendix 2), indicating that viability is a critical parameter for IVF success in these genetic backgrounds. The reasons for the increased cell death may be related to the significant damage to the plasma membrane, especially in the acrosome region, resulting in abnormal sperm morphology and susceptibility to DNA fragmentation [121, 208, 209].

In the present study, BALB/c spermatozoa appeared to be the most sensitive to cryopreservation in LN₂ and at -80°C. The lowest motility rate and the highest abnormality rate were obtained in cryopreserved spermatozoa from BALB/c even when LN₂ was used (Figures 19 and 20). Importantly, the type of abnormalities was different in cryopreserved spermatozoa from BALB/c compared to the other strains. The percentage of abnormal head was much higher than the percentage of abnormal tail in BALB/c, while we observed the opposite relationship for the other strains. Furthermore, the percentage of severely damaged spermatozoa and the level of DNA fragmentation were the highest in BALB/c under -80°C cryopreservation conditions (Figures 21 and 22).

D-Asp treatment rescues the quality of spermatozoa cryopreserved and stored at -80°C even in the most sensitive strains

We have previously shown that D-Asp has a beneficial effect on the quality of B6N spermatozoa cryopreserved in LN₂. We therefore investigated whether D-Asp could improve the quality of spermatozoa which are the most sensitive to cryopreservation and storage at -

80°C, namely B6J and BALB/c. Analysis of sperm motility and morphology showed that *in vitro* D-Asp treatment improved these two parameters in these strains at both cryopreservation temperatures (Figure 23). The cryopreservation temperature negatively affects the capacitation and the acrosome reaction rate in B6J and BALB/c spermatozoa, but not in B6N controls (Figure 24). D-Asp treatment rescues capacitation and acrosome reaction rates in all mouse strains under both cryopreservation conditions. Finally, *in vitro* D-Asp treatment in B6J and BALB/c rescues the decrease in sperm motility, morphological integrity, and capacitation and acrosome reaction rates at both cryopreservation temperatures. These are very encouraging results for the development of a LN₂-free cryopreservation method, especially for spermatozoa that are particularly sensitive to cryodamage. Pre-incubation with D-Asp for 1 hour could be recommended before performing IVF. Further studies are therefore needed to determine whether *in vitro* D-Asp treatment of spermatozoa cryopreserved and stored at -80°C results in higher IVF and improves sperm DNA and ultrastructural integrity. Further investigation is required to determine whether the ROS-mediated effect of D-Asp is involved in improving the quality of spermatozoa cryopreserved and stored at -80°C, as it was in the LN₂ condition.

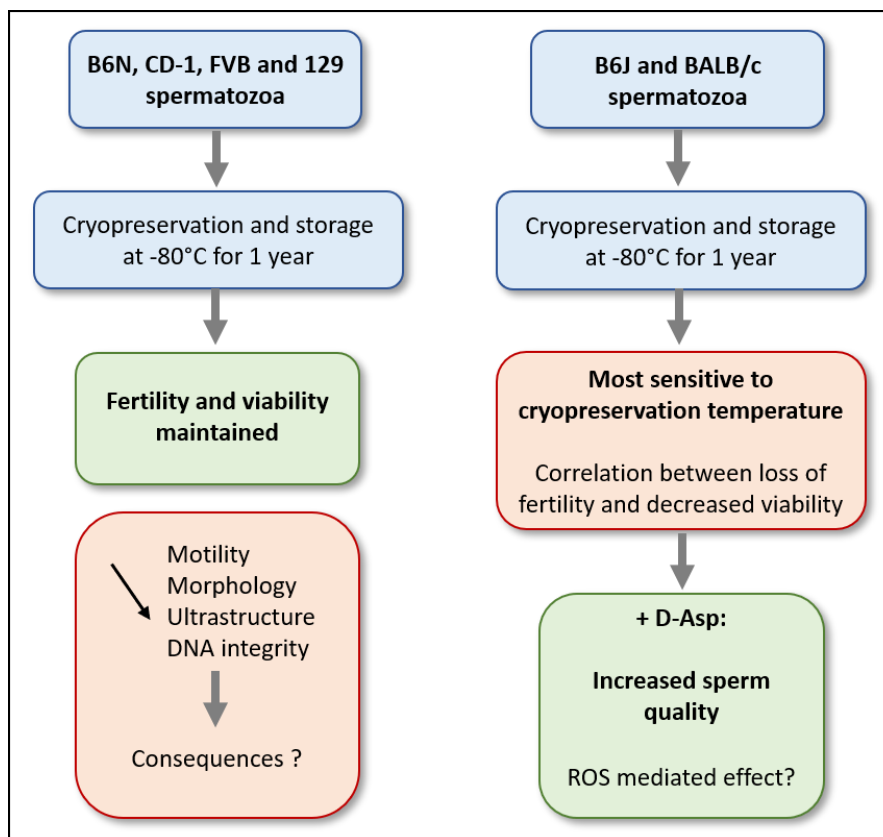


Figure 26: Mouse strain specificities related to sperm cryopreservation and storage at -80°C.

Differences in lipid metabolism may cause cryo-intolerance in B6J and BALB/c

Variations in genomic content and in the regulation of many genes result in phenotypic differences between mouse strains. In particular, differences in sperm physiology, in IVF success and sperm survival rate after cryopreservation in LN₂ depend on the genetic background [22, 39, 210]. Notably, LN₂-cryopreserved spermatozoa from B6J have a lower fertility rate than B6N (51% in B6J compared to 78% in B6N) [211]. Other studies have reported that the BALB/c strain has one of the lowest IVF success rates (48.7% compared to 66.3% in B6J), one of the lowest embryo development rates after transfer of fresh embryos (24.0% of live pups compared to 53.1% in B6J) and only 17.5% of live pups were obtained after transfer of cryopreserved embryos compared to 41.9% for B6J [22, 39]. However, the genetic regions and mechanisms involved in these differences remain to be elucidated. Genetic polymorphisms in the Y chromosome between inbred strains have been associated with differences in sperm quality, in testis weight and sperm count, which may lead to differences in fertility [210, 212]. Specific regions on chromosomes 1 and 11 have been associated with cryodamage of spermatozoa. More specifically, 15 genes have been identified to cause strain-specific differences in fertility using cryopreserved spermatozoa and at least 7 of them have a polymorphism in B6J [118]. Of these, *Soat1* is located on chromosome 1. *Soat1* encodes for the sterol O-acyltransferase 1, which is implicated in cholesterol metabolism and the regulation of plasma membrane fluidity and integrity [213]. Indeed, genetic studies in B6J mice have revealed major defects in lipid metabolism in this strain. Mutations in the nicotinamide nucleotide transhydrogenase (*Nnt*) gene, coding for a protein of the inner mitochondrial membrane implicated in the production of NADPH, contribute to obesity and various metabolic abnormalities specific to B6J [214]. In the BALB/c strain, studies show variation in plasma and liver cholesterol levels under a high-fat diet in male BALB/c compared to male B6J [215]. In addition, a naturally occurring mutation of the Niemann-Pick type C1 intracellular cholesterol transporter 1 (*Npc1*) gene leads to a dysregulation of cholesterol metabolism, making the use of this mutant ideal for studying human intracellular cholesterol trafficking disorders [216-219]. All of these differences in lipid metabolism suggest, as in B6J, potential differences in sperm lipid membrane composition and fluidity compared to other mouse strains. All of these associations point towards a key role for lipid metabolism in the resistance to cryodamage. Since lipids are key components of biological membranes and cryodamage of the plasma membrane has been linked to the degree of membrane fluidity [193-195], it is possible that strain-specific defects in lipid metabolism may be involved in the cryo-intolerance of B6J and BALB/c spermatozoa. Finally, this supports the hypothesis that the increased plasma membrane fluidity associated with ROS activity may be involved in the recovery after loss of sperm plasma membrane integrity.

5.3 Can D-Asp treatment of cryopreserved sperm be of interest for human health?

In the European Union, the human fertility rate is currently below the replacement level of 2.1 children per woman, which can be partly explained by fertility problems [220]. It is well known that male fertility is declining. The meta-analysis carried out over a period of approximately 40 years (1973-2011) shows a decline in sperm concentration of 1.4% per year and 52% during this period in Western countries [221]. A general estimation indicates that 5-8% of men of reproductive age are subfertile (reduced fertility) or infertile [111]. Another important trend observed nowadays is a delay in child conception. In the USA, the birth rate among men over 35 has increased by 40% since 1980 [222]. However, changes in semen parameters have been described as men age, with a decrease in volume, motility and normal morphology in men over 50 [223]. Other human studies have reported a loss of function of the sexual organs, dysfunction of the reproductive endocrine system and damage to sperm DNA [224-227]. Diseases, genetic abnormalities, environmental chemicals and obesity are also some of the reasons for men fertility decline [220, 228, 229]. In addition, psychological stress has been postulated to affect male fertility with a decrease in testosterone levels and spermatogenesis [230]. The reverse is also true, and whatever the cause of infertility, the psychological impact is significant. Depression, anxiety or sexual dysfunction are often reported after a diagnosis of infertility [231]. The global consequence of the decline in fertility is that the demand for assisted reproductive technologies has increased dramatically in recent years [232].

Cryobiology has revolutionised the way reproductive medicine is practiced today, requiring a detailed analysis of the cryopreservation of sperm, oocytes, embryos and ovarian tissue for both health issues and social reasons. The main purposes of human sperm cryopreservation are for donor sperm banks and for future use in the event of illness, particularly for oncological reasons. It is estimated that approximately 40% of men will be diagnosed with cancer at some point in their lives [233]. While improvements in cancer treatment have led to a decline in cancer mortality, cancer patients, especially at a young age, expect to have a future that may include the decision to start a family. However, recent research has shown that cancers of the reproductive system and the treatments associated with cancers in general (cumulative dose of chemotherapy, radiation doses and type of surgery performed) can compromise men's fertility [233, 234]. The number of cancer survivors who have used ARTs with cryopreserved sperm is reported to be between 33% and 56%, with successful paternity up to 21 years after cryopreservation [235].

Human sperm cryopreservation is also commonly performed with the use of LN₂. However, the option of using ultra-low temperature freezers is being considered for the same

reasons as for mouse repositories, namely cost reduction, inconsistent availability of LN₂ and ease of workflow. Encouraging results have been obtained with spermatozoa from men with normospermia (normal values of sperm parameters) cryopreserved and stored at -80°C for 1 month without affecting sperm concentration, motility and DNA integrity compared to LN₂ [131, 236]. However, there are many concerns associated with cryopreservation and storage of spermatozoa from subfertile men at -80°C. Indeed, these spermatozoa tend to have low motility, abnormal morphology and DNA damage. Since the use of ultra-low temperature freezers instead of LN₂ seems to increase the damage already present in the spermatozoa, a poor survival rate and IVF outcome could be expected. Therefore, the use of the BALB/c model, which shows significant cryoinjury after cryopreservation and storage at -80°C, is highly relevant for further research on cryodamage and fertility.

Surprisingly, limited research on the pharmacological use of D-Asp in humans has been conducted despite its huge therapeutic potential in fertility [158]. The effect of D-Asp in men showed that daily oral administration of 6 g of D-Asp for 12 days increased the production of LH and testosterone [154]. Another study showed that subfertile men treated orally with 6 g of D-Asp for 90 days had a higher sperm concentration and motility, leading to a higher pregnancy rate [158]. Moreover, *in vitro* treatment of spermatozoa from fertile and subfertile patients with a combination of D-Asp, zinc and coenzyme-Q10 improved the motility of spermatozoa from subfertile men, reduced lipid peroxidation in both groups but had no effect on the level of DNA fragmentation [163, 164]. However, the synergistic effects of these molecules did not provide specific information on the effect of D-Asp alone. Overall, the use of D-Asp seems very promising to improve the IVF success rate of spermatozoa from subfertile men. In the present study, we have shown that D-Asp improves sperm quality in not fully sexually mature mice and thus with a simple incubation of spermatozoa before performing IVF.

Therefore, further research should be conducted to investigate the beneficial effects of D-Asp in young men with immature spermatozoa, which would be relevant in paediatric oncology. On the other hand, research on the effect of D-Asp on spermatozoa from elderly men may support fertility in this population and contribute to the understanding of D-Asp function, ROS production and fertility.

References

1. Doke, S.K. and S.C. Dhawale, *Alternatives to animal testing: A review*. Saudi Pharm J, 2015. **23**(3): p. 223-229.
2. Stein, M., et al., *Why Animal Experiments Are Still Indispensable in Bone Research: A Statement by the European Calcified Tissue Society*. J Bone Miner Res, 2023. **38**(8): p. 1045-1061.
3. Mukherjee, P., et al., *Role of animal models in biomedical research: a review*. Lab Anim Res, 2022. **38**(1): p.18.
4. Kirk, R.G.W., *Recovering The Principles of Humane Experimental Technique: The 3Rs and the Human Essence of Animal Research*. Sci Technol Human Values, 2018. **43**(4): p. 622-648.
5. National Research Council (US) Committee for the Update of the Guide for the Care and Use of Laboratory Animals. *Guide for the Care and Use of Laboratory Animals*. 8th edition. Washington (DC): National Academies Press (US); 2011.
6. Rosenthal, N. and S. Brown, *The mouse ascending: perspectives for human-disease models*. Nat Cell Biol, 2007. **9**(9): p. 993-999.
7. Bryda, E.C., *The Mighty Mouse: the impact of rodents on advances in biomedical research*. Mo Med, 2013. **110**(3): p. 207-211.
8. Mouse Genome Sequencing, C., et al., *Initial sequencing and comparative analysis of the mouse genome*. Nature, 2002. **420**(6915): p. 520-562.
9. Justice, M.J. and P. Dhillon, *Using the mouse to model human disease: increasing validity and reproducibility*. Dis Model Mech, 2016. **9**(2): p. 101-103.
10. Kato, T. and S. Takada, *In vivo and in vitro disease modeling with CRISPR/Cas9*. Brief Funct Genomics, 2017. **16**(1): p. 13-24.
11. Gurumurthy, C.B. and K.C.K. Lloyd, *Generating mouse models for biomedical research: technological advances*. Dis Model Mech, 2019. **12**(1).
12. Kilkenny, C., et al., *Survey of the quality of experimental design, statistical analysis and reporting of research using animals*. PLoS One, 2009. **4**(11): p. e7824.
13. Donahue, L.R., et al., *Centralized mouse repositories*. Mamm Genome, 2012. **23**(9-10): p. 559-571.
14. Amos-Landgraf, J., et al., *The Mutant Mouse Resource and Research Center (MMRRC): the NIH-supported National Public Repository and Distribution Archive of Mutant Mouse Models in the USA*. Mamm Genome, 2022. **33**(1): p. 203-212.
15. Ali Khan, A., et al., *INFRAFRONTIER: mouse model resources for modelling human diseases*. Mamm Genome, 2023. **34**(3): p. 408-417.
16. Eppig, J.T., et al., *The International Mouse Strain Resource (IMSR): cataloging worldwide mouse and ES cell line resources*. Mamm Genome, 2015. **26**(9-10): p. 448-55.
17. Davisson, M.T. and R.A. Taft, *Strategies for managing an ever increasing mutant mouse repository*. Brain Res, 2006. **1091**(1): p. 255-257.
18. Mazur, P., S.P. Leibo, and G.E. Seidel, Jr., *Cryopreservation of the germplasm of animals used in biological and medical research: importance, impact, status, and future directions*. Biol Reprod, 2008. **78**(1): p. 2-12.
19. Ramaswamy, S. and G.F. Weinbauer, *Endocrine control of spermatogenesis: Role of FSH and LH/ testosterone*. Spermatogenesis, 2014. **4**(2): p. e996025.
20. Fayomi, A.P. and K.E. Orwig, *Spermatogonial stem cells and spermatogenesis in mice, monkeys and men*. Stem Cell Res, 2018. **29**: p. 207-214.
21. Muro, Y., et al., *Behavior of Mouse Spermatozoa in the Female Reproductive Tract from Soon after Mating to the Beginning of Fertilization*. Biol Reprod, 2016. **94**(4): p. 80.
22. Byers, S.L., S.J. Payson, and R.A. Taft, *Performance of ten inbred mouse strains following assisted reproductive technologies (ARTs)*. Theriogenology, 2006. **65**(9): p. 1716-1726.
23. Zhou, C.J., et al., *The beneficial effects of cumulus cells and oocyte-cumulus cell gap junctions depends on oocyte maturation and fertilization methods in mice*. PeerJ, 2016. **4**: p. e1761.

24. Dziuk, P.J. and M.N. Runner, *Recovery of blastocysts and induction of implantation following artificial insemination of immature mice*. J Reprod Fertil, 1960. **1**: p. 321-331.
25. Duselis, A., et al., *Nonsurgical Artificial Insemination in Mice*. Cold Spring Harb Protoc, 2018. **2018**(9): p. 10.
26. De Repentigny, Y. and R. Kothary, *An improved method for artificial insemination of mice--oviduct transfer of spermatozoa*. Trends Genet, 1996. **12**(2): p. 44-45.
27. Duselis, A.R. and P.B. Vrana, *Harvesting sperm and artificial insemination of mice*. J Vis Exp, 2007. (3): p. 184.
28. Parkinson, T.J. and J.M. Morrell, *43 - Artificial Insemination*, in *Veterinary Reproduction and Obstetrics (Tenth Edition)*, D.E. Noakes, T.J. Parkinson, and G.C.W. England, Editors. 2019, W.B. Saunders: St. Louis (MO). p. 746-777.
29. Nakagata, N., et al., *Rescue in vitro fertilization method for legacy stock of frozen mouse sperm*. J Reprod Dev, 2014. **60**(2): p. 168-171.
30. Skinner, M.K., *Encyclopedia of Reproduction*. 2018, San Diego, UNITED STATES: Elsevier Science & Technology.
31. Wigger, M., S.E. Tröder, and B. Zevnik, *A simple and economic protocol for efficient in vitro fertilization using cryopreserved mouse sperm*. PLoS ONE, 2021. **16**(10): p. e0259202.
32. Uehara, T. and R. Yanagimachi, *Microsurgical injection of spermatozoa into hamster eggs with subsequent transformation of sperm nuclei into male pronuclei*. Biol Reprod, 1976. **15**(4): p. 467-470.
33. Kimura, Y. and R. Yanagimachi, *Intracytoplasmic sperm injection in the mouse*. Biol Reprod, 1995. **52**(4): p. 709-720.
34. Wakayama, T., D.G. Whittingham, and R. Yanagimachi, *Production of normal offspring from mouse oocytes injected with spermatozoa cryopreserved with or without cryoprotection*. J Reprod Fertil, 1998. **112**(1): p. 11-17.
35. Moisyadi, S., J.M. Kaminski, and R. Yanagimachi, *Use of intracytoplasmic sperm injection (ICSI) to generate transgenic animals*. Comp Immunol Microbiol Infect Dis, 2009. **32**(2): p. 47-60.
36. Johnson, L.W., et al., *Optimization of embryo transfer protocols for mice*. Theriogenology, 1996. **46**(7): p. 1267-1276.
37. Takeo, T., et al., *Cryopreservation of mouse resources*. Lab Anim Res, 2020. **36**: p. 33.
38. Nakagata, N., J. Sztejn, and T. Takeo, *The CARD Method for Simple Vitrification of Mouse Oocytes: Advantages and Applications*, in *Microinjection: Methods and Protocols*, C. Liu and Y. Du, Editors. 2019, Springer New York: New York, NY. p. 229-242.
39. Glenister, P.H. and C.E. Thornton, *Cryoconservation--archiving for the future*. Mamm Genome, 2000. **11**(7): p. 565-571.
40. Saragusty, J. and A. Arav, *Current progress in oocyte and embryo cryopreservation by slow freezing and vitrification*. Reproduction, 2011. **141**(1): p. 1-19.
41. Takeo, T. and N. Nakagata, *Cryobanking and Recovery of Genetically Modified Mice*, in *Transgenic Mouse: Methods and Protocols*, M.A. Larson, Editor. 2020, Springer US: New York, NY. p. 195-209.
42. Nakagata, N., *Cryopreservation of mouse spermatozoa*. Mamm Genome, 2000. **11**(7): p. 572-576.
43. Du, Y., W. Xie, and C. Liu, *Strategies and considerations for distributing and recovering mouse lines*. Methods Enzymol, 2010. **476**: p. 37-52.
44. Sztejn, J.M., T. Takeo, and N. Nakagata, *History of cryobiology, with special emphasis in evolution of mouse sperm cryopreservation*. Cryobiology, 2018. **82**: p. 57-63.
45. Cooke, H.J. and P.T. Saunders, *Mouse models of male infertility*. Nat Rev Genet, 2002. **3**(10): p. 790-801.
46. Yan, H.H., D.D. Mruk, and C.Y. Cheng, *Junction restructuring and spermatogenesis: the biology, regulation, and implication in male contraceptive development*. Curr Top Dev Biol, 2008. **80**: p. 57-92.

47. Oatley, J.M. and R.L. Brinster, *The germline stem cell niche unit in mammalian testes*. *Physiol Rev*, 2012. **92**(2): p. 577-595.
48. Hao, S.L., F.D. Ni, and W.X. Yang, *The dynamics and regulation of chromatin remodeling during spermiogenesis*. *Gene*, 2019. **706**: p. 201-210.
49. Ibtisham, F., et al., *Progress and future prospect of in vitro spermatogenesis*. *Oncotarget*, 2017. **8**(39): p. 66709-66727.
50. Yogo, K., *Molecular basis of the morphogenesis of sperm head and tail in mice*. *Reprod Med Biol*, 2022. **21**(1): p. e12466.
51. Thompson, I.R. and U.B. Kaiser, *GnRH pulse frequency-dependent differential regulation of LH and FSH gene expression*. *Mol Cell Endocrinol*, 2014. **385**(1-2): p. 28-35.
52. Stocco, D.M., et al., *A brief history of the search for the protein(s) involved in the acute regulation of steroidogenesis*. *Mol Cell Endocrinol*, 2017. **441**: p. 7-16.
53. Skorupskaitė, K., J.T. George, and R.A. Anderson, *The kisspeptin-GnRH pathway in human reproductive health and disease*. *Hum Reprod Update*, 2014. **20**(4): p. 485-500.
54. Menkveld, R., C.A. Holleboom, and J.P. Rhemrev, *Measurement and significance of sperm morphology*. *Asian J Androl*, 2011. **13**(1): p. 59-68.
55. Kawai, Y., et al., *The relationship between sperm morphology and in vitro fertilization ability in mice*. *J Reprod Dev*, 2006. **52**(4): p. 561-568.
56. Rothmann, S.A. and A.A. Reese, *Semen analysis*, in *Infertility in the Male*, C.S. Niederberger, L.I. Lipshultz, and S.S. Howards, Editors. 2009, Cambridge University Press: Cambridge. p. 550-573.
57. Niederberger, C., *Clinical evaluation of the male*, in *An Introduction to Male Reproductive Medicine*, C. Niederberger, Editor. 2011, Cambridge University Press: Cambridge. p. 29-57.
58. Gu, N.H., et al., *Comparative analysis of mammalian sperm ultrastructure reveals relationships between sperm morphology, mitochondrial functions and motility*. *Reprod Biol Endocrinol*, 2019. **17**(1): p. 66.
59. Cornwall, G.A., *New insights into epididymal biology and function*. *Hum Reprod Update*, 2009. **15**(2): p. 213-227.
60. Vadnais, M.L., et al., *Adenine nucleotide metabolism and a role for AMP in modulating flagellar waveforms in mouse sperm*. *Biol Reprod*, 2014. **90**(6): p. 128.
61. Cornwall, G.A., et al., *The effect of sulfhydryl oxidation on the morphology of immature hamster epididymal spermatozoa induced to acquire motility in vitro*. *Biol Reprod*, 1988. **39**(1): p. 141-55.
62. Rejraji, H., et al., *Lipid remodeling of murine epididymosomes and spermatozoa during epididymal maturation*. *Biol Reprod*, 2006. **74**(6): p. 1104-13.
63. Skerget, S., et al., *Sperm Proteome Maturation in the Mouse Epididymis*. *PLoS One*, 2015. **10**(11): p. e0140650.
64. Snyder, R.L., *Collection of mouse semen by electroejaculation*. *The Anatomical Record*, 1966. **155**(1): p. 11-14.
65. Goodson, S.G., et al., *Classification of mouse sperm motility patterns using an automated multiclass support vector machines model*. *Biol Reprod*, 2011. **84**(6): p. 1207-15.
66. Dcunha, R., et al., *Current Insights and Latest Updates in Sperm Motility and Associated Applications in Assisted Reproduction*. *Reprod Sci*, 2022. **29**(1): p. 7-25.
67. Bjorndahl, L., *The usefulness and significance of assessing rapidly progressive spermatozoa*. *Asian J Androl*, 2010. **12**(1): p. 33-35.
68. Cooper, T.G., et al., *World Health Organization reference values for human semen characteristics*. *Hum Reprod Update*, 2010. **16**(3): p. 231-245.
69. Visconti, P.E., et al., *Novel signaling pathways involved in sperm acquisition of fertilizing capacity*. *J Reprod Immunol*, 2002. **53**(1-2): p. 133-150.
70. Aitken, R.J. and B. Nixon, *Sperm capacitation: a distant landscape glimpsed but unexplored*. *Mol Hum Reprod*, 2013. **19**(12): p. 785-793.

71. Gervasi, M.G. and P.E. Visconti, *Chang's meaning of capacitation: A molecular perspective*. Mol Reprod Dev, 2016. **83**(10): p. 860-874.
72. Breitbart, H. and O. Shabtay, *Sperm Acrosome Reaction*, in *Encyclopedia of Reproduction (Second Edition)*, M.K. Skinner, Editor. 2018, Academic Press: Oxford. p. 284-288.
73. Choi, Y.-H. and Y. Toyoda, *Cyclodextrin Removes Cholesterol from Mouse Sperm and Induces Capacitation in a Protein-Free Medium*. Biology of Reproduction, 1998. **59**(6): p. 1328-1333.
74. Ded, L., et al., *Fluorescent analysis of boar sperm capacitation process in vitro*. Reprod Biol Endocrinol, 2019. **17**(1): p. 109.
75. Larson, J.L. and D.J. Miller, *Simple histochemical stain for acrosomes on sperm from several species*. Mol Reprod Dev, 1999. **52**(4): p. 445-449.
76. Kerr, C.L., et al., *Characterization of zona pellucida glycoprotein 3 (ZP3) and ZP2 binding sites on acrosome-intact mouse sperm*. Biol Reprod, 2002. **66**(6): p. 1585-1595.
77. Sies, H. and D.P. Jones, *Reactive oxygen species (ROS) as pleiotropic physiological signalling agents*. Nat Rev Mol Cell Biol, 2020. **21**(7): p. 363-383.
78. Baskaran, S., et al., *Reactive oxygen species in male reproduction: A boon or a bane?* Andrologia, 2021. **53**(1): p. e13577.
79. Bardaweel, S.A.-O., et al., *Reactive Oxygen Species: the Dual Role in Physiological and Pathological Conditions of the Human Body*. Eurasian J Med, 2018. **50**(3): p. 193-201.
80. Aitken, R.J. and J.R. Drevet, *The Importance of Oxidative Stress in Determining the Functionality of Mammalian Spermatozoa: A Two-Edged Sword*. Antioxidants (Basel), 2020. **9**(2): p. 111.
81. Du Plessis, S.S., et al., *Contemporary evidence on the physiological role of reactive oxygen species in human sperm function*. J Assist Reprod Genet, 2015. **32**(4): p. 509-520.
82. Morimoto, H., et al., *ROS are required for mouse spermatogonial stem cell self-renewal*. Cell Stem Cell, 2013. **12**(6): p. 774-86.
83. Maiorino, M. and F. Ursini, *Oxidative Stress, Spermatogenesis and Fertility*. 2002. **383**(3-4): p. 591-597.
84. Miranda-Vizuete, A., et al., *The mammalian testis-specific thioredoxin system*. Antioxid Redox Signal, 2004. **6**(1): p. 25-40.
85. Tai, P. and M. Ascoli, *Reactive oxygen species (ROS) play a critical role in the cAMP-induced activation of Ras and the phosphorylation of ERK1/2 in Leydig cells*. Mol Endocrinol, 2011. **25**(5): p. 885-893.
86. Fujii, J. and H. Imai, *Redox reactions in mammalian spermatogenesis and the potential targets of reactive oxygen species under oxidative stress*. Spermatogenesis, 2014. **4**(2): p. e979108.
87. Gadella, B.M. and A. Boerke, *An update on post-ejaculatory remodeling of the sperm surface before mammalian fertilization*. Theriogenology, 2016. **85**(1): p. 113-124.
88. Aitken, R.J., M.A. Baker, and B. Nixon, *Are sperm capacitation and apoptosis the opposite ends of a continuum driven by oxidative stress?* Asian J Androl, 2015. **17**(4): p. 633-639.
89. Curry, M.R., *Cryopreservation of Mammalian Semen*, in *Cryopreservation and Freeze-Drying Protocols*, J.G. Day and G.N. Stacey, Editors. 2007, Humana Press: Totowa, NJ. p. 303-311.
90. Sherman, J.K., *Synopsis of the Use of Frozen Human Semen Since 1964: State of the Art of Human Semen Banking*. Fertility and Sterility, 1973. **24**(5): p. 397-412.
91. Paoli, D., et al., *Cryopreservation of Sperm: Effects on Chromatin and Strategies to Prevent Them*, in *Genetic Damage in Human Spermatozoa*, E. Baldi and M. Muratori, Editors. 2019, Springer International Publishing: Cham. p. 149-167.
92. Yokoyama, M., et al., *[Production of normal young following transfer of mouse embryos obtained by in vitro fertilization using cryopreserved spermatozoa]*. Jikken Dobutsu, 1990. **39**(1): p. 125-128.
93. Tada, N., et al., *Cryopreservation of mouse spermatozoa in the presence of raffinose and glycerol*. J Reprod Fertil, 1990. **89**(2): p. 511-516.
94. Takeshima, T., N. Nakagata, and S. Ogawa, *[Cryopreservation of mouse spermatozoa]*. Jikken Dobutsu, 1991. **40**(4): p. 493-497.

95. AbdelHafez, F., et al., *Techniques for cryopreservation of individual or small numbers of human spermatozoa: a systematic review*. Hum Reprod Update, 2009. **15**(2): p. 153-164.
96. Pegg, D.E., *Principles of cryopreservation*. Methods Mol Biol, 2015. **1257**: p. 3-19.
97. Fahy, G.M. and B. Wowk, *Principles of cryopreservation by vitrification*. Methods Mol Biol, 2015. **1257**: p. 21-82.
98. Critser, J.K. and L.E. Mobraaten, *Cryopreservation of murine spermatozoa*. ILAR J, 2000. **41**(4): p. 197-206.
99. Ostermeier, G.C., et al., *Conserving, distributing and managing genetically modified mouse lines by sperm cryopreservation*. PLoS One, 2008. **3**(7): p. e2792.
100. Takeo, T. and N. Nakagata, *Combination medium of cryoprotective agents containing L-glutamine and methyl- β -cyclodextrin in a preincubation medium yields a high fertilization rate for cryopreserved C57BL/6J mouse sperm*. Laboratory Animals, 2010. **44**(2): p. 132-137.
101. Borg, C.L., et al., *Phenotyping male infertility in the mouse: how to get the most out of a 'non-performer'*. Hum Reprod Update, 2010. **16**(2): p. 205-224.
102. Albert, M. and C. Roussel, *Changes from puberty to adulthood in the concentration, motility and morphology of mouse epididymal spermatozoa*. Int J Androl, 1983. **6**(5): p. 446-460.
103. Albert, M. and C. Roussel, *Strain differences in the concentration, motility and morphology of epididymal sperm in relation to puberty in mice*. Int J Androl, 1984. **7**(4): p. 334-347.
104. Koshimoto, C. and P. Mazur, *Effects of Cooling and Warming Rate to and from -70°C , and Effect of Further Cooling from -70 to -196°C on the Motility of Mouse Spermatozoa*. Biology of Reproduction, 2002. **66**(5): p. 1477-1484.
105. Seki, S., B. Jin, and P. Mazur, *Extreme rapid warming yields high functional survivals of vitrified 8-cell mouse embryos even when suspended in a half-strength vitrification solution and cooled at moderate rates to -196°C* . Cryobiology, 2014. **68**(1): p. 71-78.
106. Sharafi, M., et al., *Cryopreservation of Semen in Domestic Animals: A Review of Current Challenges, Applications, and Prospective Strategies*. Animals (Basel), 2022. **12**(23): p. 3271.
107. Ozkavukcu, S., et al., *Effects of cryopreservation on sperm parameters and ultrastructural morphology of human spermatozoa*. J Assist Reprod Genet, 2008. **25**(8): p. 403-411.
108. Nijs, M., et al., *Influence of freeze-thawing on hyaluronic acid binding of human spermatozoa*. Reprod Biomed Online, 2009. **19**(2): p. 202-206.
109. Barthelemy, C., et al., *Ultrastructural changes in membranes and acrosome of human sperm during cryopreservation*. Arch Androl, 1990. **25**(1): p. 29-40.
110. Paoli, D., et al., *Sperm cryopreservation: effects on chromatin structure*. Adv Exp Med Biol, 2014. **791**: p. 137-150.
111. Barratt, C.L.R., et al., *The diagnosis of male infertility: an analysis of the evidence to support the development of global WHO guidance-challenges and future research opportunities*. Hum Reprod Update, 2017. **23**(6): p. 660-680.
112. Quinn, P.J., K.W. White, and K.W. Cleland, *Chemical and ultrastructural changes in ram spermatozoa after washing, cold shock and freezing*. J Reprod Fertil, 1969. **18**(2): p. 209-220.
113. Nishizono, H., et al., *Decrease of fertilizing ability of mouse spermatozoa after freezing and thawing is related to cellular injury*. Biol Reprod, 2004. **71**(3): p. 973-978.
114. Irvine, D.S., et al., *DNA integrity in human spermatozoa: relationships with semen quality*. J Androl, 2000. **21**(1): p. 33-44.
115. Sztejn, J.M., J.S. Farley, and L.E. Mobraaten, *In vitro fertilization with cryopreserved inbred mouse sperm*. Biol Reprod, 2000. **63**(6): p. 1774-1780.
116. Barbas, J.P. and R.D. Mascarenhas, *Cryopreservation of domestic animal sperm cells*. Cell Tissue Bank, 2009. **10**(1): p. 49-62.
117. Hezavehei, M., et al., *Sperm cryopreservation: A review on current molecular cryobiology and advanced approaches*. Reprod Biomed Online, 2018. **37**(3): p. 327-339.
118. Liu, J., et al., *Identification of quantitative trait loci associated with the susceptibility of mouse spermatozoa to cryopreservation*. J Reprod Dev, 2018. **64**(2): p. 117-127.

119. Mochida, K., et al., *Easy and quick (EQ) sperm freezing method for urgent preservation of mouse strains*. Scientific Reports, 2021. **11**(1): p. 14149.
120. Kenyon, J., et al., *Transporting mouse embryos and germplasm as frozen or unfrozen materials*. Curr Protoc Mouse Biol, 2014. **4**(2): p. 47-65.
121. Said, T.M., A. Gaglani, and A. Agarwal. *Implication of apoptosis in sperm cryoinjury*. Reprod Biomed Online, 2010. **21**(4): p. 456-462.
122. Diogo, P., et al., *Electric ultrafreezer (-150 °C) as an alternative for zebrafish sperm cryopreservation and storage*. Fish Physiol Biochem, 2018. **44**(6): p. 1443-1455.
123. Alamo, D., et al., *Cryopreservation of semen in the dog: use of ultra-freezers of -152 degrees C as a viable alternative to liquid nitrogen*. Theriogenology, 2005. **63**(1): p. 72-82.
124. Batista, M., et al., *Influence of the freezing technique (nitrogen liquid vs ultrafreezer of -152 degrees C) and male-to-male variation over the semen quality in Canarian Mastiff breed dogs*. Reprod Dom Anim, 2006. **41**(5): p. 423-428.
125. Yavaş, T.K. and A. Daşkin, *Effect of alternative cryopreservation procedures on bull semen*. Ankara Üniversitesi Veteriner Fakültesi Dergisi, 2012. **59**(3): p. 231-234.
126. Medrano, A., et al., *Is sperm cryopreservation at -150 degree C a feasible alternative?*. Cryo Letters, 2002. **23**(3): p. 167-172.
127. Batista, M., et al., *Successful artificial insemination using semen frozen and stored by an ultrafreezer in the Majorera goat breed*. Theriogenology, 2009. **71**(8): p. 1307-1315.
128. Raspa, M., et al., *Dry ice is a reliable substrate for the distribution of frozen mouse spermatozoa: A multi-centric study*. Theriogenology, 2017. **96**: p. 49-57.
129. Mazur, P., *Freezing of living cells: mechanisms and implications*. Am J Physiol, 1984. **247**(3 Pt 1):C125-C142.
130. Buranaamnuy, K., *Cryopreservation and storage of cat epididymal sperm using -75 °C freezer vs liquid nitrogen*. Animal Reproduction Science, 2018. **191**: p. 56-63.
131. Rahana, A.R., et al., *Comparison between mechanical freezer and conventional freezing using liquid nitrogen in normozoospermia*. Singapore Med J, 2011. **52**(10): p. 734-737.
132. González, A., et al., *Frozen dog spermatozoa are negatively affected during storage at -80, -21 and -8 °C*. Animal Reproduction Science, 2019. **210**: p. 106197.
133. Buranaamnuy, K., K. Seesuan, and K. Saikhun, *Preliminary study on effects of bovine frozen semen storage using a liquid nitrogen-independent method on the quality of post-thaw spermatozoa*. Animal Reproduction Science, 2016. **172**: p. 32-38.
134. Liu, S., et al., *Ultra-low temperature cryopreservation and -80 °C storage of sperm from normal-male and pseudo-male Siniperca chuatsi*. Aquaculture, 2022. **553**: p. 738007.
135. Raspa, M., et al., *The impact of five years storage/biobanking at -80°C on mouse spermatozoa fertility, physiology, and function*. Andrology, 2021. **9**(3): p. 989-999.
136. Raspa, M., et al., *A new, simple and efficient liquid nitrogen free method to cryopreserve mouse spermatozoa at -80 degrees C*. Theriogenology, 2018. **119**: p. 52-59.
137. Chung, S.-Y. and S. Reed, *IgE binding to peanut allergens is inhibited by combined d-aspartic and d-glutamic acids*. Food Chemistry, 2015. **166**: p. 248-253.
138. Katane, M. and H. Homma, *d-Aspartate—An important bioactive substance in mammals: A review from an analytical and biological point of view*. Journal of Chromatography B, 2011. **879**(29): p. 3108-3121.
139. Brückner, H. and T. Westhauser, *Chromatographic determination of L- and D-amino acids in plants*. Amino Acids, 2003. **24**(1): p. 43-55.
140. Wolosker, H., A. D'Aniello, and S.H. Snyder, *d-Aspartate disposition in neuronal and endocrine tissues: ontogeny, biosynthesis and release*. Neuroscience, 2000. **100**(1): p. 183-189.
141. D'Aniello, S., et al., *D-Aspartic acid is a novel endogenous neurotransmitter*. FASEB J, 2011. **25**(3): p. 1014-1027.
142. Katane, M. and H. Homma, *D-aspartate oxidase: the sole catabolic enzyme acting on free D-aspartate in mammals*. Chem Biodivers, 2010. **7**(6): p. 1435-1449.

143. D'Aniello, A., et al., *A specific enzymatic high-performance liquid chromatography method to determine N-methyl-d-aspartic acid in biological tissues*. Analytical Biochemistry, 2002. **308**(1): p. 42-51.
144. Gill, S.S., et al., *Potential target sites in peripheral tissues for excitatory neurotransmission and excitotoxicity*. Toxicol Pathol, 2000. **28**(2): p. 277-284.
145. Gill, S.S. and O.M. Pulido, *Glutamate receptors in peripheral tissues: current knowledge, future research, and implications for toxicology*. Toxicol Pathol, 2001. **29**(2): p. 208-223.
146. Santillo, A., et al., *D-aspartate affects NMDA receptor-extracellular signal-regulated kinase pathway and upregulates androgen receptor expression in the rat testis*. Theriogenology, 2014. **81**(5): p. 744-751.
147. D'Aniello, G., et al., *Occurrence of D-aspartic acid in human seminal plasma and spermatozoa: Possible role in reproduction*. Fertility and Sterility, 2005. **84**(5): p. 1444-1449.
148. D'Aniello, A., *D-Aspartic acid: an endogenous amino acid with an important neuroendocrine role*. Brain Res Rev, 2007. **53**(2): p. 215-234.
149. Lamanna, C., et al., *d-Aspartic acid and nitric oxide as regulators of androgen production in boar testis*. Theriogenology, 2007. **67**(2): p. 249-254.
150. Ota, N., T. Shi, and J.V. Sweedler, *d-Aspartate acts as a signaling molecule in nervous and neuroendocrine systems*. Amino Acids, 2012. **43**(5): p. 1873-1886.
151. Di Fiore, M.M., A. Santillo, and G. Chieffi Baccari, *Current knowledge of d-aspartate in glandular tissues*. Amino Acids, 2014. **46**(8): p. 1805-1818.
152. D'Aniello, A., et al., *Occurrence of D-aspartic acid and N-methyl-D-aspartic acid in rat neuroendocrine tissues and their role in the modulation of luteinizing hormone and growth hormone release*. FASEB J, 2000. **14**(5): p. 699-714.
153. Raspa, M., et al., *Effects of oral d-aspartate on sperm quality in B6N mice*. Theriogenology, 2018. **121**: p. 53-61.
154. Topo, E., et al., *The role and molecular mechanism of D-aspartic acid in the release and synthesis of LH and testosterone in humans and rats*. Reprod Biol Endocrinol, 2009. **7**: p. 120.
155. Nagata, Y., et al., *Stimulation of steroidogenic acute regulatory protein (StAR) gene expression by D-aspartate in rat Leydig cells*. FEBS Lett, 1999. **454**(3): p. 317-320.
156. Raucci, F., A. D'Aniello, and M.M. Di Fiore, *Stimulation of androgen production by d-aspartate through the enhancement of StAR, P450scc and 3 β -HSD mRNA levels in vivo rat testis and in culture of immature rat Leydig cells*. Steroids, 2014. **84**: p. 103-110.
157. Ansari, M., et al., *Improvement of post-thawed sperm quality and fertility of Arian rooster by oral administration of d-aspartic acid*. Theriogenology, 2017. **92**: p. 69-74.
158. Di Fiore, M.M., et al., *D-Aspartic Acid in Vertebrate Reproduction: Animal Models and Experimental Designs(double dagger)*. Biomolecules, 2019. **9**(9): p. 445.
159. Macchia, G., et al., *DL-Aspartic acid administration improves semen quality in rabbit bucks*. Anim Reprod Sci, 2010. **118**(2-4): p. 337-343.
160. Raspa, M., et al., *Oral D-Aspartate Treatment Improves Sperm Fertility in Both Young and Adult B6N Mice*. Animals (Basel), 2022. **12**(11): p. 1350.
161. Gualtieri, R., et al., *Treatment with zinc, d-aspartate, and coenzyme Q10 protects bull sperm against damage and improves their ability to support embryo development*. Theriogenology, 2014. **82**(4): p. 592-598.
162. Barbato, V., et al., *Supplementation of sperm media with zinc, D-aspartate and co-enzyme Q10 protects bull sperm against exogenous oxidative stress and improves their ability to support embryo development*. Zygote, 2017. **25**(2): p. 168-175.
163. Talevi, R., et al., *Protective effects of in vitro treatment with zinc, d-aspartate and coenzyme q10 on human sperm motility, lipid peroxidation and DNA fragmentation*. Reprod Biol Endocrinol, 2013. **11**: p. 81.
164. Giacone, F., et al., *In vitro effects of zinc, D-aspartic acid, and coenzyme-Q10 on sperm function*. Endocrine, 2017. **56**(2): p. 408-415.

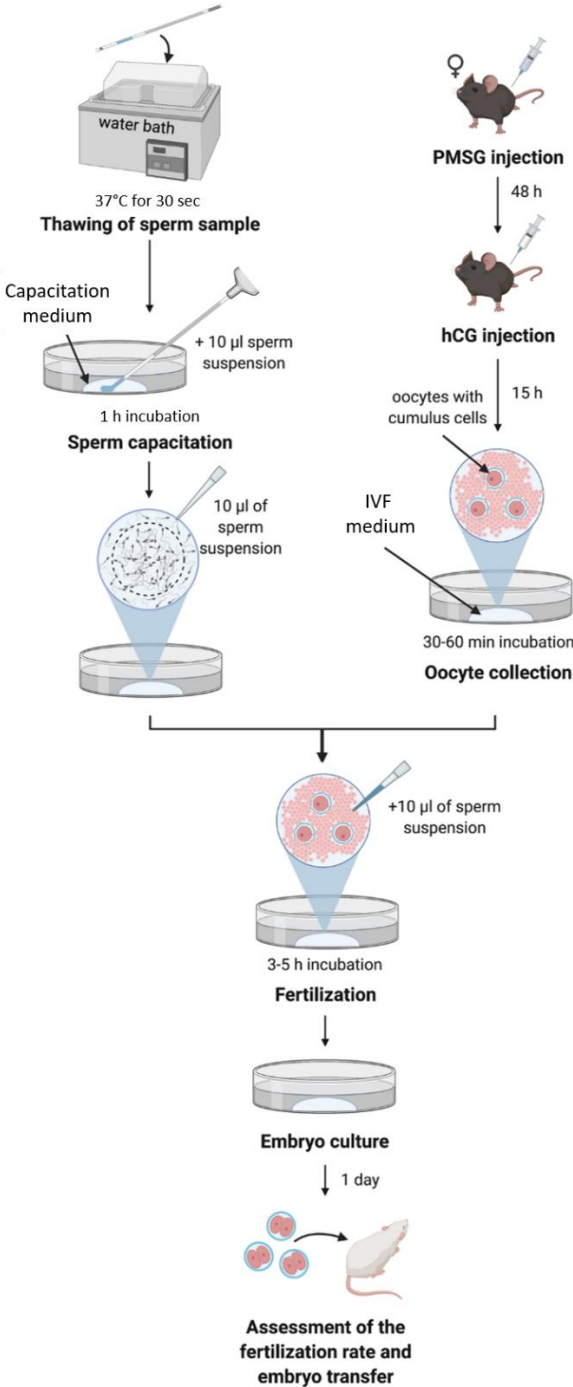
165. Raspa, M., et al., *d-aspartate treatment in vitro improves mouse sperm fertility in young B6N mice*. Theriogenology, 2020. **148**: p. 60-67.
166. Chandrashekar, K.N. and Muralidhara, *Oxidative alterations induced by D-aspartic acid in prepubertal rat testis in vitro: a mechanistic study*. Theriogenology, 2008. **70**(1): p. 97-104.
167. Chandrashekar, K.N. and Muralidhara, *D-Aspartic acid induced oxidative stress and mitochondrial dysfunctions in testis of prepubertal rats*. Amino Acids, 2010. **38**(3): p. 817-827.
168. Lamanna, C., et al., *Involvement of D-Asp in P450 aromatase activity and estrogen receptors in boar testis*. Amino Acids, 2007. **32**(1): p. 45-51.
169. Tapia, P.C., *Sublethal mitochondrial stress with an attendant stoichiometric augmentation of reactive oxygen species may precipitate many of the beneficial alterations in cellular physiology produced by caloric restriction, intermittent fasting, exercise and dietary phytonutrients: "Mitohormesis" for health and vitality*. Medical Hypotheses, 2006. **66**(4): p. 832-843.
170. Ristow, M. and K. Zarse, *How increased oxidative stress promotes longevity and metabolic health: The concept of mitochondrial hormesis (mitohormesis)*. Exp Gerontol, 2010. **45**(6): p. 410-418.
171. Ristow, M. and K. Schmeisser, *Mitohormesis: Promoting Health and Lifespan by Increased Levels of Reactive Oxygen Species (ROS)*. Dose Response, 2014. **12**(2): p. 288-341.
172. Mahler Convenor, M., et al., *FELASA recommendations for the health monitoring of mouse, rat, hamster, guinea pig and rabbit colonies in breeding and experimental units*. Lab Anim, 2014. **48**(3): p. 178-192.
173. Kilkenney, C., et al., *Improving bioscience research reporting: the ARRIVE guidelines for reporting animal research*. PLoS Biol, 2010. **8**(6): p. e1000412.
174. Wang, Q. and M.H. Zou, *Measurement of Reactive Oxygen Species (ROS) and Mitochondrial ROS in AMPK Knockout Mice Blood Vessels*. Methods Mol Biol, 2018. **1732**: p. 507-517.
175. Ribas-Maynou, J., et al., *Alkaline and neutral Comet assay profiles of sperm DNA damage in clinical groups*. Hum Reprod, 2012. **27**(3): p. 652-658.
176. Aldini, G., et al., *N-Acetylcysteine as an antioxidant and disulphide breaking agent: the reasons why*. Free Radic Res, 2018. **52**(7): p. 751-762.
177. N Nikolettos, N., et al., *Fertilization potential of spermatozoa with abnormal morphology*. Hum Reprod, 1999. **14**(1): p. 47-70.
178. L Lasiene, K., et al., *Evaluation of morphological criteria of sperm quality before in vitro fertilization and intracytoplasmic sperm injection*. Pol J Vet Sci, 2013. **16**(4): p. 773-785.
179. Burrone, L., M.M. Raucci, and M.M. Di Fiore, *Steroidogenic gene expression following D-aspartate treatment in frog testis*. Gen Comp Endocrinol, 2012. **175**(1): p. 109-117.
180. Kishida, K.T., et al., *NADPH oxidase is required for NMDA receptor-dependent activation of ERK in hippocampal area CA1*. J Neurochem, 2005. **94**(2): p. 299-306.
181. Girouard, H., et al., *NMDA receptor activation increases free radical production through nitric oxide and NOX2*. Neurosci, 2009. **29**(8): p. 2545-2552.
182. Kim, E.Y., M. Anderson, and S.E. Dryer, *Sustained activation of N-methyl-D-aspartate receptors in podocytes leads to oxidative stress, mobilization of transient receptor potential canonical 6 channels, nuclear factor of activated T cells activation, and apoptotic cell death*. Mol Pharmacol, 2012. **82**(4): p. 728-737.
183. A Agarwal, A., G. Ahmad, and R. Sharma, *Reference values of reactive oxygen species in seminal ejaculates using chemiluminescence assay*. J Assist Reprod Genet, 2015. **32**(12): p. 1721-1729.
184. Murphy, M.P., et al., *Guidelines for measuring reactive oxygen species and oxidative damage in cells and in vivo*. Nature Metabolism, 2022. **4**(6): p. 651-662.
185. S Schieber, M. and N.S. Chandel, *ROS function in redox signaling and oxidative stress*. Curr Biol, 2014. **24**(10): p. 453-462.
186. MacLeod, J., *The rôle of oxygen in the metabolism and motility of human spermatozoa*. American Journal of Physiology-Legacy Content, 1943. **138**(3): p. 512-518.

187. Sanocka, D., et al., *Effect of reactive oxygen species and the activity of antioxidant systems on human semen; association with male infertility*. International Journal of Andrology, 1997. **20**(5): p. 255-264.
188. Brouwers, J.F.H.M. and B.M. Gadella, *In situ detection and localization of lipid peroxidation in individual bovine sperm cells*. Free Radical Biology and Medicine, 2003. **35**(11): p. 1382-1391.
189. Cassani, P., M.T. Beconi, and C. O'Flaherty, *Relationship between total superoxide dismutase activity with lipid peroxidation, dynamics and morphological parameters in canine semen*. Animal Reproduction Science, 2005. **86**(1): p. 163-173.
190. Awda, B.J., M. Mackenzie-Bell, and M.M. Buhr, *Reactive Oxygen Species and Boar Sperm Function1*. Biology of Reproduction, 2009. **81**(3): p. 553-561.
191. Mayorga-Torres, B.J.M., et al., *Are oxidative stress markers associated with unexplained male infertility?*. Andrologia, 2017. **49**(5).
192. Peña, F.A.-O., et al., *Redox Regulation and Oxidative Stress: The Particular Case of the Stallion Spermatozoa*. Antioxidants (Basel), 2019. **8**(11): p. 567.
193. Giraud, M.N., et al., *Membrane fluidity predicts the outcome of cryopreservation of human spermatozoa*. Hum Reprod, 2000. **15**(10): p. 2160-2164.
194. Bailey, J.L., N. Bilodeau, and N. Cormier, *Semen cryopreservation in domestic animals: a damaging and capacitating phenomenon*. J Androl, 2000. **21**(1): p. 1-7.
195. Oehninger, S., et al., *Assessment of sperm cryodamage and strategies to improve outcome*. Mol Cell Endocrinol, 2000. **169**(1-2): p. 3-10.
196. Goldman, R., U. Ferber, and U. Zort, *Reactive oxygen species are involved in the activation of cellular phospholipase A2*. FEBS Lett, 1992. **309**(2): p. 190-192.
197. Flesch, F.M. and B.M. Gadella, *Dynamics of the mammalian sperm plasma membrane in the process of fertilization*. Biochim Biophys Acta, 2000. **1469**(3): p. 197-235.
198. Tomita, K., et al., *The Effect of D-Aspartate on Spermatogenesis in Mouse Testis*. Biol Reprod, 2016. **94**(2): p. 30.
199. Raspa, M., et al., *Long term maintenance of frozen mouse spermatozoa at -80 degrees C*. Theriogenology, 2018. **107**: p. 41-49.
200. Trummer, H., et al., *Effect of storage temperature on sperm cryopreservation*. Fertil Steril, 1998. **70**(6): p. 1162-1164.
201. Olexikova, L.A.-O., et al., *Cryodamage of plasma membrane and acrosome region in chicken sperm*. Anat Histol Embryol, 2019. **48**(1): p. 33-39.
202. Keskin, N., et al., *Cryopreservation Effects on Ram Sperm Ultrastructure*. Biopreserv Biobank, 2020. **18**(5): p. 441-448.
203. Da Costa, R., K. Redmann, and S.A.-O. Schlatt, *Simultaneous detection of sperm membrane integrity and DNA fragmentation by flow cytometry: A novel and rapid tool for sperm analysis*. Andrology, 2021. **9**(4): p. 1254-1263.
204. Donnelly, E.T., et al., *In vitro fertilization and pregnancy rates: the influence of sperm motility and morphology on IVF outcome*. Fertil Steril, 1998. **70**(2): p. 305-314.
205. Li, M.W., et al., *Cryorecovery of Mouse Sperm by Different IVF Methods Using MBCD and GSH*. J Fertil In Vitro, 2016. **4**(2): p. 175.
206. Poch, M.A. and M. Sigman, *Clinical Evaluation and Treatment of Male Factor Infertility*, in *Reproductive Endocrinology and Infertility: Integrating Modern Clinical and Laboratory Practice*, D.T. Carrell and C.M. Peterson, Editors. 2010, Springer New York: New York, NY. p. 367-377.
207. Ribas-Maynou, J.A.-O. and J. Benet, *Single and Double Strand Sperm DNA Damage: Different Reproductive Effects on Male Fertility*. Genes (Basel), 2019. **10**(2): p. 105.
208. Spanò, M., et al., *Nuclear chromatin variations in human spermatozoa undergoing swim-up and cryopreservation evaluated by the flow cytometric sperm chromatin structure assay*. Mol Hum Reprod, 1999. **5**(1): p. 29-37.

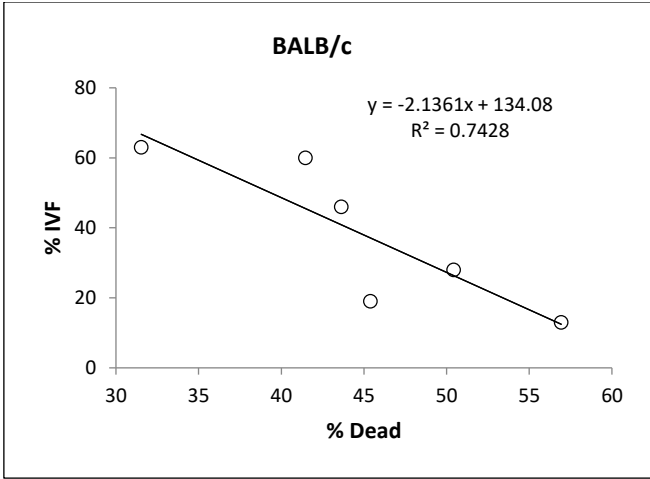
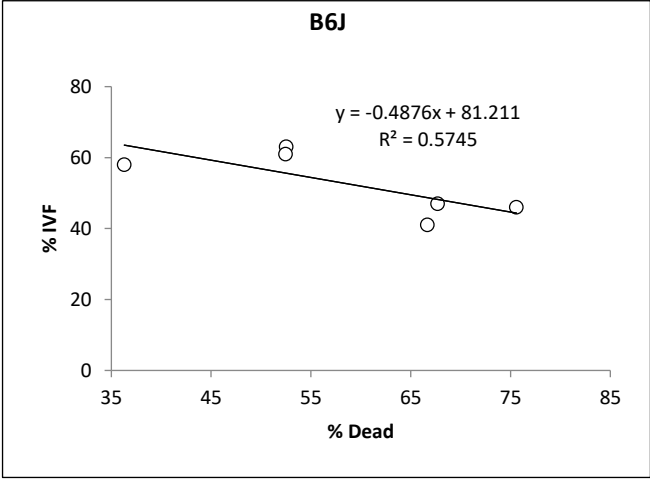
209. Donnelly, E.T., et al., *Assessment of DNA integrity and morphology of ejaculated spermatozoa from fertile and infertile men before and after cryopreservation*. Hum Reprod, 2001. **16**(6): p. 1191-1199.
210. Portela, J.M.D., et al., *Strains matter: Success of murine in vitro spermatogenesis is dependent on genetic background*. Dev Biol, 2019. **456**(1): p. 25-30.
211. Hasegawa, A., et al., *Microdroplet in vitro fertilization can reduce the number of spermatozoa necessary for fertilizing oocytes*. J Reprod Dev, 2014. **60**(3): p. 187-193.
212. S Styrna, J. and H. Krzanowska, *Sperm select penetration test reveals differences in sperm quality in strains with different Y chromosome genotype in mice*. Arch Androl, 1995. **35**(2): p. 111-118.
213. T Tu, T., H. Zhang, and H. Xu, *Targeting sterol-O-acyltransferase 1 to disrupt cholesterol metabolism for cancer therapy*. Front Oncol, 2023. **13**: p. 1197502.
214. N Nemoto, S.A.-O., T. Kubota, and H. Ohno, *Metabolic differences and differentially expressed genes between C57BL/6J and C57BL/6N mice substrains*. PLoS One, 2022. **17**(12): p. e0271651
215. Rebholz, S.L., et al., *Hypercholesterolemia with consumption of PFOA-laced Western diets is dependent on strain and sex of mice*. Toxicol Rep, 2016. **3**: p. 46-54.
216. Pentchev, P.G., et al., *The cholesterol storage disorder of the mutant BALB/c mouse. A primary genetic lesion closely linked to defective esterification of exogenously derived cholesterol and its relationship to human type C Niemann-Pick disease*. J Biol Chem, 1986. **261**(6): p. 2772-2777.
217. Reue, K. and M.H. Doolittle, *Naturally occurring mutations in mice affecting lipid transport and metabolism*. Journal of Lipid Research, 1996. **37**(7): p. 1387-1405.
218. Akpovi, C.D., et al., *Dysregulation of testicular cholesterol metabolism following spontaneous mutation of the niemann-pick c1 gene in mice*. Biol Reprod, 2014. **91**(2): p. 42.
219. Cologna, S.M., et al., *Alterations in Cholesterol and Phosphoinositides Levels in the Intracellular Cholesterol Trafficking Disorder NPC*. Adv Exp Med Biol, 2023. **1422**: p. 143-165.
220. Skakkebaek, N.E., et al., *Male Reproductive Disorders and Fertility Trends: Influences of Environment and Genetic Susceptibility*. Physiol Rev, 2016. **96**(1): p. 55-97.
221. Levine, H., et al., *Temporal trends in sperm count: a systematic review and meta-regression analysis*. Hum Reprod Update, 2017. **23**(6): p. 646-659.
222. Alshahrani, S., et al., *Infertile men older than 40 years are at higher risk of sperm DNA damage*. Reprod Biol Endocrinol, 2014. **12**: p. 103.
223. Kidd, S.A., B. Eskenazi, and A.J. Wyrobek, *Effects of male age on semen quality and fertility: a review of the literature*. Fertil Steril, 2001. **75**(2): p. 237-248.
224. Wyrobek, A.J., et al., *Advancing age has differential effects on DNA damage, chromatin integrity, gene mutations, and aneuploidies in sperm*. Proc Natl Acad Sci USA, 2006. **103**(25): p. 9601-9606.
225. Sampson, N., et al., *The ageing male reproductive tract*. J Pathol, 2007. **211**(2): p. 206-218.
226. Kunimura, Y., et al., *Age-related alterations in hypothalamic kisspeptin, neurokinin B, and dynorphin neurons and in pulsatile LH release in female and male rats*. Neurobiology of Aging, 2017. **50**: p. 30-38.
227. Paul, C. and B. Robaire, *Ageing of the male germ line*. Nat Rev Urol, 2013. **10**(4): p. 227-34.
228. Nguyen, R.H., et al., *Men's body mass index and infertility*. Hum Reprod, 2007. **22**(9): p. 2488-2493.
229. Vested, A., et al., *Persistent organic pollutants and male reproductive health*. Asian J Androl, 2014. **16**(1): p. 71-80.
230. Nargund, V.H., *Effects of psychological stress on male fertility*. Nat Rev Urol, 2015. **12**(7): p. 373-382.
231. Luk, B.H. and A.Y. Loke, *The Impact of Infertility on the Psychological Well-Being, Marital Relationships, Sexual Relationships, and Quality of Life of Couples: A Systematic Review*. J Sex Marital Ther, 2015. **41**(6): p. 610-625.

232. Donnez, J. and M.-M. Dolmans, *Fertility preservation in men and women: Where are we in 2021? Are we rising to the challenge?* Fertility and Sterility, 2021. **115**(5): p. 1089-1090.
233. Brannigan, R.E., R.J. Fantus, and J.A. Halpern, *Fertility preservation in men: a contemporary overview and a look toward emerging technologies.* Fertility and Sterility, 2021. **115**(5): p. 1126-1139.
234. De Vos, M., J. Smits, and T.K. Woodruff, *Fertility preservation in women with cancer.* Lancet, 2014. **384**(9950): p. 1302-1310.
235. Feldschuh, J., et al., *Successful sperm storage for 28 years.* Fertil Steril, 2005. **84**(4): p. 1017.
236. Wang, X., et al., *A Simple and Efficient Method to Cryopreserve Human Ejaculated and Testicular Spermatozoa in -80°C Freezer.* Front Genet, 2022. **12**: p. 815270.

Appendix



Appendix 1: IVF protocol according to the Nakagata method and sperm thawing protocol according to the Ostermeier method. (Modified from [31])



Appendix 2: Correlation between IVF success rate and percentage of dead spermatozoa from B6J (A) and BALB/c (B) males.

Curriculum Vitae

For reasons of data protection, my curriculum vitae will not be published in the electronic version of my work.

ERKLÄRUNG

Hiermit versichere ich an Eides statt, dass ich die vorliegende Dissertationsschrift selbstständig und ohne die Benutzung anderer als der angegebenen Hilfsmittel angefertigt habe. Alle Stellen - einschließlich Tabellen, Karten und Abbildungen -, die wörtlich oder sinngemäß aus veröffentlichten und nicht veröffentlichten anderen Werken im Wortlaut oder dem Sinn nach entnommen sind, sind in jedem Einzelfall als Entlehnung kenntlich gemacht. Ich versichere an Eides statt, dass diese Dissertationsschrift noch keiner anderen Fakultät oder Universität zur Prüfung vorgelegen hat; dass sie - abgesehen von unten angegebenen Teilpublikationen - noch nicht veröffentlicht worden ist sowie, dass ich eine solche Veröffentlichung vor Abschluss der Promotion nicht ohne Genehmigung der / des Vorsitzenden des IPHS-Promotionsausschusses vornehmen werde. Die Bestimmungen dieser Ordnung sind mir bekannt. Die von mir vorgelegte Dissertation ist von Prof. Dr. Esther Mahabir-Brenner betreut worden.

Darüber hinaus erkläre ich hiermit, dass ich die Ordnung zur Sicherung guter wissenschaftlicher Praxis und zum Umgang mit wissenschaftlichem Fehlverhalten der Universität zu Köln gelesen und sie bei der Durchführung der Dissertation beachtet habe und verpflichte mich hiermit, die dort genannten Vorgaben bei allen wissenschaftlichen Tätigkeiten zu beachten und umzusetzen.

Übersicht der Publikationen:

- Raspa, M.; Paoletti, R.; **Peltier, M.**; Majjouti, M.; Protti, M.; Mercolini, L.; Mahabir, E.; Scavizzi, F. Oral D-Aspartate Treatment Improves Sperm Fertility in Both Young and Adult B6N Mice. *Animals* **2022**, 12, 1350

Ich versichere, dass ich alle Angaben wahrheitsgemäß nach bestem Wissen und Gewissen gemacht habe und verpflichte mich, jedmögliche, die obigen Angaben betreffenden Veränderungen, dem IPHS-Promotionsausschuss unverzüglich mitzuteilen.

Köln, den 10.06.2024

.....
Unterschrift